

SIMULATION OF NON-ISOTHERMAL AROMATIC EXTRACTION COLUMN

*A Thesis Submitted in Partial
Fulfillment of the Requirements
for the degree of*
Master of Technology

by

RAJESH KUMAR JAISWAL

**Department of Chemical Engineering
Indian Institute of Technology,
Kanpur**

June, 1998

***Dedicated
To
My
Parents***

CENTRAL LIBRARY
I. I. T., KANPUR

~~MA~~ A 126233

Entered In System.

CHE-1998-JAI-M-SIM



A126233

CERTIFICATE

It is certified that the work contained in the thesis titled
“**Simulation of Non-isothermal Aromatic Extraction Column**”, by
RAJESH KUMAR JAISWAL, has been carried out under my supervision
and that this work has not been submitted elsewhere for a degree.



Dr. Ashok Khanna

Professor

Department of Chemical Engg.

I. I. T. Kanpur, (INDIA)

June, 1998

ACKNOWLEDGEMENT

To acknowledge the help and affection of all the people known to me would perhaps be impossible, nor would it be any way a measure of my gratitude to them. However, as a duty, it is sacred.

I express my deep gratitude to my thesis supervisor, **Dr. Ashok Khanna** for his able guidance, constant encouragement, constructive advice and painstaking effort in completing my thesis work. His critical remarks were great source of inspiration to me.

I would like to thank all the faculties of Dept. of Chemical Engg. for providing an excellent academic environment here. Computational facilities in Computer Centre, IIT Kanpur and especially in our lab will always remain forever in my memory as positive facets of my educational experience.

Among many friends, wonderful BITians like, Parmanadjee, Prashant, Ravishankar, Mukesh, Jaikishore, Sujit, Ajay deserve a special mention for having always boosted my morale. I am also thankful to Tribhuvan, Brajesh, Phalguni, Amit, Abha and Ansarijee for providing happy environment in our lab. Special thanks to Suman for inspiring and encouraging at various moments and for her help in my thesis preparation.

I am also thankful to Engineers' India Limited (EIL) for providing partial financial support.

Rajesh K. Jaiswal

CONTENTS

CERTIFICATE	II
ACKNOWLEDGEMENT.....	III
CONTENTS	IV
LIST OF FIGURES	VI
LIST OF TABLES	VIII
NOMENCLATURE	IX
ABSTRACT	X
1 INTRODUCTION	1
1.1 General	1
1.2 Literature Review	3
1.3 Objective	6
2 NON-ISOTHERMAL LIQUID-LIQUID EXTRACTION	8
2.1 Introduction	8
2.2 Overall simulation model.....	9
2.3 Degree of freedom analysis	12
2.4 Estimation of mass transfer coefficient matrix	14
2.4.1 Estimation approach	14
2.4.2 Estimation of binary mass transfer coefficient.....	16
2.5 Estimation of heat transfer coefficient	16
2.5.1 Heat transfer coefficient for continuous phase	16
2.5.2 Heat transfer coefficient for dispersed phase	17
2.6 Estimation of physical properties.....	17
2.6.1 Liquid density.....	17
2.6.2 Liquid viscosity.....	18
2.6.3 Interfacial tension.....	19
2.6.4 Diffusion coefficient.....	20
2.6.5 Thermal conductivity	21
2.6.6 Specific heat capacity	21
2.7 Estimation of thermodynamic properties	22
2.8 Estimation of hydrodynamic properties	24
3 MODEL DEVELOPMENT ON ASPEN PLUS & SPEEDUP	26
3.1 Modeling on ASPEN PLUS	26
3.2 Modeling on SPEEDUP	31

4 RESULTS AND DISCUSSION	37
4.1 Computation time	39
4.2 Validation of results with ASPEN PLUS at 30 °C temperature difference	40
4.3 Results at various temperature differences across the column...	45
4.4 Execution of SPEEDUP model	52
5 CONCLUSIONS AND SUGGESTIONS	87
APPENDIX A	90
APPENDIX B	97
BIBLIOGRAPHY	101

LIST OF FIGURES

2.1 Schematic representation of extraction column	10
2.2 Schematic representation of k^{th} plate.....	11
3.1 Flow sheet of extraction column on ASPEN PLUS	28
4.1 Concentration of n-Heptane in extract.....	55
4.2 Concentration of n-Heptane in raffinate.....	55
4.3 Concentration of Methyl cyclo-hexane in extract.....	56
4.4 Concentration of Methyl cyclo-hexane in raffinate	56
4.5 Concentration of Benzene in extract	57
4.6 Concentration of Benzene in raffinate	57
4.7 Concentration of Toluene in extract.....	58
4.8 Concentration of Toluene in raffinate.....	58
4.9 Concentration of o-Xylene in extract.....	59
4.10 Concentration of o-Xylene in raffinate.....	59
4.11 Concentration of Sulfolane in extract.....	60
4.12 Concentration of Sulfolane in raffinate	60
4.13 Density of dispersed phase	61
4.14 Density of continuous phase	61
4.15 Temperature profile	62
4.16 Molar flow rate of extract.....	62
4.17 Concentration profile of n-Heptane in extract	63
4.18 Concentration profile of n-Heptane in raffinate	63
4.19 Concentration profile of Methyl cyclo-hexane in extract	64
4.20 Concentration profile of Methyl cyclo-hexane in raffinate	64
4.21 Concentration profile of Benzene in extract.....	65
4.22 Concentration profile of Benzene in raffinate	65
4.23 Concentration profile of Toluene in extract	66
4.24 Concentration profile of Toluene in raffinate.....	66
4.25 Concentration profile of o-Xylene in extract	67
4.26 Concentration profile of o-Xylene in raffinate	67
4.27 Concentration profile of Sulfolane in extract.....	68
4.28 Concentration profile of Sulfolane in raffinate	68
4.29 Density of dispersed phase	69
4.30 Density of continuous phase	69
4.31 Density difference.....	70
4.32 Interfacial tension	70
4.33 Concentration of n-Heptane at interface (dispersed phase).....	71
4.34 Concentration of n-Heptane at interface (continuous phase)	71
4.35 Concentration of Methyl cyclo hexane at interface (dispersed phase).....	72
4.36 Concentration of Methyl cyclo hexane at interface (continuous phase).....	72
4.37 Concentration of Benzene at interface (dispersed phase).....	73
4.38 Concentration of Benzene at interface (continuous phase)	73
4.39 Concentration of Toluene at interface (dispersed phase).....	74

4.40	Concentration of Toluene at interface (continuous phase)	74
4.41	Concentration of o-Xylene at interface (dispersed phase)	75
4.42	Concentration of o-Xylene at interface (continuous phase)	75
4.43	Concentration of Sulfolane at interface (dispersed phase)	76
4.44	Concentration of Sulfolane at interface (continuous phase)	76
4.45	Temperature of bulk dispersed phase	77
4.46	Temperature of bulk continuous phase	77
4.47	Interphase mass transfer rate of n-Heptane	78
4.48	Interphase mass transfer rate of Methyl cyclo hexane	78
4.49	Interphase mass transfer rate of Benzene	79
4.50	Interphase mass transfer rate of Toluene	79
4.51	Interphase mass transfer rate of o-Xylene	80
4.52	Interphase mass transfer rate of Sulfolane	80
4.53	Superficial velocity of dispersed phase	81
4.54	Superficial velocity of continuous phase	81
4.55	Drop diameter profile	82
4.56	Interfacial area profile	82
4.57	Temperature of interface	83
4.58	Static holdup of dispersed phase	83
4.59	Operational holdup of dispersed phase	84
4.60	Total holdup of dispersed phase	84
4.61	Forward flow-rate of dispersed phase	85
4.62	Forward flow-rate of continuous phase	85
4.63	Flooding curve	86
4.64	Heat transfer rate from dispersed to continuous phase	86

LIST OF TABLES

2.1 Summary of equations	12
2.2 No. of variables	13
2.3 No. of equations per stage	13
2.4 Constants of modified Antoine equation	20
3.1 Stream specifications in ASPEN PLUS	29
3.2 Summary of sections in SPEEDUP	32
4.1 Column specifications	38
4.2 System specifications	38
4.3 Operating conditions	39
4.4 Percentage of CPU time taken by some of functions	40
4.5 Stage efficiency of components in ASPEN PLUS	41
4.6 Percentage recovery of aromatics from naphtha	42
4.7 Average relative absolute difference	43
4.8 Distribution coefficient range for components	48
4.9 Percentage recovery of aromatics	50
A.1 Modified UNIFAC parameters	96
A.2 Physical properties of components	97

NOMENCLATURE

a	interfacial area, m^2
c	mixture molar density, $moles/m^3$.
c_p	specific heat capacity, $J/mol\ K$
d	drop diameter, m
d_N	tray perforation diameter, m
d_J	Jet diameter, m
D	axial dispersion coefficient, m^2/s
D°	infinite dilution diffusivity, m^2/s
F	sidestream feed flow rate, $moles/s$
g	acceleration due to gravity, m/s^2
h	heat transfer coefficient, $W/m^2\ K$
h_s	static holdup
h_N	layer thickness required to overcome friction through perforations, m
h_γ	layer thickness required to overcome interfacial effects; m
h_c	layer thickness required to overcome the resistance in downspout, m
Δh	effective mass transfer height of real stage, m
J^*	diffusive flux, $moles/m^2\ s$
k	binary mass transfer coefficient, $moles/m^2\ s$
k_{th}	thermal conductivity, $W/m\ K$
K	distribution coefficient.
M	molecular weight.
n	effective carbon number.
N	interphase mass transfer rate, $moles/s$.
NC	number of components.
ND	number of drop classes.
NS	number of stages.
P	volume fraction of each drop class in a stage.

P_c	critical pressure, bar.
Re	Reynolds number.
S	column cross sectional area, m^2 .
T	temperature, K
T_c	critical temperature, K .
T_b	boiling temperature, K .
T_r	reduced temperature.
u	velocity, m/s .
u_t	terminal velocity, m/s .
u_r^*	characteristic velocity of drop, m/s .
U_{in}	column feed (continuous phase), $moles/s$
U_n	jet velocity, m/s .
V	(without subscript), effective volume for mass transfer in each stage, m^3
V_{in}	column feed (dispersed phase), $moles/s$
x	mole fraction of dispersed phase.
y	mole fraction of continuous phase.

Greek letters

ϕ	operational holdup
γ	activity coefficient
σ	surface tension, N/m
ρ	liquid density, kg/m^3
μ	viscosity, $kg/m.s$
ω	acentric factor.
ε	heat transfer rate, J/s
ψ	temperature dependent group interaction parameter.

Subscripts

av	average
c	continuous phase

d	dispersed phase
i, m	component
in	inlet
j	drop class
k	stage

Superscripts

c	continuous phase
d	dispersed phase
f	feed
I	interface
r	relative
+	in the direction of solvent
-	in the opposite direction of solvent.

ABSTRACT

Recovery of aromatics from naphtha is very important for petrochemical industries. Liquid-liquid extraction process is applied for this purpose using Sulfolane as solvent. A non-equilibrium stage model for non-isothermal operation has been used for simulation of counter-current multi-component extraction column. The present simulator has been tested for 5 different temperature differences across the column and validated with another model developed on ASPEN PLUS. Although ASPEN PLUS utilizes the equilibrium stage approach, stage efficiency profiles for components have been used to make the comparison feasible. It has been found on comparison that aromatics have stage efficiency of 49 – 55 % whereas non-aromatics have 19 – 22 %.

The non-isothermal operation of extraction process results in increased recovery of benzene and xylene whereas toluene recovery decreases. Favorable hydrodynamic behavior has been observed for non-isothermal operation. The solvent loss increases slightly by increasing the temperature difference.

Reduction in CPU time by a factor of 30 has been achieved compared to previous version of the simulator after implementing modified coding in the simulator. This incorporates detailed study of effects of temperature difference on physical, thermodynamic and hydrodynamic properties (density, viscosity, interfacial tension, activity coefficient, drop size, interfacial area operational holdup, etc.).

The present work also includes a simulator developed on commercial application software SPEEDUP.

CHAPTER 1

INTRODUCTION

1.1 General

Separation of different components from the mixture is one of the important tasks of unit operation in chemical process industries. There are various unit operations applied to achieve this goal. Distillation, extraction, absorption, etc are used to separate the components of homogeneous liquid mixtures.

These days more emphasis is given on the economical use of energy in all the industries. Distillation process requires huge amount of energy to vaporize the feed. The feed may contain different components having close boiling points. Thus it is very difficult to separate them in higher purity. This is one of the main drawbacks of the distillation process. When some components form azeotropes having same compositions in liquid and vapor phases, then distillation process is limited by this phenomenon. Some mixtures are heat sensitive, so they can not be separated using high temperature.

The difference in volatility of components is the main source of separation by distillation. When the relative volatility is low, distillation is expensive. Some components have higher solubility in some solvents compared to other components. This factor is utilized in extraction. In extraction, the addition of the solvent is equivalent to the addition of heat in the case of separation by distillation.

The success of liquid-liquid extraction process is strongly dependent on selection of the most appropriate solvent. The final choice of the solvent is a compromise between solvent selectivity, solvent capacity, toxicological constraints, system physical properties and solvent recovery difficulties.

Fields of usefulness of extraction:

- In competition with other mass transfer operations.
- As a substitute for chemical methods.

- For separation not possible by other methods such as distillation, evaporation etc.

The various fields where liquid-liquid extraction is used, are described by Lo, Baird and Hanson (1983). In pharmaceutical industry, penicillin and other antibiotics such as erythromycin, tetracycline, basitracin, cephalosporin and some non-antibiotics are manufactured by liquid-liquid extraction.

LLX is also employed in food industries to produce lipids, coffee, flavors, aromas etc. Extraction is also used with chemical reaction in aromatic nitration, aromatic sulfonation, alkylation reactions, and hydrolysis of salts. This is known as extractive reaction process. Increasing environmental concern about toxic organic compound such as phenol, hydrocarbons and their halogenated derivatives, organonitrogens and organosulfur compounds etc suggests that solvent extraction may play an increasing role in wastewater effluent treatment.

Inorganic and nuclear industries also apply solvent extraction. Some examples are hydrometallurgical extraction of copper from aqueous solution, separation of nickel and cobalt from ammonium carbonate solution containing amines of these metals, acid extraction of zinc and cadmium, production of uranium from ores, recovery of uranium and plutonium from irradiated nuclear fuels etc.

Production of high purity fiber-grade caprolactum can be achieved by solvent extraction. Commercial production of anhydrous acetic acid by solvent extraction provides substantial savings in plant investment and operating costs. Here solvent is used to recover acid from aqueous phase to reduce the amount of water in the product.

In petroleum and petrochemicals processing, the need to separate mixtures of aliphatic and aromatic hydrocarbons provided one of the first large-scale applications for solvent extraction. It represents a physical method for separating groups of components of similar chemical types. The solvent extraction is used extensively for the production of high purity aromatic extracts from the catalytic

reformates containing 45-60 % aromatics. Benzene, toluene and xylene (BTX) extraction is a major example.

Udex process was the first efficient method using glycol based solvent to separate aromatics from aliphatic hydrocarbons. Currently, sulfolane and N-methyl pyrrolidone (NMP) are used for this purpose. Other solvents are polyethylene glycol water mixture, N-formylmorpholine (NFM), dimethyl sulfoxide (DMSO) and tetra ethylene glycol (TEG). Lube oils are purified by extraction to remove certain aromatics or polar components having poor stability or viscometric properties. For this purpose, sulfur dioxide, $\text{SO}_2\text{-C}_6\text{H}_6$, phenol, furfural, NMP, Duo-sol, propane are used as solvents.

Choice of solvent depends on:

- Selectivity
- Distribution coefficient
- Insolubility of solvent
- Recoverability
- Density and density difference with the feed
- Interfacial tension
- Chemical reactivity
- Viscosity, vapor pressure, boiling and freezing points
- Non-toxicity, non-flammability, low cost etc.

1.2 Literature review

Modeling of extraction process

Any chemical process needs to be properly represented in mathematical form to take care of proper operation and design. Extraction process may be expressed as the combination of differential and algebraic equations as that for the distillation and absorption assuming equilibrium-state at each of the stages. But extraction process gives a very low efficiency of the order of 20-25 % Laddha (1976). Hence it is not practical to apply this approach because the efficiency may vary from stage to stage as well as component-wise.

Ricker(1981), Spencer(1981), Henley & Seader (1981), Smith and Brinkley (1960) and others have applied the equilibrium stage model. The phenomenon of axial dispersion or backmixing drastically reduces the driving force for mass transfer from continuous phase to dispersed phase or vice-versa. Treybal (1963 & 1981), Laddha & Degaleesan (1976), Ricker (1981), Spencer (1981), Baird (1983) have described this effect by taking some fraction of main flow as backward flow. Now more stress has been given on rigorous modeling as in the case of the distillation Krishnamurthy (1985a & 1985b), Krishna and Taylor (1993) encourage use of such models incorporating interaction of different components in mass transfer including reverse osmotic effects, pressure diffusion etc. Zimmermann (1992) proposed a model for extraction applying non-equilibrium stage approach.

Modeling for drop breakage and coalescence

Khani, Gourdon and Casamatta (1989) have used the drop population balance model for dispersed phase behavior. This takes into account the drop transport, break up, coalescence and mass transfer for dispersed phase. Ramakrishna (1985) has presented a review article on status of drop population balance model. The mass transfer rate during drop formation, rise or fall through continuous phase and coalescence vary according to Skelland & Minhas (1971), Coulaloglou and Tavlarides (1977) and Baird (1983). They have proposed a phenomenological model to describe drop breakage and coalescence in turbulently agitated liquid-liquid dispersion. Sovova (1981) worked out the same model for the batch stirred extraction operation and discretized it on the real stage. Sovova (1983) also applied this model for vibrating plate extractor incorporating drop population balance approach. Hsia and Tavlarides (1980) discussed about the stirred tank, whereas Rubio et al (1994) described the various possible theoretical drop spectrum distributions in Wirz extraction column fitting them to real extraction operation. Recently, Tsouris and Tavlarides (1994a & 1994b) further extended the model

developed earlier by Coulaloglou (1977). The model has been analyzed for drop breakage and coalescence behavior and control of operational holdup in a multi-stage extraction column.

Rate based mass transfer and axial dispersion

Zimmermann (1992) synthesized both drop population and non-equilibrium approach and proposed a detailed mathematical model for steady state extraction operation. Jiricny (1979) explained the polydispersed phase model which has a drop spectrum of different drop classes (drops of same volume) interacting with the bulk continuous phase. Backmixing is represented by axial dispersion coefficients D^c and D^d . Krishnamurthy (1985a & 1985b) used rigorous transport relations in distillation and suggested for use in extraction also. Taylor and Krishna (1993) have used the film theory for mass transfer between continuous and dispersed phase. Smith and Taylor (1983) proposed a film model for multi-component mass transfer.

Equilibrium relations

The equilibrium relations at the interface (separating continuous and dispersed phases) are described in the form of distribution coefficient as $y_i^I = K_i x_i^I$. Aromatics form highly non-ideal solution; hence care must be taken to calculate the distribution coefficient between the phases. The experimental data for liquid-liquid equilibria are not available in large amount. Its scarcity is strongly felt for multi-component systems. The distribution coefficient requires the knowledge of activity coefficient of a component in both the phases. There are various thermodynamic models for the calculations of activity coefficient of liquids. NRTL model proposed by Renon & Prausnitz (1968) and UNIQUAC model proposed by Abrams and Prausnitz (1975) are two of the methods applied to calculate the activity coefficients of liquids. UNIFAC method is the most relied method for VLE as well as LLE calculations. Larsen et al (1987) introduced two modifications with respect to the original UNIFAC

model having combinatorial and residual terms. Their model includes three group interaction parameters for temperature effect for hydrocarbons, alcohols, water, ether, esters, amines and aldehydes. Gmehling (1993) proposed modified UNIFAC method for prediction of multi-component liquid-liquid equilibria. It can be applied to systems having molecules of very different sizes. The temperature dependent group interaction parameters have been fitted for 45 main groups (more than the original UNIFAC for LLE containing 32 groups).

Empirical correlations

Extraction process contains a large number of equations for various types of extractors. Several empirical correlations are applied for prediction of various parameters. These correlations vary from extractor to extractor and are described in the textbooks Transport Phenomena in Liquid Extraction by Laddha and Degaleesan (1976), Handbook of Solvent Extraction edited by Baird (1983), Handbook of Separation Technology Rousseou (1987), Perry's Chemical Engineer's Handbook (1984), Reid & Prausnitz (1988) etc. These correlations are used for liquid density, specific heat capacity, thermal conductivity, diffusivity, viscosity, interfacial tension, characteristic velocity, drop size, mass transfer coefficient, heat transfer coefficient etc.

1.3 Objective

Simulation of any chemical process is a design tool that predicts the behavior of the process with respect to the various process variables. Steady state and dynamic simulations can be used to evaluate equipment configuration and control schemes to determine the reliability and safety of a design before capital is committed to a project. In existing units, these simulations can be helpful to study the feasibility and economical applicability of a major process modification. Simulation also helps to compare the results with that of an existing plant and avoids unnecessary capital expenditure.

Simulation study on a simulator helps to learn how the process variables will respond to a change and this helps to find out the optimum operating conditions under which plant must be operated for maximum economic gain.

Availability of commercial advanced application software packages helps to simulate the process conditions accurately and speedily. ASPEN PLUS, PROCESS, SIMMOD, SPEEDUP, etc are some of the widely used packages for the simulation of chemical processes, Edgar & Himmelblau (1989).

The present work involves the development of a model for liquid-liquid extraction for multi-stage sieve tray column for multi-component system. The steady state model for process was simulated using ASPEN PLUS (Aspen Technology Inc.) and the simulator developed earlier by Rajeev Kumar (1996). This simulator was extended for non-isothermal operation of the counter current extraction column. The performance of unit for changes in various process variables was studied through the simulation.

Chapter 2 provides a detailed description of the mathematical model for the extraction. It also includes the various correlations used. Chapter 3 explains the steady state model development on ASPEN PLUS and dynamic modeling on SPEEDUP. Simulation and comparison of results of two simulations; one on ASPEN PLUS and other on our simulator, is the subject matter for chapter 4. It also includes details of results of simulations applying 5 temperature differences across the column. Chapter 5 provides the final conclusion and recommendations for future work.

CHAPTER 2

NON-ISOTHERMAL LIQUID-LIQUID EXTRACTION

2.1 INTRODUCTION

The equilibrium stage model approach for distillation, absorption, etc is widely used. The model includes the assumption that the streams leaving any particular stage are in equilibrium with each other. Component Material balances, the equation of phase equilibrium, Summation equations and Heat balance for each stage (the so-called MESH equations) are solved using one of the very many ingenious algorithms presently available to give product distributions, flow rates, temperatures and so on.

In actual operation stages rarely operate at equilibrium despite attempts to approach this condition by proper design and choice of operating conditions. Incorporating stage efficiency into the equilibrium relations is the usual way of dealing with the departure from the equilibrium. Many different models of stage efficiency have been proposed for binary systems, there is no consensus for the best one.

The schematic diagrams of the extraction column and a stage are given in Fig. 2.1 and 2.2. A non-equilibrium stage model has been developed for the simulation of a counter-current multi-component extraction operation avoiding the use of empirical correction factor such as efficiency. HETP is completely avoided. The dispersed phase behavior, the change in holdup, mean drop size d_{32} , drop population along the column have to be considered in order to describe the hydrodynamics of the extraction column.

The model is based on the following assumptions:

1. The stages are assumed to be in mechanical equilibrium i.e. pressures of both the continuous and dispersed phases are same.
2. There is no resistance to mass transfer at the interface.
3. All the properties (density, viscosity, interfacial tension, diffusivity, specific heat capacity, thermal conductivity etc) are temperature and composition dependent.
4. Trays are numbered in the direction of the dispersed phase flow (Sulfolane in the present case).
5. Mixture molar densities are assumed uniform for all drops of the same drop-class in a particular stage.

Mass and energy balances are split into two parts, one for each phase. Mass transfer across the interface is modeled using rate based approach (here flux is not used). Stage efficiency (Murphree type) or HETU is completely avoided. Back mixing is assumed in the form of axial dispersion between adjacent stages applying axial dispersion coefficient. Whenever flooding occurs, it is checked. The distribution coefficient K_i has been predicted by use of modified UNIFAC group contribution model. Several empirical correlations have been used for different parameters.

2.2 Overall simulation model

The details of equations are given in Appendix (A), which describes the model for any general multi-stage counter-current extraction column. The summary of equations is given in Table 2.1. The model is discretized in such a way that it can be applied to any type of extraction column (agitated and unagitated) such as sieve-tray column, pulsed sieve-tray column, RDC etc. However the correlations used in the model will be different for different type of columns.

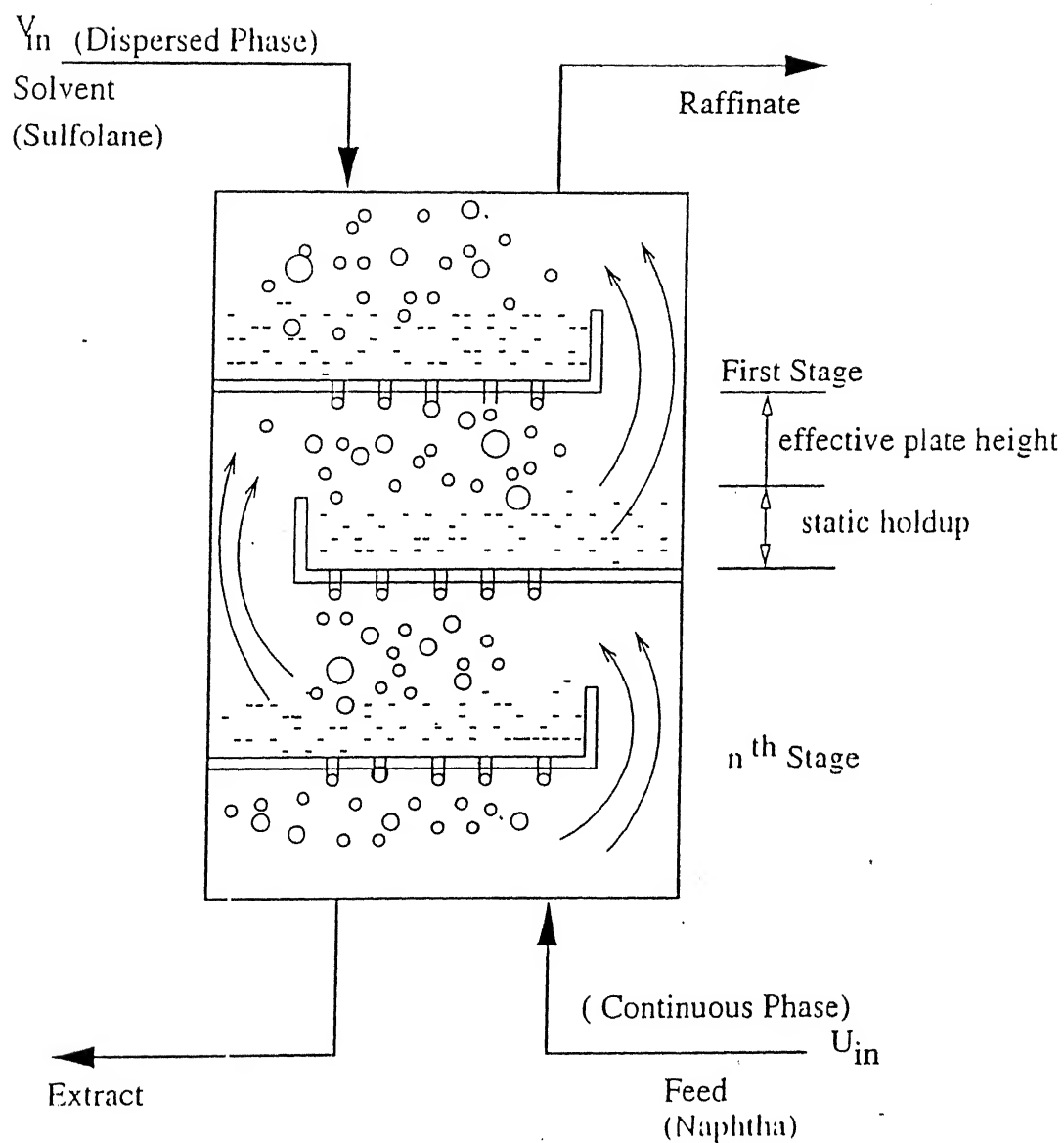


Fig 2.1: Schematic representation of extraction column
(Heavy Phase Dispersed)

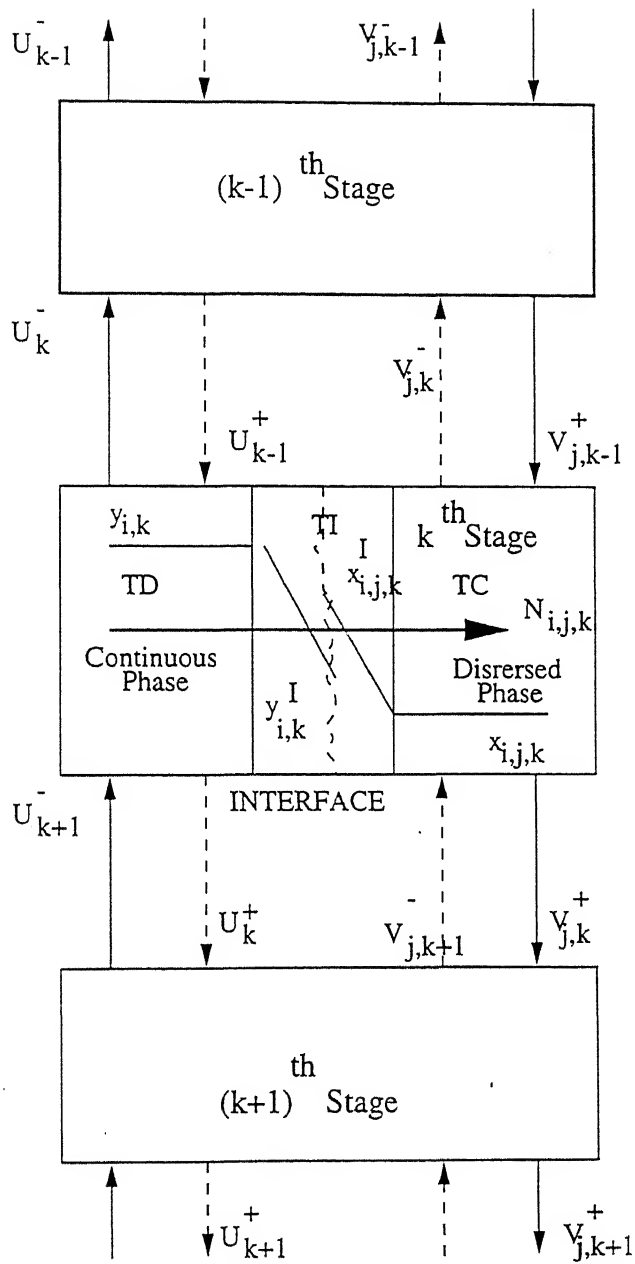


Fig 2.2 Schematic representation of k th stage

Table 2.1: Summary of equations

$V_{jk-1}^+ x_{ijk-1} - (V_{jk}^+ + V_{jk}^-) x_{ijk} + V_{jk+1}^- x_{ijk+1} + N_{ijk} + F_{jk}^d x_{ik}^f + \Pi_{ijk} = 0$	
$U_{k-1}^+ y_{ik-1} - (U_k^+ + U_k^-) y_{ik} + U_{k+1}^- y_{ik+1} - \sum_{j=1}^{ND} N_{ijk} + F_k^c y_{ik}^f = 0$	
$V_{jk}^+ = (u_{jk}^d + \frac{D_k^d}{\Delta h_k}) P_{jk} c_{jk}^d S$	$V_{jk}^- = (\frac{D_{k-1}^d}{\Delta h_{k-1}}) P_{jk} c_{jk}^d S$
$U_k^- = (u_k^c + \frac{D_{k-1}^c}{\Delta h_{k-1}}) (1 - \phi_k) c_k^c S$	$U_k^+ = (\frac{D_k^c}{\Delta h_k}) (1 - \phi_k) c_k^c S$
$\sum_{j=1}^{ND} V_{jk}^+ \sum_{i=1}^{NC} x_{ijk-1} H_{ik-1}^d - \sum_{j=1}^{ND} (V_{jk}^+ + V_{jk}^-) \sum_{i=1}^{NC} x_{ijk} H_{ik}^d + \sum_{j=1}^{ND} V_{jk+1}^- \sum_{i=1}^{NC} x_{ijk+1} H_{ik+1}^d +$	
$\sum_{j=1}^{ND} F_{jk}^d \sum_{i=1}^{NC} x_{ik}^f H_{ik}^f + \sum_{j=1}^{ND} \sum_{i=1}^{NC} \Pi_{ijk} H_{ijk}^d + \varepsilon^d = 0$	
$U_{k-1}^+ \sum_{i=1}^{NC} y_{ik-1} H_{ik-1}^c - (U_k^+ + U_k^-) \sum_{i=1}^{NC} y_{ik} H_{ik}^c + U_{k+1}^- \sum_{i=1}^{NC} y_{ik+1} H_{ik+1}^c +$	
$F_k^c \sum_{i=1}^{NC} y_{ik}^f H_{ik}^c - \varepsilon^c = 0$	
$N_{ijk} = y_{ik} \sum_{i=1}^{NC} N_{ijk} + a_{jk} \sum_{m=1}^{NC-1} K_{imjk}^c (y_{mk} - y_{mjk}^f)$	
$N_{ijk} = x_{ik} \sum_{i=1}^{NC} N_{ijk} + a_{jk} \sum_{m=1}^{NC-1} K_{imjk}^d (x_{mjk}^f - x_{mjk})$	
$\varepsilon^d = h^d a_k (TD_k - TI_k) + \sum_{j=1}^{ND} \sum_{i=1}^{NC} N_{ijk} H_{ik}^d \quad \varepsilon^c = h^c a_k (TI_k - TC_k) + \sum_{j=1}^{ND} \sum_{i=1}^{NC} N_{ijk} H_{ik}^c$	
$y_{ijk}^f = K_{ijk} x_{ijk}^f$	
$\sum_{i=1}^{NC} x_{ijk}^f = 1.0$	$\sum_{i=1}^{NC} y_{ijk}^f = 1.0$
$\sum_{i=1}^{NC} x_{ijk} = 1.0$	$\sum_{i=1}^{NC} y_{ik} = 1.0$
$i = 1, 2, 3, \dots, NC; j = 1, 2, 3, \dots, ND; k = 1, 2, 3, \dots, NS$	

2.3 Degree of freedom Analysis

Table 2.1 lists the set of equations for a single stage k. Similar equations can be written for other stages. For any stage k, following independent variables exist:

Table 2.2: No. of independent variables

Independent variables	Total no. of variables
Flow rates of each drop class (V_{jk}^+, V_{jk}^-) in the dispersed phase.	2^{ND}
Flow rates of continuous phase (U_k^+, U_k^-)	2
Bulk mole fractions (x_{ijk}, y_{ik})	$(ND \times NC) + NC$
Interface mole fraction (x_{ijk}^I, y_{ijk}^I)	$2(ND \times NC)$
Mass transfer rate (N_{ijk})	$(ND \times NC)$
Drop class volume fractions for the dispersed phase (P_{jk})	ND
Velocity of continuous phase (u_k^c)	1
Temperature of dispersed phase (TD_k)	1
Temperature of continuous phase (TC_k)	1
Temperature at the interface (TI_k)	1
Total no. of variable/stage	$4(ND \times NC) + 3ND + NC + 6$

Similarly for any stage k , following number of equations are to be solved:

Table 2.3: No. of equations per stage

Independent equations	Number of equations
Material balance equation MBD_{ijk}	$(ND \times NC)$
Material balance MBC_{ik}	NC
Flow Equation $VP_{jk}, V_{jk}, UP_k, UM_k$	$2(ND + 1)$
Transport relation $MBID_{ijk}, MBIC_{ijk}$	$2ND(NC - 1)$
Equilibrium relations EQ_{ijk}	$(ND \times NC)$
Normalization relations NDI_{jk}, NCI_k	2^{ND}
Normalization relations ND_{jk}, NC_k	$ND + 1$
Energy equations EBD_k, EBC_k	2
Transport relations EBI_k	1
Total no. equations/stage	$4(ND \times NC) + 3ND + NC + 6$

Thus the above simulation problem becomes a set of non-linear algebraic equations for steady simulation. These can be solved by any

non-linear equation-solver such as multi-variable Newton-Raphson method or Block-Thomas method

2.4 Estimation of mass transfer coefficient matrix

The multi-component mixture mass transfer is very complicated as compared with the binary mixtures. This is because of possible coupling between the individual concentration gradients. Reverse and osmotic diffusions are also possible in multi-component system Krishna & Taylor (1993). The rate of mass transfer depends upon the concentration gradient across the film. Bulk concentrations are assumed uniform and thermodynamic equilibrium is assumed at the interface. Many other factors such as temperature, concentration, physical properties like, density, density difference, viscosity, interfacial tension, etc, system geometry and hydrodynamics influence the rate of mass transfer. Mass transfer rate for component i in multi-component mixture is described as $[N_i = y_i \sum_i N_i + \bar{J}_i^*]$ by Bird (1960) and Krishna & Taylor (1993). The first term on the right hand side of this expression represents the convective mass transfer and the second term represents the diffusive mass transfer.

2.4.1 Estimation approach

Resistance for mass transfer (for both the phases) can be accounted for by using separate rate equations incorporating interactive mass transfer coefficient. The interfacial area between the bulk continuous phase and any drop class can be easily calculated by eq. (A.16).

Krishnamurthy (1985a, 1985b) proposed the method for distillation and absorption, which is implicit in fluxes or transfer rate. This can be applied here for extraction also. This can be extended to extraction as

$$N_{ijk} = y_{ik} \sum_{i'=1}^{NC} N_{i'jk} + a_{jk} \bar{J}_{ijk}^* \quad (2.1)$$

Flux $\overline{J_{ijk}^*}$ can be written by incorporating interaction effects into account by using generalized Fick's law Krishna & Taylor (1993) based on mass transfer coefficient instead of diffusivity. Equation (2.1) can be rewritten as

$$N_{ijk} = y_{ik} \sum_{i=1}^{NC} N_{i,jk} + a_{jk} \sum_{m=1}^{NC-1} K_{mjk}^c (y_{mk} - y_{mjk}^I) \quad (2.2)$$

In matrix form the above equation can be written for each drop class j and stage k as

$$(N)_{jk} = (y)_{jk} N_I + a_{jk} [K^c]_{jk} (y - y^I)_{jk} \quad (2.3)$$

where $N_I = \sum_{i=1}^{NC} N_{i,jk}$

() represents vector,

[] represents matrix in eq. (2.3).

Equation (2.3) consists of (NC-1) equations for any drop class j at stage k, since $\sum_{i=1}^{NC} \overline{J_{ijk}^*} = 0.0$, hence only (NC-1) independent equations will exist.

The same approach may be applied for the dispersed phase. In general mass transfer coefficient K depends on bulk concentration, interfacial concentration, flux or transfer rate, etc. Mass transfer matrix of size (NC-1) x (NC-1) are then evaluated as:

$$[K^c]_{jk} \cdot a_{jk} = [B]_{jk}^{-1} a_{jk} [\phi]_{jk} \{ \exp[\phi]_{jk} - [I] \}^{-1} \quad (2.4)$$

This expression is then evaluated by the following procedure:

- Krishna and Standart method: This method is used in the present study.

$$\frac{[B]_{jk}}{a_{jk}} = [M]_{jk} \quad \text{with } m_{ijk} = y_{ik} \quad (2.5)$$

$$[\phi]_{jk} = [M]_{jk} \quad \text{with } m_{ijk} = N_{ijk} \quad (2.6)$$

where $[M]_{jk}$ components are evaluated as given below:

$$M_{ijk} = \frac{m_{ijk}}{k_{incjk} a_{jk}} + \sum_{\substack{m=1 \\ m \neq i}}^{NC} \frac{m_{mjk}}{k_{mjk}} \quad i = 1, 2, \dots, (NC - 1) \quad (2.7)$$

$$M_{imjk} = -m_{ijk} \left(\frac{1}{k_{imjk} a_{jk}} - \frac{1}{k_{incjk} a_{jk}} \right) \quad i \neq m' \quad I = 1, 2, \dots, (NC-1) \quad (2.8)$$

This method is described in detail in Krishna & Taylor (1993) and it is based on the film theory.

2.4.2 Estimation of binary mass transfer coefficient K_{imjk}

The binary local mass transfer coefficient k_{imjk} for any drop class j at stage k can be evaluated by the empirical correlation Baird (1983):

$$k^d = 0.0432 \frac{d}{t} \left(\frac{\rho^d}{M^d} \right)_{av} \left(\frac{U_n^2}{dg} \right)^{0.089} \left(\frac{d^2}{tD^d} \right)^{-0.334} \left(\frac{\mu^d}{\sqrt{\rho^d d\gamma}} \right)^{-0.601} \quad (2.9)$$

$$k^c = 0.386 \left(\frac{\rho^c}{M^c} \right)_{av} \left(\frac{D^c}{t} \right)^{0.5} \left(\frac{\rho^c \gamma}{\Delta \rho g t \mu^c} \right)^{0.407} \left(\frac{gt^2}{d} \right)^{0.148} \quad (2.10)$$

Rise time t is given by

$$t = \frac{n_o (\pi/6) d^3}{Q^d} \quad (2.11)$$

$\left(\frac{\rho^d}{M^d} \right)_{av}$ and $\left(\frac{\rho^c}{M^c} \right)_{av}$ are equivalent to c^d and c^c respectively.

2.5 Estimation of heat transfer coefficient

There are two phases in which the dispersed phase is in the form of droplets. The heat transfer coefficient depends on the physical properties of the system as well as the drop size and the velocity of the bulk fluid. It is function of Reynolds and Prandtl numbers.

2.5.1 Heat transfer coefficient for the dispersed phase

The correlation for Nusselt number is obtained from Bird (1960) as follows:

$$\frac{h_k^d d_{32}}{k_{th,k}^d} = 2.0 + 0.6 \left(\frac{c_{p,k}^d \mu^d}{k_{th,k}^d} \right)^{1/3} \left(\frac{d_{32} u_k^d \rho^d}{\mu^d} \right)^{1/2} \quad (2.12)$$

This correlation has been satisfactorily applied for various operations in which heat transfer between spherical drops and bulk fluid takes place, Wang et al (1983).

2.5.2 Heat transfer coefficient for the continuous phase

Same correlation can be used for the prediction of continuous phase heat transfer coefficient for heat transfer between the bulk continuous phase and the interface using the physical properties for that phase:

$$\frac{h_k^c d_{32}}{k_{th,k}^c} = 2.0 + 0.6 \left(\frac{c_{p,k}^c \mu^c}{k_{th,k}^c} \right)^{1/3} \left(\frac{d_{32} u_k^c \rho^c}{\mu^c} \right)^{1/2} \quad (2.13)$$

2.6 Estimation of physical properties

Experimental data for the physical properties are essential for the proper design of any equipment. Due to scarcity of experimental data over the wide range of operating conditions Estimation and Prediction are often used. Estimates may be based on theory, on correlation of experimental values or on a combination of both. Completely empirical correlations are often useful, but one must avoid the temptation to use them beyond the prescribed range of conditions on which they are based, Reid (1988). In general, the correlations are more reliable when they have theoretical basis.

2.6.1: Liquid density

Liquid density is one of the important properties for the proper operation of liquid-liquid extraction. A difference in the densities of the liquid phases is necessary. The larger this difference, the better is the extraction. Larger density difference increases the capacity of the contacting equipment. It is necessary for proper operation that a satisfactory density difference should be maintained throughout the process.

Hankinson and Thomson (1979) proposed the following correlation for the prediction of the liquid density:

$$\frac{V_s}{V^*} = V_R^{(0)} [1 - \omega_{SRK} V_R^{(\delta)}] \quad (2.14)$$

$$\text{where } V_R^{(0)} = 1 + a(1 - T_r)^{\frac{1}{3}} + b(1 - T_r)^{\frac{2}{3}} + c(1 - T_r) + d(1 - T_r)^{\frac{4}{3}} \quad (2.14a)$$

$$0.25 < T_r < 0.95$$

$$V_R^{(\delta)} = \frac{[e + fT_r + gT_r^2 + hT_r^3]}{(T_r - 1.00001)} \quad (2.14b)$$

$$0.25 < T_r < 1.0$$

Values of a, b, c,, h are given below, Reid et al (1988).

a	-1.52816	b	1.43907
c	-0.81446	d	0.190454
e	-0.296123	f	0.386914
g	-0.0427258	h	-0.0480645

Values of V^* and ω_{SRK} are available in literature Reid et al (1988).

Mixture density is given as:

$$\frac{1}{\rho_m} = \sum_{i=1}^{NC} \frac{x_i}{\rho_i} \quad (2.15)$$

2.6.2 Liquid viscosity

Low viscosity of the liquid consumes small amount of power for pumping, rapid extraction, settling of dispersions. High mass and heat transfer coefficients are achieved for low viscosity. The viscosity of continuous phase should be as low as possible.

Viscosity influence the terminal velocity of the drops which can be seen by Navier-Stokes equation

$$u_t = \frac{\Delta \rho g d_p^2}{18 \mu^c} \left(\frac{1 + \frac{\mu^d}{\mu^c}}{\frac{2}{3} + \frac{\mu^d}{\mu^c}} \right) \quad (2.16)$$

Quantity within the parenthesis is the correction required to account for internal circulation of the drops.

The viscosity of the liquid can be calculated by the correlation proposed by Allan and Teja (1991) which is based on the effective carbon number:

$$\ln \mu = A \left[\frac{-1}{B} + \frac{1}{(T+C)} \right] \quad (2.17)$$

$$\text{where } A = 145.73 + 99.01 n + 0.83 n^2 - 0.125 n^3 \quad (2.17a)$$

$$B = 30.48 + 34.01 n - 1.230 n^2 + 0.017 n^3 \quad (2.17b)$$

$$C = -3.07 - 1.99 n \quad (2.17c)$$

The effective carbon number for the mixture is calculated using a simple mixing rule

$$n_m = \sum_{i=1}^N x_i n_i \quad (2.18)$$

The value of n_m can be used to calculate the viscosity of the mixture at a given temperature.

2.6.3 Interfacial tension

Interfacial tension is one of the parameters, which affects the size of drops formed. Drop diameter is function of $\sigma^{0.5}$. Hence lower the interfacial tension, lower is the size of drop formed. Small drops enhance the rates of heat and mass transfer. Higher value of interfacial tension increases coalescence of drops. The capacity of separation will be higher for low interfacial tension. Antonoff (Treybal, 1981) proposed the difference of surface tension of liquid phases as the interfacial tension of the system.

Hakim (1971) proposed the following correlation for i^{th} component as:

$$\sigma_i = P_{c_i}^{2/3} T_{c_i}^{1/3} Q_{p_i} \left(\frac{1 - T_r}{0.4} \right)^{m_i} \quad (2.19)$$

where

$$Q_{p_i} = 0.1560 + 0.365 \omega_i - 0.1754 X_i - 13.57 X_i^2 - 0.506 \omega_i^2 + 1.287 \omega_i X_i \quad (2.19a)$$

$$m_i = 1.210 + 0.5385\omega_i - 14.61X_i - 32.07X_i^2 - 1.656\omega_i^2 + 22.03\omega_iX_i \quad (2.19b)$$

$$X_i = \log P_{\text{vpr}}(0.6) + 1.70 \omega_i + 1.552 \quad (2.19c)$$

$$\omega_i = \frac{3}{7} \left(\frac{\theta_i}{1 - \theta_i} \right) \log P_c - 1 \quad (2.19d)$$

$$\theta_i = \frac{T_{b_i}}{T_{c_i}} \quad (2.19e)$$

$$P_{\text{vpr}} = \frac{P_{\text{vap}}}{P_c} \quad (2.19f)$$

P_{vpr} is estimated by the following Extended Antoine vapor pressure equation

$$\ln P_i = C_1 + \frac{C_2}{T + C_3} + C_4 T + C_5 \ln T + C_6 T^2 \quad (2.20)$$

Values of all constants C_1 to C_7 for all components are given in Table 2.4. These values have been taken from ASPEN PLUS Reference Manual Vol. III (1996).

Table 2.4 Constants of modified Antoine eq.

Components	C ₁	C ₂	C ₃	C ₄	C ₅	C ₆	C ₇
N-Heptane	42.853	-5684.3	0	0	-4.658	8.688x10 ⁻¹⁸	6
MCH	39.874	-5502.21	0	0	-4.249	7.452x10 ⁻¹⁸	6
Benzene	46.114	-5758.85	0	0	-5.08	1.1338x10 ⁻¹⁷	6
Toluene	42.072	-5872.82	0	0	-4.5	6.256x10 ⁻¹⁸	6
O-xylene	46.79	-6661.1	0	0	-5.067	4.678x10 ⁻¹⁸	6
Sulfolane	63.831	-9603.58	0	0	-5.561	7.6338x10 ⁻¹⁹	6

The surface tension of mixture can be calculated by:

$$\sigma_m^{1/4} = \rho_m \sum_{i=1}^{N_c} \frac{x_i \sigma_i^{1/4}}{\rho_i} \quad (2.21)$$

$$\gamma_m = \frac{\sigma_{md} - \sigma_{mc}}{\sigma_{mc}} \quad (2.22)$$

2.6.4 Diffusion coefficient

Diffusion refers to the net transport of material within a single phase. Whenever a concentration gradient occurs for a component in

any phase, diffusion takes place. Diffusivity of the components are calculated using the famous Wilke-Chang correlation Reid (1988):

$$D_{im} = 7.4 \times 10^{-8} \left(\frac{(\phi_m M_m)^{\frac{1}{2}} T}{\mu(m) V_i^{0.6}} \right) \quad (2.23)$$

2.6.5 Thermal conductivity

Latini (1984) and his coworkers proposed the correlation for thermal conductivity of components as:

$$k_{th,i} = \frac{A(1 - T_r)^{0.38}}{T_r^{1/6}} \quad (2.24)$$

where $A = \frac{A^* T_{bi}^{\alpha}}{M_i^{\beta} T_{ci}^{\gamma}}$ (2.24a)

Values of A^* , α , β , γ are available in Reid (1988).

Mixture thermal conductivity is calculated by the correlation proposed by Li (1976):

$$k_{th,m} = \sum_{i=1}^{NC} \sum_{j=1}^{NC} \phi_i \phi_j k_{th,ij} \quad (2.25)$$

where

$$k_{th,ij} = \frac{2}{\left(\frac{1}{k_{th,i}} + \frac{1}{k_{th,j}} \right)} \quad (2.25a)$$

and

$$\phi_i = \frac{x_i V_i}{\sum_{j=1}^{NC} x_j V_j} \quad (2.25b)$$

V_j = molar volume of component j.

2.6.6 Specific heat capacity of liquid:

The liquid specific heat capacity for pure components is calculated by using the DIPPR (Design Institute for Physical Property) data. It uses the correlation proposed by Rowlinson (1969).

$$\frac{c_{pi} - c_{pi}^*}{R} = 1.45 + 0.45(1 - T_r)^{-1} + 0.25\omega[17.11 + 25.2(1 - T_r)^{1/3} T_r^{-1} + 1.742(1 - T_r)^{-1}] \quad (2.26)$$

where c_{pi}^* = specific heat capacity at any reference temperature (298.15 °K)

Mixture specific heat capacity can be calculated by:

$$c_{pm} = \sum_{i=1}^{Nc} x_i c_{pi} \quad (2.27)$$

2.7 Estimation of thermodynamic properties

The liquid mixtures behave different from the vapor mixtures. Their thermodynamic properties are also more sensitive than those of vapor mixtures are. These changes greatly affect the operation of extraction for non-isothermal conditions. Small change in activity coefficient of any component results in large variation in liquid-liquid equilibrium data. Various methods have been proposed for calculations of liquid activity coefficients. Gmehling (1993) proposed modified UNIFAC model for prediction of multi-component liquid-liquid equilibrium. The activity coefficient is combination of two terms – combinatorial and residual.

$$\ln \gamma_i = \ln \gamma_i^c + \ln \gamma_i^R \quad (2.28)$$

The combinatorial part takes into account the non-idealities caused by difference in size and shape and the residual part checks the energy interactions between the molecules of various species.

The combinatorial part of the expression for activity coefficient may be written as:

$$\ln \gamma_i^c = \ln \frac{\phi_i}{x_i} + 1 - \frac{\phi_i}{x_i} - \frac{z}{2} q_i \left(\ln \frac{\phi_i}{\theta_i} + 1 - \frac{\phi_i}{\theta_i} \right) \quad (2.28a)$$

where ϕ_i = molecular volume fraction,

θ_i = surface area fraction.

ϕ_i and θ_i can be calculated using group volume parameter R_k and group surface area parameter Q_k .

$$\phi_i = \frac{x_i r_i^{3.4}}{\sum_i x_i r_i^{3.4}} \quad \text{where} \quad r_i = \sum_k v_k^{(i)} R_k \quad (2.28b)$$

$v_k^{(i)}$ = no. of groups of type k in molecule i.

$$\text{and } \theta_i = \frac{x_i q_i}{\sum_i x_i q_i} \quad \text{where} \quad q_i = \sum_k v_k^{(i)} Q_k \quad (2.28c)$$

k = 1, 2, 3,, all groups.

j = 1, 2, 3,, NC.

x_i is the mole fraction of component i.

The residual part is given as:

$$\ln \gamma_i^R = \sum_k v_k^{(i)} [\ln \Gamma_k - \ln \Gamma_k^{(i)}] \quad (2.28d)$$

where Γ_k is the residual group activity coefficient at the actual group composition

and $\Gamma_k^{(i)}$ is the residual group activity coefficient at the group composition corresponding to pure component i

$$\ln \Gamma_k = Q_k \left[1 - \ln \left(\sum_m \theta_m \psi_{mk} \right) - \sum_m \frac{\theta_m \psi_{km}}{\sum_n \theta_n \psi_{mn}} \right] \quad (2.28e)$$

where group area fraction θ_m is given by

$$\theta_m = \frac{Q_m X_m}{\sum_n Q_n X_n} \quad (2.28f)$$

Group mole fraction, X_m is expressed as:

$$X_m = \frac{\sum_i v_m^{(i)} x_i}{\sum_i \sum_n v_n^{(i)} x_i} \quad (2.28g)$$

i = 1, 2, 3,, NC.

m, n = 1, 2, 3,, all groups in the mixture.

The group interaction parameter ψ_{mn} is temperature dependent as:

$$\psi_{mn} = \exp \left\{ - \left(\frac{a_{mn} + b_{mn} T + c_{mn} T^2}{T} \right) \right\} \quad (2.28h)$$

ψ_{mn} is temperature dependent parameter between groups m and n , which gives better description of real behavior of liquid mixtures. The values of R_k , Q_k , a_{mn} , b_{mn} , c_{mn} are given in the Table A.1. taken from Gmehling (1993).

2.8 Estimation of hydrodynamic properties

There are two types of holdup in liquid-liquid extraction column – *static holdup* (coalesced layer on the plate or beneath it) and *operational holdup* (drops moving in the continuous phase). Static holdup, h_s is combination of three terms Laddha(1976).

$$h_s = h_\gamma + h_N + h_c \quad (2.29)$$

h_γ , the head required to overcome interfacial tension effects

h_N , the head required to overcome friction through perforations

h_c , the head required to overcome the effects of flow of continuous phase.

The correlations for these three terms are taken from Laddha (1976):

$$h_\gamma = \frac{0.01\gamma\mu_d^{0.4}\mu_c^{0.2}}{\Delta\rho(d_N)^4} \quad (2.29a)$$

$$h_N = \frac{U_N^2[1 - (\frac{S_u}{S_i})^2]\rho_d}{2g_c C_v^2 \Delta\rho} \quad (2.29b)$$

$$C_v = 1 - \frac{0.71}{\log N_{Re}} \quad (2.29c)$$

$$h_c = 4.5\left(\frac{u_c^2 \rho_c}{2g_c \Delta\rho}\right) \quad (2.29d)$$

The other hydrodynamic variables are jet velocity, jet diameter, characteristic velocity, mean drop diameter, etc. These variables depend on the physical properties as well as column specification, like nozzle diameter. Physical properties of the system change on stages, which results in change of these variables. In non-isothermal operation, these changes are significant than that in isothermal operation.

Jet velocity U_N is given as:

$$U_N = 2.69 \left(\frac{d_J}{d_N} \right)^2 \left[\frac{\gamma/d_J}{0.5137\rho_d + 0.4719\rho_c} \right]^{1/2} \quad (2.30)$$

Jet diameter, d_J :

$$\text{for } \frac{d_N}{(\gamma/\Delta\rho g)^{0.5}} < 0.785; \quad \frac{d_N}{d_J} = 1 + 0.485 \left[\frac{d_N}{(\gamma/\Delta\rho g)^{0.5}} \right]^2 \quad (2.31a)$$

$$\text{for } \frac{d_N}{(\gamma/\Delta\rho g)^{0.5}} \geq 0.785; \quad \frac{d_N}{d_J} = 0.12 + \left[\frac{1.51d_N}{(\gamma/\Delta\rho g)^{0.5}} \right] \quad (2.31b)$$

Characteristic velocity u_r^*

$$u_r^* = 1.088 \left(\frac{U_n^2}{2gd_n} \right)^{-0.0818} \left(\frac{\gamma\Delta\rho g}{\rho_c^2} \right)^{1/4} \quad (2.32)$$

Mean drop diameter d_{32} :

$$d_{32} = 1.592 \left(\frac{U_n^2}{2gd_n} \right)^{-0.0665} \left(\frac{\gamma}{\Delta\rho g} \right)^{1/2} \quad (2.33)$$

Operational holdup is the volume of dispersed phase drops moving in the continuous phase during the operation of the column.

$$\text{Operational holdup, } \phi = \frac{\text{total holdup} - S_T \sum_{k=1}^{\text{no. of stages}} h_{sk}}{\text{total volume} - S_T \sum_{k=1}^{\text{no. of stages}} h_{sk}} \quad (2.34)$$

S_T = total area of cross-section of the column.

Total holdup is the sum of static holdup and operational holdup.

CHAPTER 3

MODEL DEVELOPMENT ON ASPEN PLUS & SPEEDUP

3.1 Modeling on ASPEN PLUS

Process simulation with ASPEN PLUS allows to predict the behavior of a process using basic engineering relationships such as mass and energy balances, phase equilibrium etc. ASPEN PLUS can simulate actual plant behavior giving reliable thermodynamic data and results. It also gives the facility to interactively change the specifications such as flowsheet configuration, operating conditions, and feed compositions to run new cases and analyze alternatives.

ASPEN PLUS is an advanced chemical engineering software package which offers rigorous models for steady state simulation of process varying from simple flash unit to complex processes like absorption, crude refining, electrolytic reaction, distillation, gas processing, pharmaceuticals, hydrometallurgy, rigorous multistage distillation, liquid-liquid extraction, liquid-solid separators etc. It can help to design better plants and increase profitability in existing plants, ASPEN PLUS User Guide Release 9, Vol. I (1996).

PROPERTIES PLUS is an in-built databank which provides specialized thermodynamic models and represents the non-ideal behavior of liquid phase components to get accurate results. ASPEN PLUS has an advanced graphical user interface (GUI) based model manager where the flowsheet of a process can be created. The various units put into the workspace and connected together through the process streams. For each of the units operations simple to highly rigorous models are available in the ASPEN PLUS model manager library.

In the liquid-liquid extraction process, the important units present are the main multi-stage extractor, feed units and the product units. Extractor is a 40-stage column, which consists of two feed streams and two product streams as shown in Fig. 3.1. The solvent stream (pure sulfolane) enters from the top of the column. The counting of the stages are done from the top to the bottom. The continuous phase (naphtha) enters at the bottom (40th stage) of the column. These streams are connected to the feed units, which provide the continuous flow rates of the streams at the specified rate and compositions. The heavy dispersed phase product (extract) comes out of the column at the last stage (bottom of the column) separating different components from the continuous naphtha phase, whereas the light continuous phase product (raffinate) emerges from the first stage (top of the column). These streams are counter-currently contacted on each of the stages for the separation of aromatics from the naphtha feed.

In the COMPONENT section all the components present in the feed streams are chosen from the list available in that section. The components are listed as unique numbers, their chemical formula and their names. It also provides to assign short names for component e. g. MCH for methyl cyclo-hexane, B for benzene etc.

All the graphical units are put together on the main workspace Fig. 3.1. Then the streams need to be completely specified. The top and the bottom feed streams are described as per the specifications given in Table 3.1. Here the units for measurements also need to be specified. ASPEN PLUS provides all types of units of measurements used in engineering like SI, FPS, MKS etc. The compositions of components in the feed streams, temperatures, pressure and flow rates are specified.

Extractor model needs the temperature and pressure specifications for the top and bottom stages. ASPEN PLUS extractor model runs on the equilibrium stage approach. It also gives the facility of specifying the component efficiencies varying from stage to stage. In

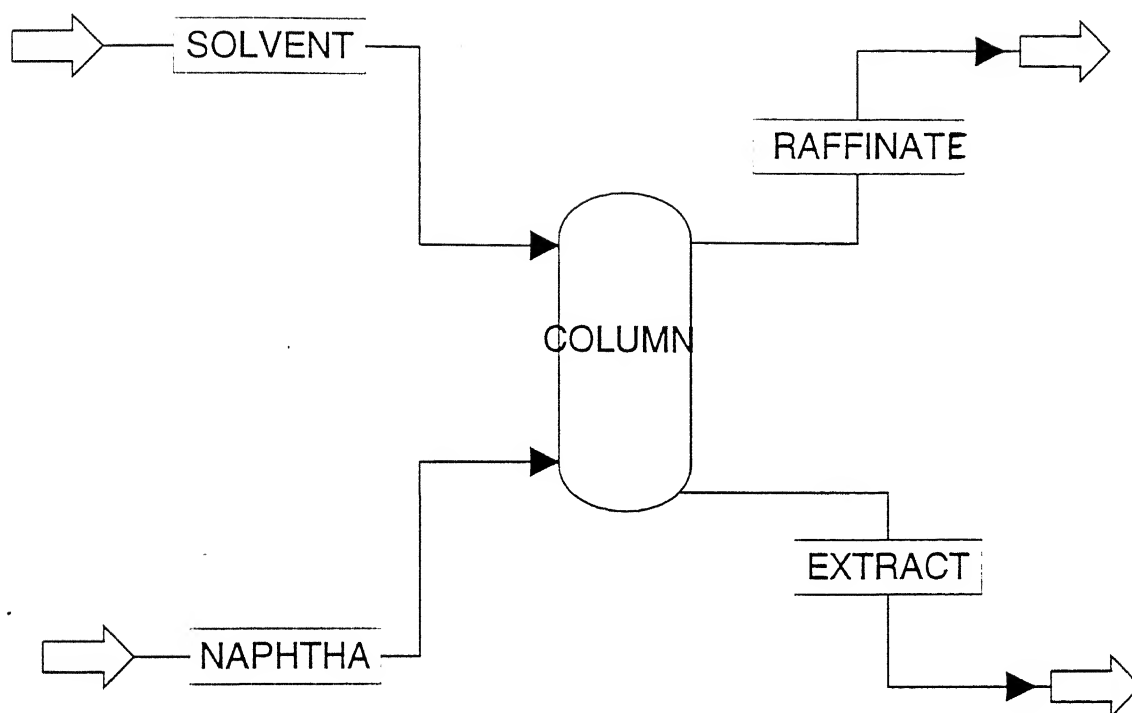


Fig. 3.1 Flow sheet of extraction column on ASPEN PLUS.

Table 3.1 Stream specifications

	Top feed (Solvent)	Bottom feed (Naphtha)
Temperature (°C)	105	75
Pressure (bar)	5.0	5.0
Flow rate (mol/s)	4.5	2.0
Composition (molefraction)		
N-Heptane	0.0	0.37
Methyl cyclo-hexane	0.0	0.37
Benzene	0.0	0.05
Toluene	0.0	0.16
O-xylene	0.0	0.05
Sulfolane	1.0	0.0

liquid-liquid extraction, it has been found that the separation efficiency varies for components on different stages. There are two liquid phases present in the liquid-liquid extraction. Hence it is also necessary to indicate the types of the streams for each of the feeds and products. The solvent feed and the bottom product should be of same types. The same is also true for the bottom feed and the top product. It also needs to mention the key components in each of the streams. In present case n-heptane and methyl cyclo-hexane are the main components in the continuous (raffinate) phase whereas sulfolane is that for the dispersed (extract) phase.

There is an optional section for assigning the temperature and pressure profiles along the column. It is not required in the present case because temperature and pressure specifications are not the constraints on the stages.

The physical property calculations for streams and components are necessary for simulation of the column. PROPERTIES PLUS provides a wide range of options for these calculations. The density, specific heat capacity, viscosity, interfacial tension, distribution coefficient etc are some of the physical and thermodynamic properties, which are needed to be estimated. ASPEN PLUS has the facility for EOS approach as well as the activity coefficient approach for thermodynamic calculations as given below.

1. BWR-LS (Benedict-Webb-Rubin)
2. LK-PLOCK (Lee-Kesler-Plocker)
3. PR (Peng-Robinson)
4. PR-BM (PR with Boston-Mathias alpha function)
5. PR-WS (PR with Wong-Sandler mixing rule)
6. PR-MHV2 (PR with modified Huron-Vidal mixing rule)
7. PSRK (Predictive Soave-Redlich-Kwong)
8. RKS-WS (Redlich-Kwong-Soave with Wong-Sandler mixing rule)
9. SRK-MHV2 (SRK with modified Huron-Vidal mixing rule)
10. RK-ASPEN
11. SRK-BM (SRK with Boston-Mathias alpha function)
12. SR-POLAR (Schwartzentruber-Renon)

Similarly activity coefficient methods available are:

1. NRTL
2. UNIFAC
3. Dortmund-modified UNIFAC
4. Lyngby-modified UNIFAC
5. UNIFAC for liquid-liquid systems (UNIF-LL)
6. UNIQUAC
7. van Laar
8. Wilson
9. Chao-Seader corresponding states model

The recommended option set for the liquid-liquid system is UNIF-LL Aspen Plus Properties Plus Reference Manual (1996); hence this option set has been used.

Once the problem specifications are complete, it is ready to run the simulation. The status of the flowsheet development is shown all the times in the status toolbar area of the main window. When the required inputs are complete, it indicates the completion of the flowsheet.

ASPEN PLUS runs the simulations in two ways:

1. Interactive.
2. Batch (background).

Interactive runs are easy to examine the simulation progress and the results, whereas the background simulation restricts it after the completion of the simulation. Batch simulations are useful for long

simulations or when it is required to run several simulations simultaneously. Any simulation can be stopped or paused during its progress by simply clicking the STOP or PAUSE button on the simulation control panel. It also displays the message regarding the progress of runs. Whenever the simulation is completed successfully, the status is displayed. The convergence status and the number of iterations of a run can be easily examined on the simulation control panel. The results can be displayed as the pre-specified fashion. The profiles for different variables may be plotted after the complete simulation.

3.2 Model development on SPEEDUP

SPEEDUP is a package designed to model processes as they occur in chemical or process engineering as a series of unit operation interconnected by process streams. The model may be any type of process that can be described in terms of algebraic and differential equations [SPEEDUP USER MANUAL](1997). It is an equation based flow-sheeting package. This means when the time come for solution problems are viewed as set of equations rather set of operations.

It can be used to perform dynamic modeling, optimization, parameter estimation, data reconciliation and steady state simulation using the same program input. Mathematical model for complex processes can be developed in a purpose-designed high level language.

In the present work, SPEEDUP is used for dynamic modeling of multi-stage unagitated sieve tray liquid-liquid extraction. The model is translated into SPEEDUP high level language. The required physical thermodynamic and transport properties are made available through PROPERTIES PLUS library databank. It needs a SAIRUN (Speedup Aspen Interface Run).

A problem description in SPEEDUP is composed of a number of input sections. Each input section describes a specific aspect of the problem. The sections for use depend upon the nature of the problem.

The sections needed for use are described in the Table 3.2 in the next page.

TABLE 3.2 Summary of sections in SPEEDUP

Input section Name	Used for
Flow-sheet, Unit	Describing the topology of a flow-sheet
Model	Model equations of equipment.
Macro	Connecting the various units
Operation	Providing specification and initial guess for variables involved
Options	Simulation options, like no. of iterations, tolerance, time, step etc.
Report, Profiles	Defining presentation of output.
Declare, Title	Specifying lower and upper bounds of variables, units of measurement and declaring stream variables and title of the model.

All the simulations require minimum of five sections.

1. Unit
2. Flow-sheet
3. Declare
4. Operation
5. Options

Other sections are optional.

There are three model sections used in the present liquid-liquid extraction problem: one each for top stage, bottom stage and intermediate stages. The FLOWSHEET section defines the source and destination for each stream. In the present model there are two feed streams (extract and raffinate). These streams are connected to the main column by declaring in this section.

UNIT section represents each unit in the FLOWSHEET. SPEEDUP assumes each stage of the column as a separate unit. Hence in a 40-stage column, there will be 40 units for all stages and 2 units for top and bottom feeds (total 42 units). Each unit has equations based on its nature, so every unit needs to be described in detail in MODEL section separately. Models can contain a wide variety

of relationships. Based on the objectives, only those relations are required to describe in SPEEDUP language, which are needed for the problem description.

In the present extractor there are 4 input streams (2 for each phase) including back-mixing effects and 4 output streams on each stage except at the 1st and the last stage, which include 3 inputs/outputs, as shown in the Fig. 2.1 and 2.2. The details of equations are given in Appendix (A). These equations are written in SPEEDUP codes. All the stream variables are type declared in TYPE sub-section in MODEL STAGE. Some fixed parameters like acceleration due to gravity, column diameter, inter-stage height, nozzle diameter, no. of holes, no. of components, value of π , etc are set in the SET sub-section.

All the 4 inputs and 4 outputs for a stage are specified in STREAM sub-section. Various stream variables for all these streams are defined here, like flow rate of dispersed and continuous phases, back-mixing flow rates, their compositions, etc. The main body of a MODEL section is the EQUATION sub-section. IN this sub-section all the equations are put together. They need not be in any particular order. The different equations put here are:

- Mass balance for dispersed phase (all components) MBD_k
- Mass balance for continuous phase (all components) MBC_k
- Energy balance for dispersed phase (EBD_k)
- Energy balance for continuous phase (EBC_k)
- Flow relations (VP_k, VM_k, UM_k, UP_k)
- Mass transfer relations at interface ($MBIC_k, MBID_k$)
- Energy transfer relations at interface ($EBIC_k, EBID_k$)
- Equilibrium relations (EQ_k for all components)
- Normalization equations (NDI_k, NCI_k, ND_k, NC_k)

Additionally, more equations are also included for operational holdup, effective volume of stage, characteristic velocity, interfacial area, drop diameter, jet diameter and velocity, mass transfer coefficients of

components in both phases, heat transfer coefficients for both phases, etc.

All the physical, thermodynamic and transport properties are calculated using in-built PROPERTIES PLUS library procedures in PROCEDURE sub-section. Here these procedures are declared as functions and the various required inputs for calculation are provided as in the FORTRAN programming. User-written functions for these calculations may also be put here instead of using library procedures.

In TITLE section a title for the problem may be given which should be a single line up to 80 characters.

The OPERATION section is used to provide specifications of different units. The following specifications are given in the SET sub-section for the feed units:

- Temperature
- Pressure
- Flow rate
- Compositions

It has a PRESET subsection, which is used to give individual initial guess for all the variables across the column. These values are taken from the simulator developed in C programming language separately. The lower and upper bounds for individual variables are specified here. In the INITIAL sub-section, all the derivatives are initialized to zero.

MACRO section helps to connect a number of UNITS, which have same MODEL description. In the present problem, STAGE_SVT, STAGE and STAGE_L are the three models for the first, intermediate and last stages. The 38 intermediate stages have the same model equations. MACRO section helps to interconnect these stages without writing separate MODEL sections for all the stages. The types of streams also needed to be specified here. In the present case, there are two types of streams: LIQUID1 (continuous or raffinate) and LIQUID2 (dispersed or extract).

OPTIONS section is used to specify the solution routines and other execution related parameters. The available routines for ROUTINE sub-section are NEWTON, FASTNEWTON and HYBRID for steady state and initialization runs and DAE, SUPERDAE, EULER and RK4 for dynamic simulation. EXECUTION sub-section provides the facility to assign various types of tolerances (absolute, relative, etc), convergence test, number of iterations required, size of time-step, target of result display (terminal or file), debugging facility, etc. All of these parameters have in-built default values. If one wants to use different values, then needs to specify in this sub-section; otherwise it needs not be written in the SPEEDUP input program.

The DECLARE section is used to describe the starting values, lower and upper bounds for variables. All the variables, which are arrays or of same types may be given the same values together here. The units of measurement for variables are also specified in the TYPE sub-section. The streams LIQUID1 and LIQUID2 are also defined in this section. Each of streams carries information regarding flow rate, composition of each components, enthalpy, temperature, pressure, etc. The STREAM sub-section of DECLARE section defines the stream structure for the FLOWSHEET comprising:

- The number of components
- The component names
- The information to be carried by the streams (stream vectors)
- The thermodynamic options

No. of components (6 in the present case) and their names are mentioned in the COMPONENT sub-section. The thermodynamic property calculation options for streams needed to be specified (like various options of EOS, activity coefficient method, etc). The sample files for all these sections are given in Appendix (B)

The necessary property interfacing has to be done before the SPEEDUP steady state or dynamic run. PROPERTIES PLUS is interfaced to SPEEDUP through speedup aspen interface run (SAIRUN). SAIRUN must be done before entering into SPEEDUP

executive environment. Once all this is done, the problem description is complete and the simulation can be carried out either in steady state or dynamic mode. Steady state or initialization run initializes the dynamic model. Once the dynamic model has been initialized, one can study the behavior of the system for a change in any process variable by giving a disturbance, say a step change in the value of that variable in the desired direction.

SPEEDUP executive provides a DIAGNOSE facility. It is a very efficient and useful sub-environment for determining the cause of failure to converge the solution. It provides information regarding the equations that were having the maximum residue in the last iteration. This also informs the values of variables for last iteration and which variables are on their lower or upper bounds. The unconverged variables are shown flagged with a * (star) mark. This helps to find out those equations causing converge failure and hence the necessary corrective measures can be taken.

The SPEEDUP executive environment is used to run a simulation problem. It needs the problem, to be put in its database. Various commands are given here. e. g.

- new llx (Here llx.spe is the input file name).
- store llx (The problem is stored in database containing all the sections).
- ss run (for steady state simulation).
- ini run (for initialization run).
- dyn run (for dynamic simulation).

If any error occurs during translation and execution, then it gives the information. The details may be get by giving “errors” command. The various steps during translation and solution are also displayed on the terminal. SPEEDUP decomposes the whole problem into small BLOCKS are solved one by one. Once the simulation is successfully complete, the results may be examined by going into PLOT or RESULT sub-environment.

CHAPTER 4

RESULTS AND DISCUSSION

The model described in the previous chapters may be used to simulate any types of extractor. The empirical co-relations will be different. Here this simulator has been used to investigate the results for aromatic extraction from naphtha feed using pure sulfolane as the solvent. The column and system specifications are listed in Tables 4.1 and 4.2. This is a 40 stage unagitated sieve tray extractor with 30 cm column diameter and 10 cm inter-stage height. The solvent (heavy dispersed phase) is fed from the top of the column whereas the naphtha feed (light continuous phase) is introduced at the bottom stage.

The simulator consists of 20 files written in C programming language developed by Rajeev Kumar (1996) for the isothermal operation and later modified by Phalguni Banerjee (1997) for non - isothermal operation. Previously original UNIFAC model was being used for thermodynamic property calculations and it was found that the results were not satisfactory. Now modified UNIFAC model by Gmehling (1993) has been used in this simulator. All the physical, transport and thermodynamic property functions have been made temperature and composition dependent. All the three previous workers had taken drop size constant. This is not justified because the drop size of the dispersed phase depends on the system physical properties, which vary as compositions, temperature and pressure change on different stages. The drop size function has been implemented as per the correlation available in Laddha (1976). As the drop size changes on different stages, the interfacial area between the dispersed and continuous phases will also vary for heat and mass transfer.

The non-isothermal model consists of 39 independent variables per stage. Bulk composition of six components in dispersed and continuous phases (6 + 6 variables), interfacial composition at the interface on both phase sides (6 + 6 variables), mass transfer rates for all the components (6 variables), forward and backward molar flow rate of both phases (4 variables), operational holdup of dispersed phase and superficial velocity of continuous phase (2 variables), temperatures of bulk dispersed phase, bulk continuous phase and interface (3 variables) are the 39 independent variables on a stage. Hence there are 1560 variables for the 40 stages of the column. The details of independent equations and variables are listed in the Appendix (A).

The simulator was run for five temperature difference across the column. The details of operating conditions are given in Table 4.3. The first run was taken isothermally at 90 °C. Other runs at temperature difference of 10, 20, 30 and 40 °C were taken. In other words there is a gradual increase of 5 °C in solvent feed temperature and decrease of 5 °C in naphtha feed temperature.

Table 4.1 Column specifications

Description	Value
Column diameter (m)	0.30
Tray spacing (m)	0.10
No. of stages	40
Nozzle diameter (mm)	3.175
Pitch (cm) and type	1.0, triangular
No. of holes per plate	384

Table 4.2 System specifications

Description	Value
No. of components	6
Molecular weight of each component	100.2, 98.18, 78.11, 92.13, 106.16, 120.00
Association parameter for each component (for Wilke-Chang correlation for diffusivity calculations)	1.0, 1.0, 1.0, 1.0, 1.0, 1.0

- The components are n-Heptane(1), Methyl cyclo-hexane(2), Benzene(3), Toluene(4), o-Xylene(5) and Sulfolane(6).

Table 4.3 Operating conditions

Description	Value
Operating pressure (bar)	5.0
Feed flow rate of naphtha (mol/s)	2.0
Composition (mole-fraction)	0.37, 0.37, 0.05, 0.16, 0.05, 0.0
Temperature of naphtha feed (°C)	• 90.0
Feed flow rate of sulfolane (mol/s)	4.5
Composition (mole-fraction)	0.0, 0.0, 0.0, 0.0, 0.0, 1.0
Temperature of solvent feed (°C)	• 90.0

- This is the temperature for isothermal run. Other temperatures are 85, 80, 75, 70 °C for naphtha and 95, 100, 105, 110 °C for sulfolane respectively.

4.1 Computation time

The simulator has been tested on UNIX machines DEC 2000 α XP and HP9000/850 platforms. UNIX has a *prof* command to get the information regarding number of calls of functions, CPU time for various functions and percentage CPU time taken by a function. Recently (Mukesh Kumar, 1998) one iteration for steady state simulation had been taking approximately 30 minutes of CPU time for isothermal conditions. For the desired convergence when the number of iterations increases the CPU time also increases proportionately. The functions for dispersed phase density, continuous phase density, interfacial tension, drop diameter, jet diameter, jet velocity, average molecular weight and viscosity of both phases were called several million times for any iteration. These functions had been taking more than 94% of CPU time for calculations as shown in Table 4.4: This not acceptable as these days more emphasis is being given on quick and accurate calculations using less CPU time.

Initially we thought that perhaps the inefficient and inadequate use of pointers (and pointers to pointers) in C program is the main factor behind high CPU time. However it is simply resolved by declaring some of these functions as arrays of stages and calculated only once for any iteration. The values are stored as the arrays. On next procedure the functions are not called, instead the values stored

in these arrays are accessed for use in equations. In the first attempt the density calculation functions were made arrays and the execution time was reduced from 30 minutes to 8.5 minutes. Further average molecular weight, interfacial tension, jet diameter, jet velocity, drop diameter and viscosity of both phases were modified as arrays. It has been found that the CPU time greatly reduced and it is now taking about 1 minute for single iteration. This has reduced the CPU time by a factor of 40. Additionally relative tolerance has been changed from 10^{-9} to 10^{-7} and the accuracy for golden section search method has been changed from 0.001 to 0.005. The results have been found to converge in lesser number of iterations as compared to the previous observations.

Table 4.4 Percentage CPU time taken by some of functions

Functions	Before modifications	After modifications
Avg. mol. weight	39.09 %	≈0.00 %
Continuous phase density	26.07 %	0.01 %
Dispersed phase density	18.19 %	0.01 %
Interfacial tension	10.88 %	0.01 %

One can use *prof* command as:

- (i) `pixie simul.` (Here `simul` is the executable file generated after the compilation).
- (ii) `simul.pixie.` (This is the alternative of executing the program. Without `prof`, only `simul` is needed to run program).
- (iii) `prof -pixie simul simul.Addrs simul.Counts >[name of file to store the profile of percentage CPU time for all the functions].`

4.2 Validation of results with ASPEN PLUS at 30 °C temperature difference

In the absence of any running plant data, the simulator's results were compared with that from ASPEN PLUS results. ASPEN PLUS utilizes thermodynamic equilibrium stage approach whereas our simulator utilizes a rate-based approach to mass transfer between the

two phases. Hence, stage efficiencies for all the six components have been introduced for feasible comparison of results. The stage efficiencies at end points for all six the components are given in Table 4.5. It is very difficult to compare and present all the results of both simulations for all operating conditions due to the reason that ASPEN PLUS runs on PC DOS and our simulator on the UNIX operating system. The simulated results at 30 °C temperature difference on ASPEN PLUS and this simulator are compared and presented here.

Table 4.5 Stage efficiency of components (%)

Stage no.	n-heptane	MCH	Benzene	Toluene	o-Xylene	Sulfolane
1	20.2	19.6	51.55	51.0	54.5	63.5
40	20.4	19.8	53.28	51.33	49.2	66.67

Bulk composition profile of non-aromatics (n-Heptane and Methyl cyclo-hexane) Fig. 4.1 - 4.4:

These figures show the bulk composition of n-heptane and methyl cyclo-hexane (non-aromatics) in the extract and raffinate streams. The composition profiles for these components are exactly matching in raffinate phase at the tabulated efficiencies, Fig. 4.2 and 4.4. Naphtha enters with 37% n-heptane and MCH each. It is found that the raffinate stream exits at 45.7% n-heptane and 45.36% MCH in ASPEN PLUS run and 43.82% and 43.79% respectively for this simulator. These are in good accordance. Extract stream contains 0.15% and 0.25% respectively in case of ASPEN PLUS and 0.0218% n-heptane and 0.152% MCH in case of the simulator. In ASPEN PLUS run these values are slightly higher.

Bulk composition profile of BTX (aromatics) Fig. 4.5 - 4.10:

The main objective behind this extraction is the recovery of aromatics from naphtha using sulfolane as solvent. It is desirable for raffinate to contain amounts of aromatics as small as possible. The

benzene composition in the outgoing extract stream is found to be matching for ASPEN PLUS and the simulated results. The composition of benzene in the outgoing raffinate streams match nearly in both ASPEN PLUS and simulated results at stage 1, Fig. 4.6. Compositions are 1.85% and 1.90% respectively for extract leaving 40th stage and 0.75% and 0.84% for raffinate leaving 1st respectively.

In case of toluene composition in extract and profiles are matching between stages 25 to 40. The extract contains same composition of toluene for the simulations (5.30%). There is slight difference in raffinate profile of toluene in both the simulations.

O-xylene composition in extract are 1.48% (simulator) and 1.37% (ASPEN PLUS), Fig. 4.9 whereas it is 3.42% (simulator) and 2.96% (ASPEN PLUS) in raffinate, Fig. 4.10.

The recovery of aromatics for ASPEN PLUS and simulator is given in table 4.6.

Table 4.6 Percentage recovery of aromatics from naphtha

	ASPEN PLUS	SIMULATOR
Benzene	90.65%	86.15%
Toluene	70.39%	67.43%
Xylene	59.45%	69.93%

Bulk composition profile of sulfolane Fig. 4.11 & 4.12:

Sulfolane is one of the most widely used solvent for aromatic extraction and also very costly. Hence it is desirable that raffinate should contain negligible amount of sulfolane. The extract stream contains 89.75% (simulator) and 91.4% (ASPEN PLUS). In case of raffinate, simulator reports 0.2% whereas ASPEN PLUS results show 1.4% of sulfolane, Fig.4.12.

The average relative absolute difference of the present simulated results with respect to the ASPEN PLUS results are given for all the components in Table 4.7 in the next page.

Table 4.7 Average relative absolute difference

Components	Extract	Raffinate
n-Heptane	6.235 %	0.0094%
MCH	7.475 %	0.0091%
Benzene	2.272 %	0.964 %
Toluene	1.246 %	1.672 %
Xylene	5.438 %	1.539 %
Sulfolane	0.274 %	13.25 %

Profile of mass density Fig 4.13 & 4.14:

Figures 4.13 and 4.14 show the profile of mixture mass density of dispersed (extract) phase and continuous (raffinate) phase respectively. The simulator shows that the dispersed phase density remains almost constant along the stages. It contains heavier sulfolane in large amount and when it travels down the column its composition decreases. Hence its density should decrease but there is also decrease in temperature down the column, so its density remains fairly constant. It slightly decreases between stages 37 and 40. The dispersed phase density at first stage is 1179.9 kg/m³ (simulator) and 1179.73 kg/m³ (ASPEN PLUS). The density reported by ASPEN PLUS is slightly higher than that by the simulator.

The continuous phase density values are different at the first stage and this difference decreases up to 27th stage. After that ASPEN PLUS reports higher values than that by the simulator. The simulator shows the variation from 689 kg/m³ at stage 1 to 706.3 kg/m³ at 40th stage. ASPEN PLUS reports 661.5 and 717 (kg/m³) respectively. Hankinson & Thomson method has been used in the simulator whereas ASPEN PLUS uses Rackett's method. The difference may exist due different methods. The average relative absolute difference for the simulated results from ASPEN PLUS for dispersed phase density is 0.13 % whereas it is 4.131 % for continuous phase density.

Temperature profile Fig. 4.15:

Figure 4.15 shows the variation of temperature along the stages. In the non isothermal model of the simulator there are three temperatures for bulk dispersed, interface and bulk continuous phase have been used whereas ASPEN PLUS assumes thermal equilibrium on stage (i.e. the temperatures of both the phases are same on a stage). The simulator reports the temperature difference between bulk dispersed and continuous phases less than 0.9 °C at all the stages. The bulk temperature of dispersed phase is higher by 0.48 - 0.55 °C than the interface temperature whereas bulk temperature of continuous is found to be 0.40 - 0.45 °C lower than interface temperature. The temperature profile reported by ASPEN PLUS matches very well with the interface temperature by the simulator as shown in the figure. Both the simulators show the linear variation of temperature along the stages. Hence imposition of an average linear temperature profile in the simulator may be a good substitute for detailed energy balance.

Molar flow rate of extract Fig. 4.16:

The molar flow rate of dispersed phase is shown in Fig. 4.16. The value is higher by ASPEN PLUS compared to that by the simulator. It changes from 4.5 (mol/s) at entry to 4.8118 (mol/s) at the exit (40th stage). It may be possible because of backmixing in the continuous phase has been considered in the simulator. The average relative absolute difference for extract flow rate is 1.9 %.

In the above comparison between the two simulated results there exists difference and they may not match with each other, but it gives a good insight of the extraction process.

4.3 Results at various temperature differences across the column

The simulator has been run at five temperature differences across the column, keeping the average temperature at 90 °C. The first simulation has been taken isothermally at 90 °C. The successive simulations have been taken by increasing the solvent feed temperature by 5 °C and decreasing the naphtha feed temperature by 5 °C. The results are shown in the forthcoming figures 4.17 onwards.

Bulk composition profile of n-heptane and MCH Fig. 4.17 – 4.20:

The composition profiles of these components in extract and raffinate are shown in Fig. 4.17 – 4.20. In Fig. 4.17 and 4.19, it is found that the compositions of non-aromatic components decrease in the extract stream with the increase in temperature difference across the column. The extract contains 0.0248% n-heptane and 0.169% MCH at the 40th at isothermal condition whereas they decreased to 0.0212% and 0.149% respectively at 40 °C temperature difference. Decrease of 13.5 % in mole fraction of non-aromatics in extract has been found for 40 °C temperature difference compared to isothermal operation. It results in purer extract, which can increase savings insolvent recovery by distillation. Here this is the advantage of operating the column at higher temperature. The concentration profiles of these components in raffinate are shown Fig. 4.18 and 4.20 respectively. There is only slight variation for various temperature differences. The raffinate at higher temperature difference shows about 0.7 % decrease in mole fraction of non-aromatics compared to isothermal conditions. This decrease is negligible than the decrease in extract.

Bulk composition profile of BTX (aromatics) Fig 4.21 – 4.26:

Figures 4.21 and 4.22 show the composition profile of benzene at various temperature differences. They show a unique feature of this component. There is no affect of temperature-change on benzene as found in the graph. All the curves coincide for all temperature differences. There is slight difference at starting stages in both the phases. But these values are exactly similar at 40th stage.

The profiles for toluene and o-xylene are shown in Fig. 4.23 – 4.26. The behavior is slightly different as compared to that of benzene. Toluene and xylene have higher values, at higher temperature difference in both the extract and raffinate, but at the last stage they are same for toluene. Xylene shows a slight decrease at exit point with increase in temperature difference.

Bulk composition profile of sulfolane Fig. 4.27 & 4.28:

Sulfolane shows lower value in extract at higher temperature difference after 35th stage. After that it matches and exits at slight higher value at 40th stage at higher temperature difference, Fig. 4.27. Its composition in raffinate has higher value at higher temperature difference. Since sulfolane is a costly solvent, its value should be low in raffinate. Hence it is found that operating at higher temperature difference is not advantageous, because loss of solvent is increased.

Density of mixtures & density difference Fig. 4.29 – 4.31

Figures 4.29 and 4.30 show the density of dispersed and continuous phases respectively at different stages. The density of dispersed phase continuously decreases as it travels down the column at isothermal condition. This results in decrease in the density difference between the phases, Fig. 4.31. It has been found that the dispersed phase density remains almost constant at 1180 kg/m³ up to 35 stages at 30 °C temperature difference. The continuous phase density change is shown in Fig. 4.30. Its value increases with increasing temperature difference. It is desirable to maintain the

density difference at fairly constant and higher value for better hydrodynamic characteristics of extraction column, Treybal (1981). Hence the isothermal operation does not fulfill this requirement. The density difference at various temperature differences has been shown in Fig. 4.31. Its profile is hydrodynamically favorable at higher temperature difference. At 40 °C temperature difference it remains fairly stable; perhaps at 45 °C temperature difference it will reach an optimal density difference.

Interfacial tension Fig. 4.32:

The figure shows the interfacial tension profile between the drops and the continuous phase. This value decreases down the stages at isothermal condition. Higher value of interfacial tension results in more drop coalescence which decreases the available interfacial area for mass and heat transfer resulting in lower value of extraction capacity for the column. At 20 °C temperature difference the interfacial tension remains fairly constant as shown in the figure. With increase in temperature difference up to 40 °C across the column it increases up to 32 stages after that it starts decreasing.

Interfacial composition of components Fig 4.33 – 4.44:

The compositions of components at the interface are in equilibrium for both the phases. The compositions of non-aromatics increase at the dispersed phase side interface as we move down the column at isothermal operation, which is reversed in continuous phase side interface. In the dispersed phase interface, the increase in composition of non-aromatics is governed by increasing the temperature difference across the column, Fig. 4.33 and 4.35. Continuous phase side interface shows slight variation for non-aromatics as we go up the column, Fig. 4.34 and 4.36. This results in decrease in driving force for mass transfer of non-aromatics because composition in dispersed phase side increases whereas it decreases in continuous phase side with increasing temperature difference. The

benzene composition at the interface is found to be almost independent of temperature difference (Fig. 4.37 and 4.38) as in the bulk composition profile. There is no effect of non-isothermal operation on benzene composition. This behavior is not found in case of toluene, xylene and sulfolane, Fig. 4.39 – 4.44. These show same behavior at the interface as in the bulk composition. Sulfolane composition at the continuous phase side interface shows a flat profile at 40 °C temperature difference.

The distribution coefficient range for all the components for various runs is given in Table 4.8

Table 4.8 Distribution coefficient range for all runs

Comp.	00°C	10 °C	20 °C	30 °C	40 °C
n-Heptane	0.0004 – 0.000652	0.000413 – 0.00064	0.00032 – 0.000612	0.000452 – 0.000588	0.000471 – 0.000565
MCH	0.00306 – 0.0045	0.00318 – 0.004366	0.0033 – 0.00424	0.00343 – 0.00408	0.003551 – 0.00394
Benzene	0.627 – 0.6316	0.6276 – 0.6338	0.6263 – 0.6354	0.6246 – 0.6369	0.62284 – 0.6383
Toluene	0.418 – 0.4295	0.4194 – 0.4295	0.4196 – 0.4285	0.4199 – 0.4275	0.4202 – 0.4266
o-Xylene	0.2775 – 0.292	0.2794 – 0.291	0.2809 – 0.2889	0.282 – 0.287	0.2817 – 0.285
Sulfolane	267.73 – 570.45	281.37 – 539.66	295.5 – 504.03	310.75 – 471.47	327.01 – 441.7

Temperature profiles of bulk dispersed and continuous phases:

Figure 4.45 shows the temperature of the bulk dispersed phase for different runs. It shows the linear variation along the stages. The 20th stage is found to be at the same temperature (363.5 °K) for all the temperature differences across the column. Similar linear variation has been observed in case of continuous phase bulk temperature. Here also the temperature at 20th stage is same (362.7 °K) for all the runs Fig 4.46.

Interphase mass transfer rate of components Fig. 4.47 – 4.52:

The interface between the drops and continuous phase provides the media for mass and heat transfer between the phases. The variation in the mass transfer rate is very important. All the

components show different nature for interphase mass transfer rate. n-heptane and MCH show the same nature; their rates sharply decrease up to 5th, then they remain almost constant at this low value up to 28th stage; after which these rates again start increasing (Fig. 4.47 and 4.48). The interphase mass transfer rates from continuous to dispersed phase for non-aromatics decrease at higher temperature difference, this being favorable for aromatic extraction. At 40 °C temperature difference mass transfer rate of n-heptane reaches approximately zero between 14 and 26 stages.

Benzene mass transfer rate is again found to be unique compared to other components. It is not affected by the temperature variation. This is major cause of same composition of benzene in the bulk dispersed, continuous phases and at the interfaces on a stage at all the temperature differences as observed previously. The extraction of benzene up to 15th stage after that its mass transfer rate sharply increases to 0.0158 mol/s at the 40th Fig. 4.49. Benzene is mainly extracted between 25 to 40 stages.

Toluene shows the variation in the interphase mass transfer rates along the column. It sharply decreases up to 4th stage for all runs Fig. 4.50. Its value remains higher at higher temperature difference up to 19th stage, after that the rate at higher temperature difference is found to be less than the isothermal operation.

Xylene shows the opposite nature compared to benzene. Its mass transfer rate is highest at the first stage. It steeply decrease up to 10th stage then remains fairly constant up to 40th stage, Fig. 4.51. It is found that the extraction of o-xylene mainly takes place between the first and 15th stage. The transfer rate at higher temperature difference remains higher than the isothermal operation till the end of the column. It means its extraction is favorable at higher temperature difference.

Interphase mass transfer rate for sulfolane is nearly zero up to 35 stages and after that it is negative up to the last stage, Fig. 4.52. It means sulfolane is transferred from dispersed to continuous phase

between 35 and 40th stages. It is disadvantageous, as most of sulfolane should be present in the dispersed phase.

The percentage recovery of aromatics for all the runs is given in Table 4.9

Table 4.9 Percentage recovery of aromatics

Temp diff (°C)	Benzene	Toluene	Xylene
00	85.639	67.775	65.301
10	85.810	67.425	66.814
20	85.981	66.787	68.405
30	86.147	66.128	69.929
40	86.263	65.474	71.117

Hydrodynamic variables Fig. 4.53 – 4.62:

Figure 4.53 shows the variation of velocity of dispersed phase for all the runs. The *dispersed phase velocity* increases as it goes from top to down of the column, because the molar flow rate increases after recovering components from naphtha. Dispersed phase velocity is higher at higher temperature difference up to 23rd stage after that it is lower than the isothermal and lower temperature differences.

Same behavior has been observed for the *continuous phase velocity* (Fig. 4.54). It decreases as it goes from the bottom stage to top of the column because it loses moles of components to the dispersed phase resulting in the decrease of molar flow rate.

Fig. 4.55 and 4.56 show the profiles of *drop diameter* and *interfacial area*. The drop size slightly changes from stage 1 to stage 40 for isothermal operation. This change increases as the temperature difference increases as found in the figure. Lower size of drops provides more interfacial area. At isothermal conditions the drop diameter varies between 3.106 to 3.114 mm from top to bottom of column, whereas it ranges from 3.065 to 3.156 mm for 40 °C temperature difference across the column. The drop size depends on jet velocity, interfacial tension, density difference and nozzle diameter. Except nozzle diameter, all other variables change from stage to stage.

126233

The change in interfacial area is very fast for isothermal operation. As the temperature difference is increased, the interfacial area remains fairly constant on stages, Fig. 4.56. Overall there is an increase in interfacial area for higher temperature difference.

Fig. 4.57 shows the variation of interface temperature at various stages and it also shows linear variation as that by the bulk temperatures.

Fig. 4.58 shows the *static holdup* of dispersed phase on stages. At isothermal conditions, it varies from 14.5 % at 1st stage to 14.72 % at the last stage. It ranges from 14.25 % to 15.05 % for 40 °C temperature difference. At higher temperature on a stage, static holdup remains low and it increases as the temperature decreases.

The *operational holdup* profile is shown in Fig. 4.59. It is very important to maintain higher operational holdup for large interfacial area for mass transfer. It has been found that operational holdup is low at starting stages and increases fast in the last stages for isothermal operation, whereas non-isothermal operation results in increased operational holdup at initial stages and it is not so much higher in the last stages. An increase in overall operational holdup along the column has been found for higher temperature difference. It remains same at 23rd stage for all the runs. The operational holdup varies from 4.1 % to 4.695 % for isothermal and from 4.24 % to 4.58 % for 40 °C temperature difference.

The *total holdup* profile of dispersed phase is given in Fig. 4.60. It remains low at starting stages and gradually increases till the last stage because of increased molar flow rate of dispersed phase. It is varying from 18.59 % to 19.41 % for isothermal operation and 18.49 % to 19.63 % for 40 °C.

Fig. 4.61 and 4.62 show the molar *forward flow rate* of dispersed and continuous phases respectively. Forward flow rate of dispersed phase increases from top to bottom of the column. The variation is very low for all runs. The continuous phase flow rate suddenly jumps at 40th stage, gradually decreases up to 4th stage and

then it suddenly drops up to first stage. It is due to end effects. This effect is not observed in dispersed phase because axial mixing is negligible in the dispersed phase.

Fig. 4.63 shows the *flooding curves* at various operating conditions. Dispersed phase flooding velocity is plotted against continuous phase flooding velocity. The safe operating zone for extraction column is below the flooding curve. At flooding conditions ($u_{cf} = 5$ mm/s, $u_{df} = 16.5 - 17.0$ mm/s) the operational holdup has been found in the range of 19 – 22 %.

Energy transfer from dispersed to continuous phase Fig. 4.64:

The dispersed phase bulk temperature is higher than that of continuous phase throughout the column for all runs. Thus heat transfer takes place from dispersed to continuous phase. The variation in heat transfer rate is shown in Fig. 4.63. The amount of heat transfer across the interface is higher for higher temperatures and it decreases with decrease in temperature on stage. For 10 °C temperature difference it varies from 365 J/s at the first stage to 295.5 J/s at the last stage and 376.9 J/s to 306 J/s respectively for 40 °C temperature difference.

4.4 Execution of SPEEDUP model

The model described in chapter 3 and Appendix (B) has been processed sequentially through translation, compilation, linking and execution. Initially various translation errors have been found. Sulfolane was not included in the default list of 36 components, specifically provided for SPEEDUP. Hence it was included in the PROPERTIES PLUS input file (LLX.INP) and fresh SAIRUN was done. After this modification, it was found that the units were not properly connected with each other as per the MACRO text processor. A modified MACRO section had to be re-written to overcome this error.

Later in the PROCEDURE section (calls library routine for physical, thermodynamic and transport properties calculations)

arguments were not as per the specifications in the LIBRARY models. This section was modified accordingly. SPEEDUP is a versatile package and it has in-built degree of freedom analysis for a problem. When the number of unknown variables and independent equations did not match, "SPECIFY" sub-environment gave an illegal "STATUS" to the problem. This mismatch was overcome by putting normalization equations ($\sum x_i = 1.0$ etc.).

After the successful translation, the program did not run – though the compositions, mass transfer rates and distribution coefficients for components being very different in magnitude, it is not possible to give separate initial values for elements of array in DECLARE section (this is the limitation of this section). This problem could only be overcome by invoking PRESET subsection in the OPERATION section. In the PRESET subsection converged values from our simulator have been assigned. Separate lower and upper bounds were also specified for each of the variables.

After complete specifications and a legal STATUS, the problem translated successfully. SPEEDUP then generated 20 FORTRAN files, compiled and linked them before execution. At this stage, the problem is decomposed into blocks – the first two linear blocks (for overfeed and underfeed units) are solved and when it enters the third non-linear block (for extraction column), it gives "MEMORY PROTECTION FAULT" and the program abnormally terminates. Though PC version of SPEEDUP does not support a DEBUG facility, we have traced the problem to CALL SOL1 function (for further solution of equations) in SPEEDP.FOR file; the actual source of abnormal termination is still untraced.

After several attempts, we are unable to execute the program. Only two inputs/outputs (without backmixing effect) and equilibrium stage approach in place of rate-based mass transfer approach have been applied to simplify the program. It invariably gives the "MEMORY PROTECTION FAULT". The problem has been sent to New Delhi, Hong Kong and USA offices of Aspen Tech. Inc. in April. They are also

unable to resolve the situation till now. Currently, "Scaling" option is under detailed trial and investigation. Only after successful SS simulation and INI run can dynamic simulation (DYN RUN) be undertaken.

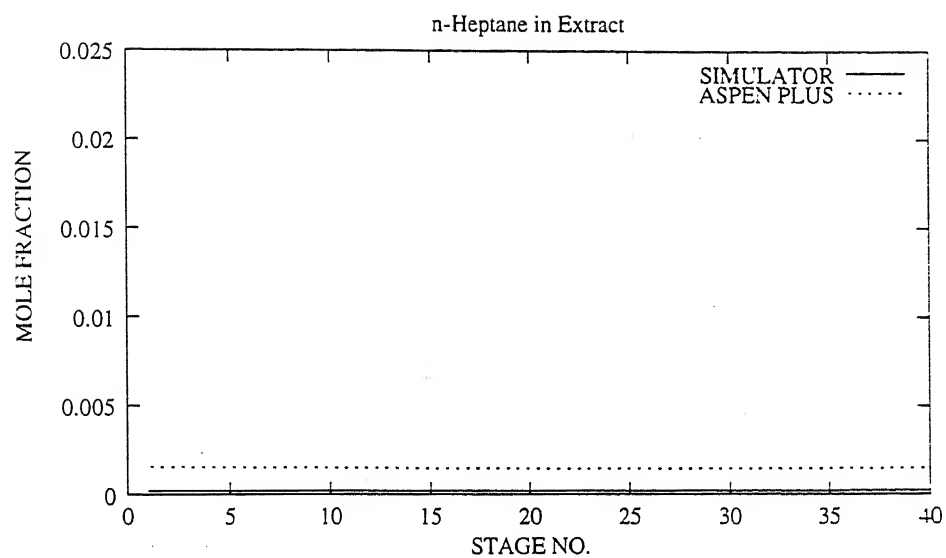


Fig. 4.1 Concentration of n-Heptane in Extract

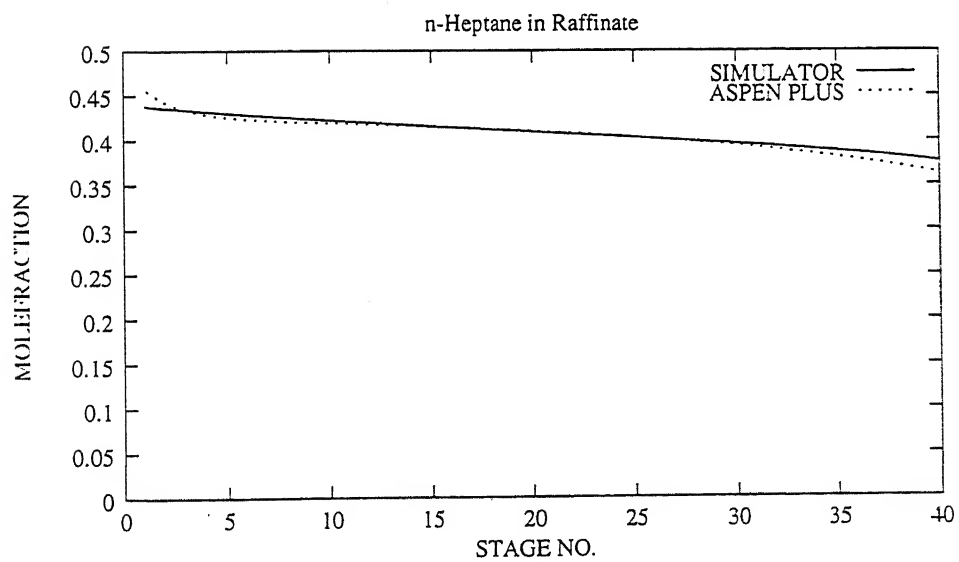


Fig. 4.2 Concentration of n-Heptane in Raffinate

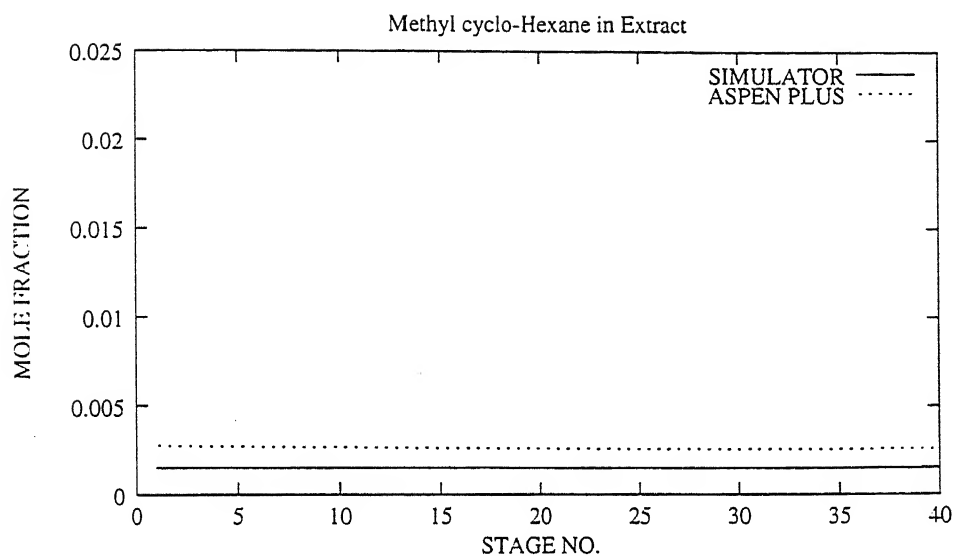


Fig. 4.3 Concentration of Methyl cyclo-Hexane in Extract

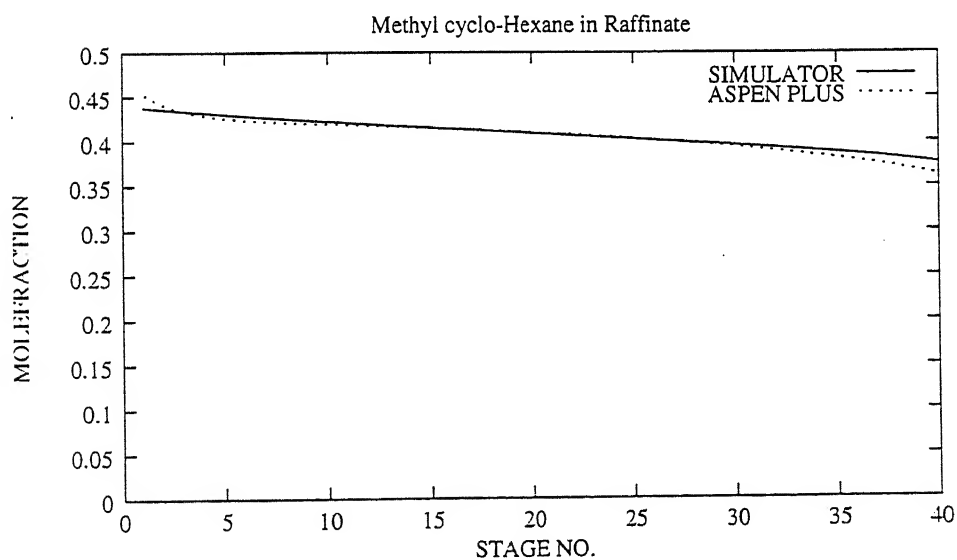


Fig. 4.4 Concentration of Methyl cyclo-Hexane in Raffinate

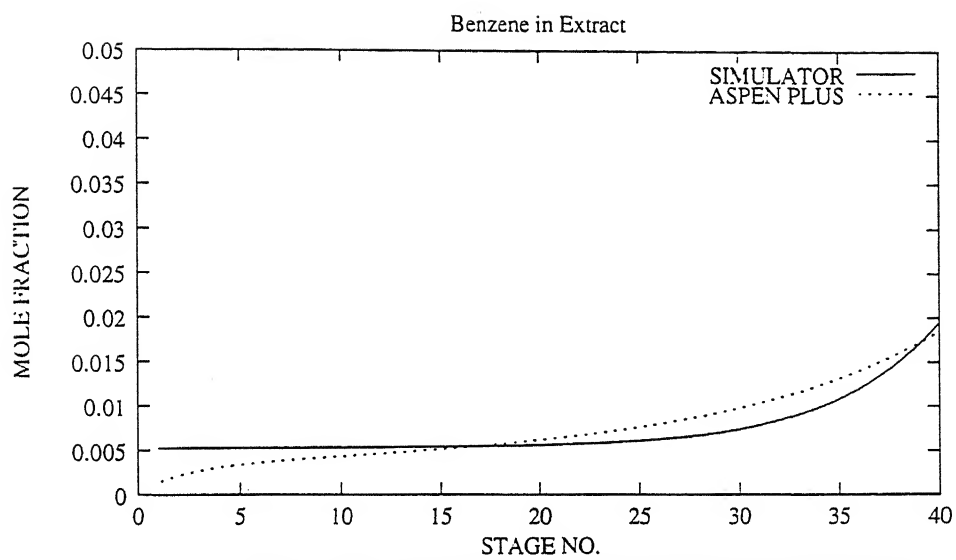


Fig. 4.5 Concentration of Benzene in Extract

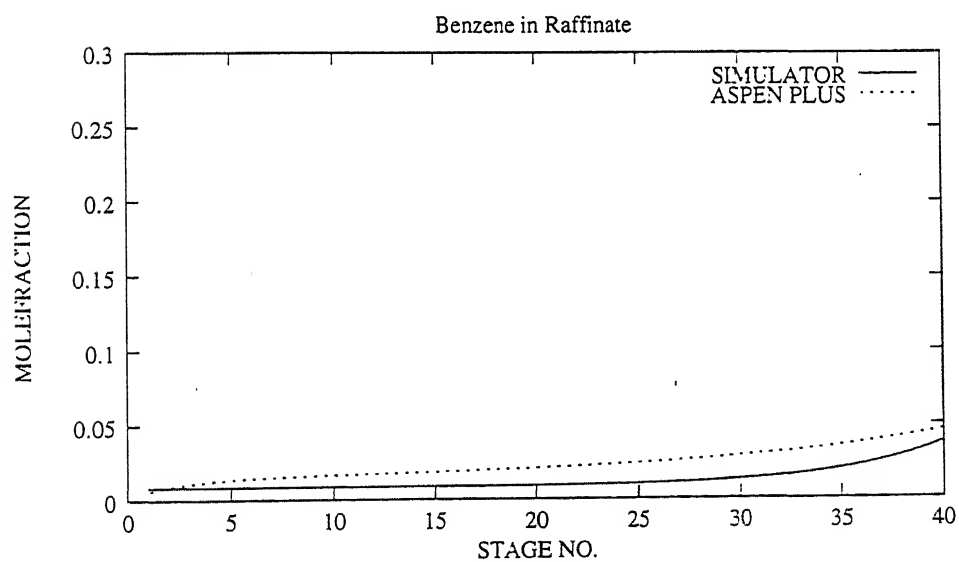


Fig. 4.6 Concentration of Benzene in Raffinate

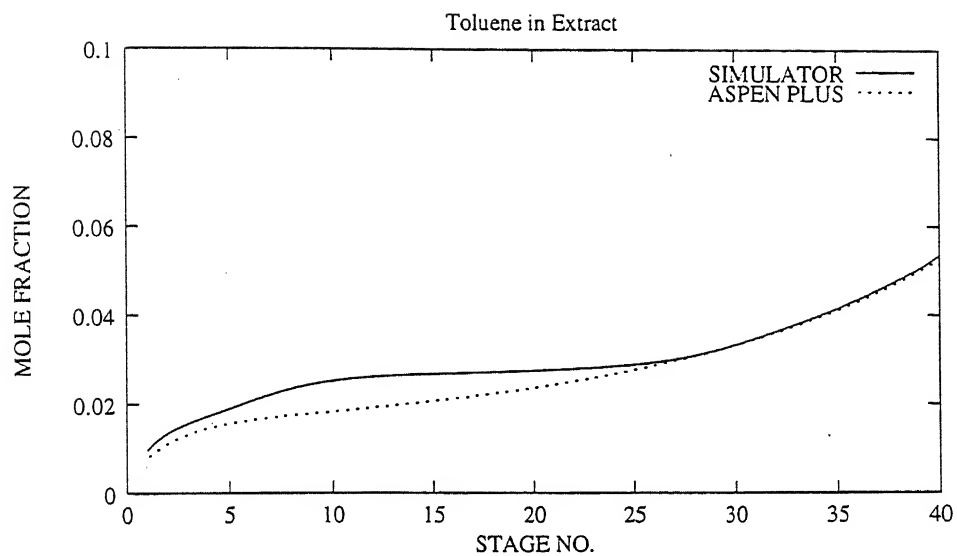


Fig. 4.7 Concentration of Toluene in Extract

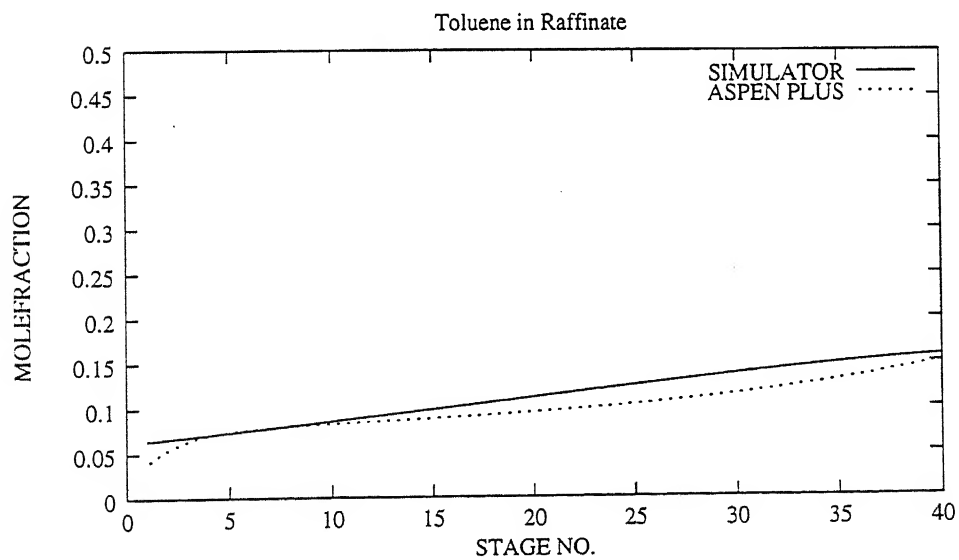


Fig. 4.8 Concentration of Toluene in Raffinate

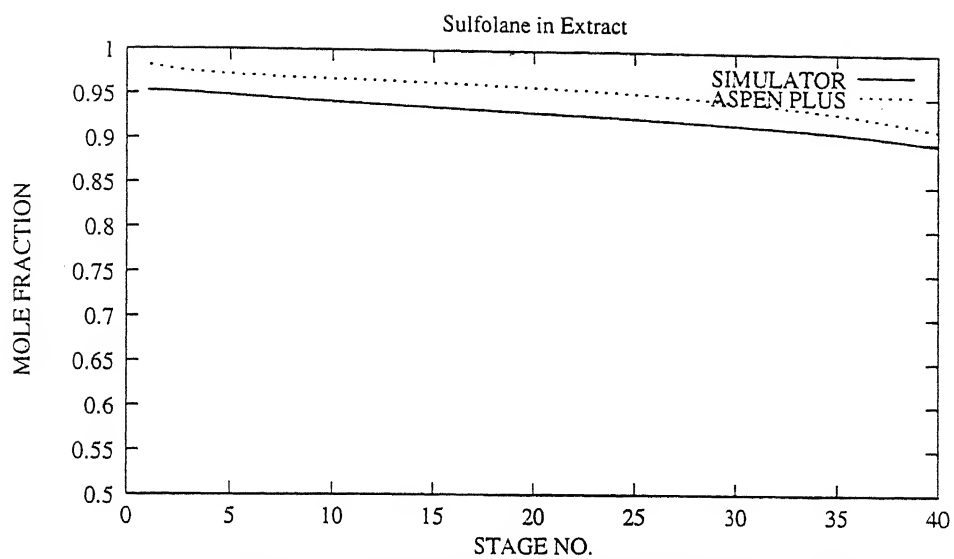


Fig. 4.11 Concentration of Sulfolane in Extract

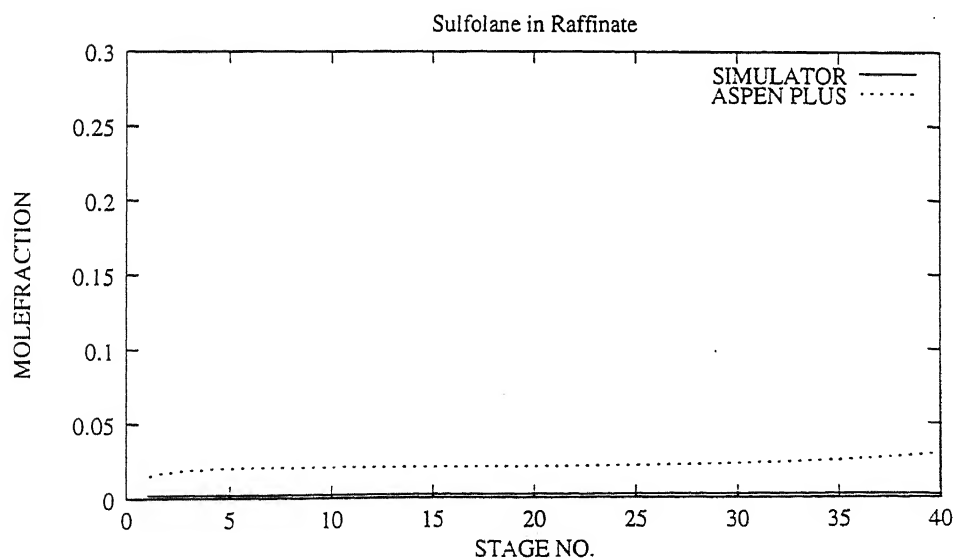


Fig. 4.12 Concentration of Sulfolane in Raffinate

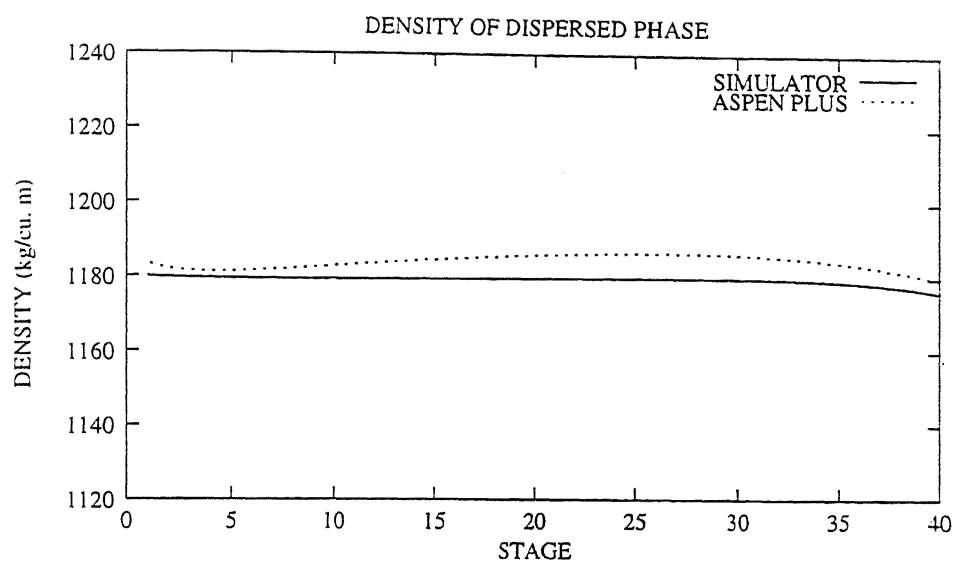


Fig. 4.13 Density of Dispersed Phase

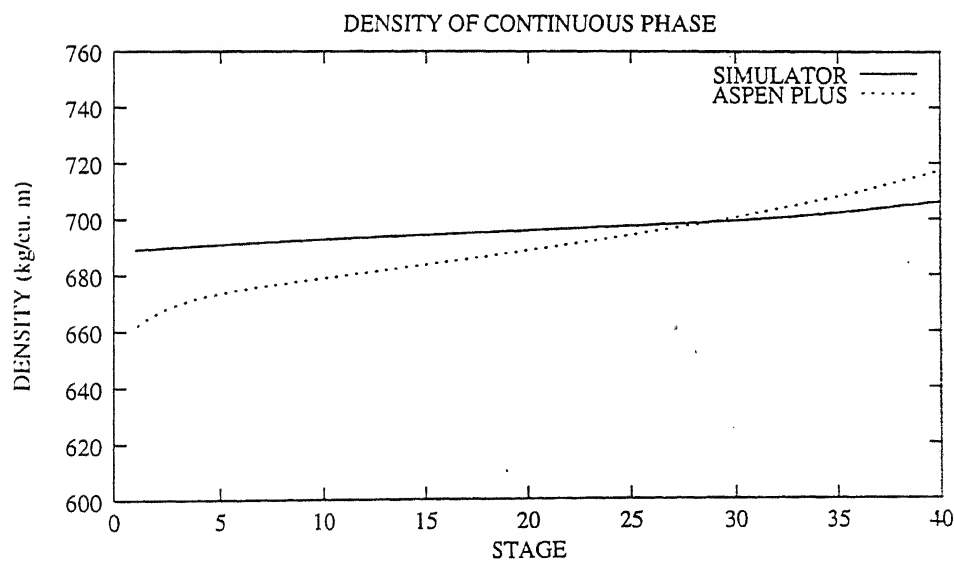


Fig. 4.14 Density of Continuous Phase

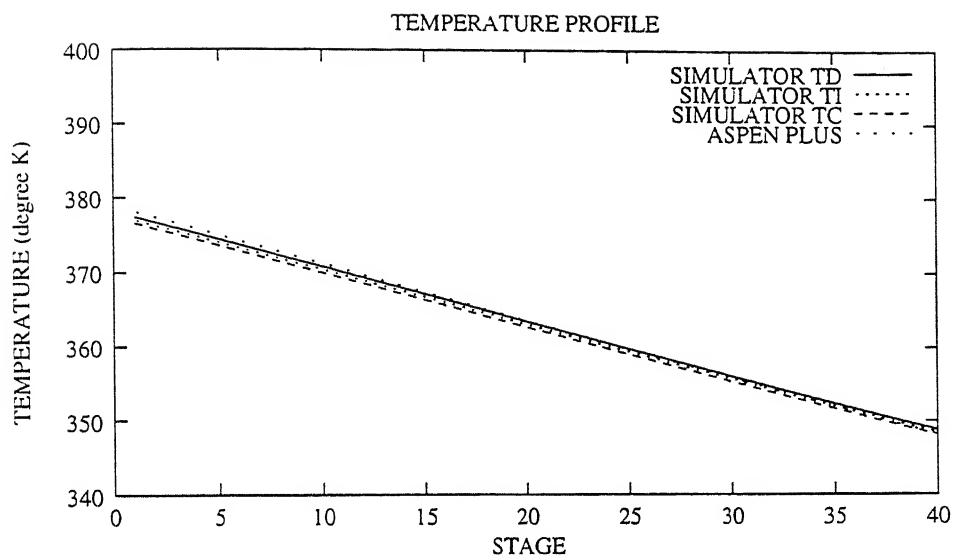


Fig. 4.15 Temperature Profile

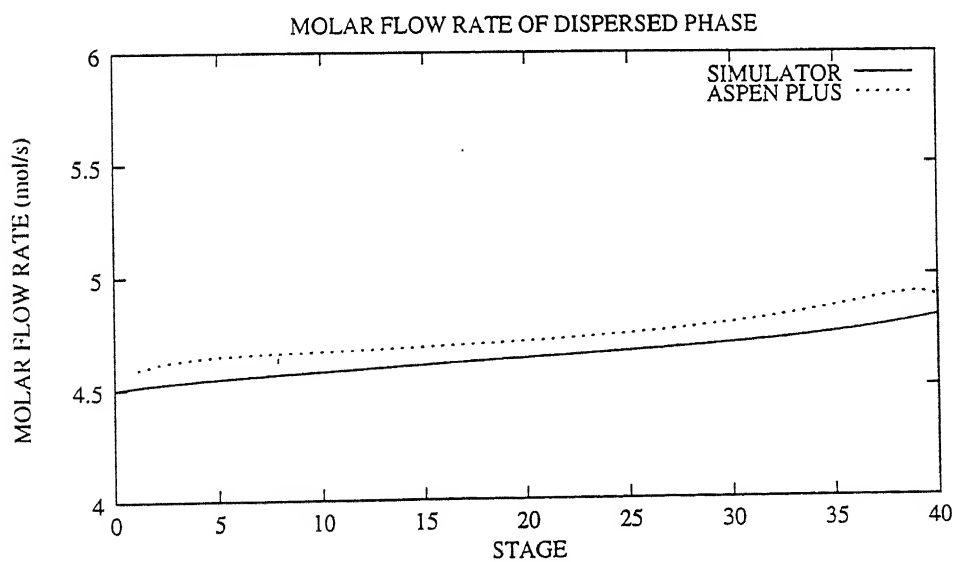


Fig. 4.16 Molar Flow Rate of Extract

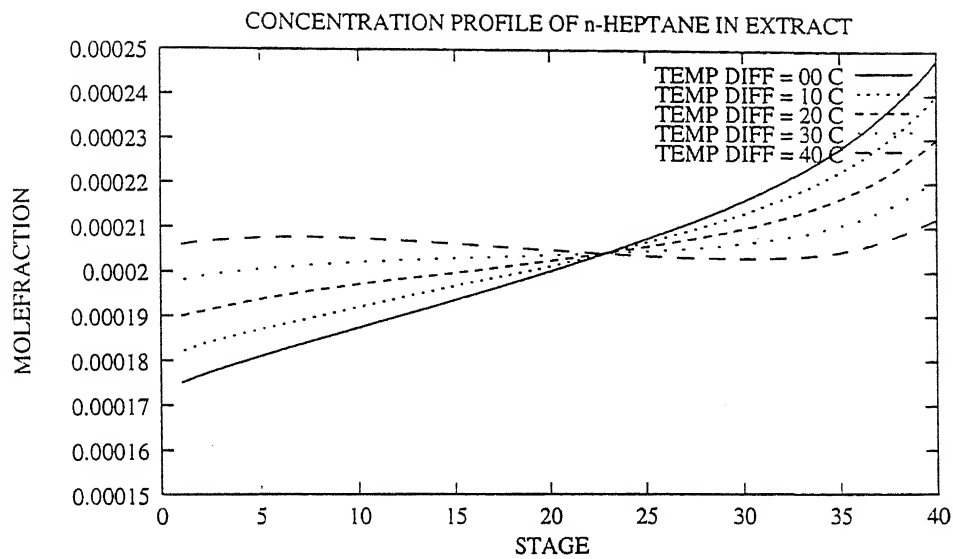


Fig. 4.17 Concentration of n-Heptane in Extract

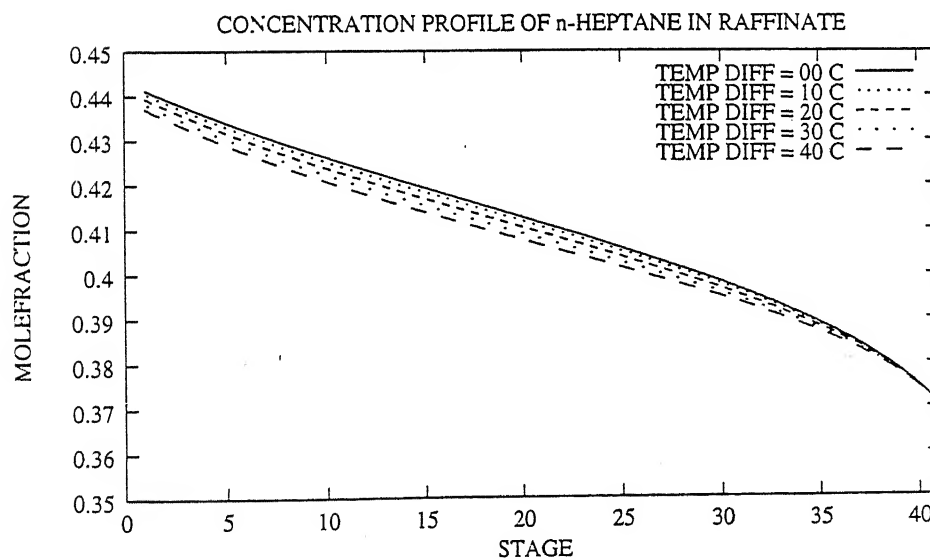


Fig. 4.18 Concentration of n-Heptane in Raffinate

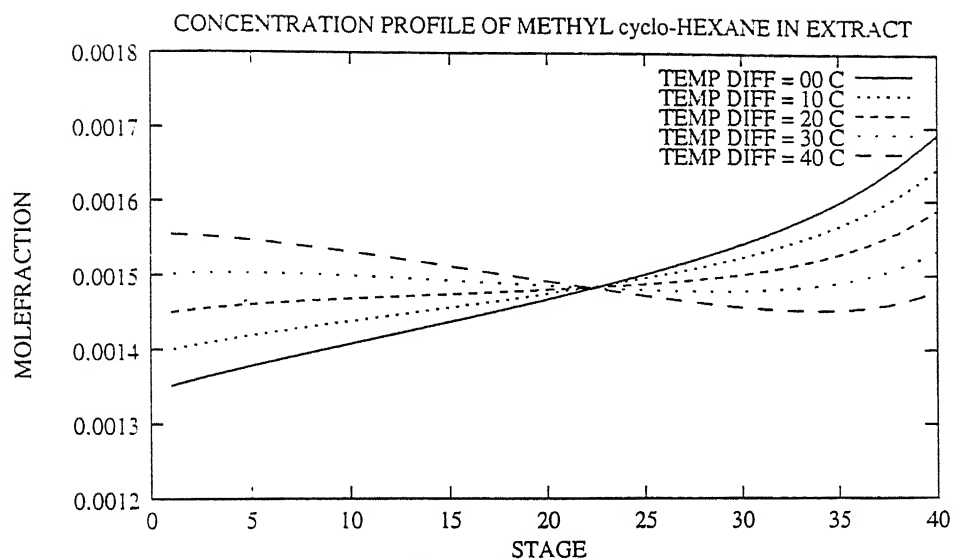


Fig. 4.19 Concentration of Methyl cyclo-Hexane in Extract

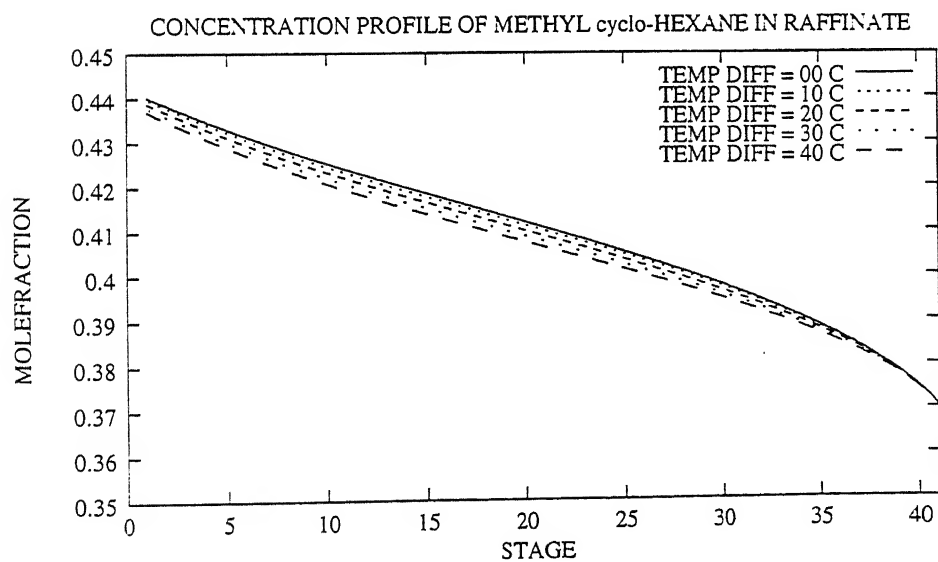


Fig. 4.20 Concentration of Methyl cyclo-Hexane in Raffinate

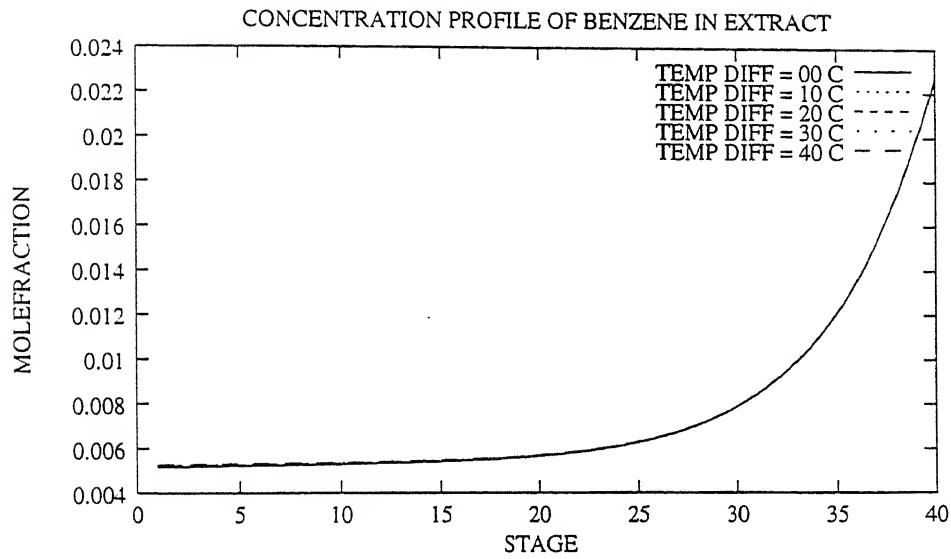


Fig. 4.21 Concentration of Benzene in Extract

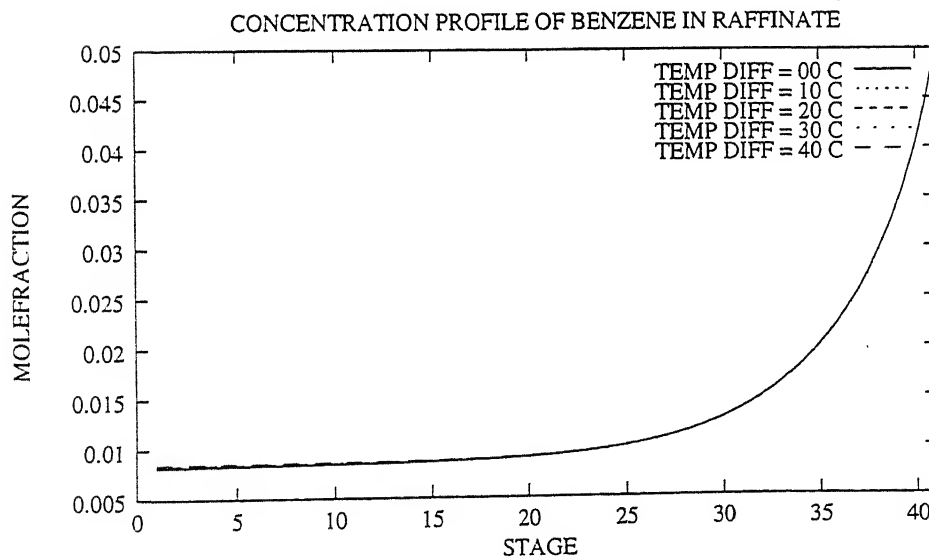


Fig. 4.22 Concentration of Benzene in Raffinate

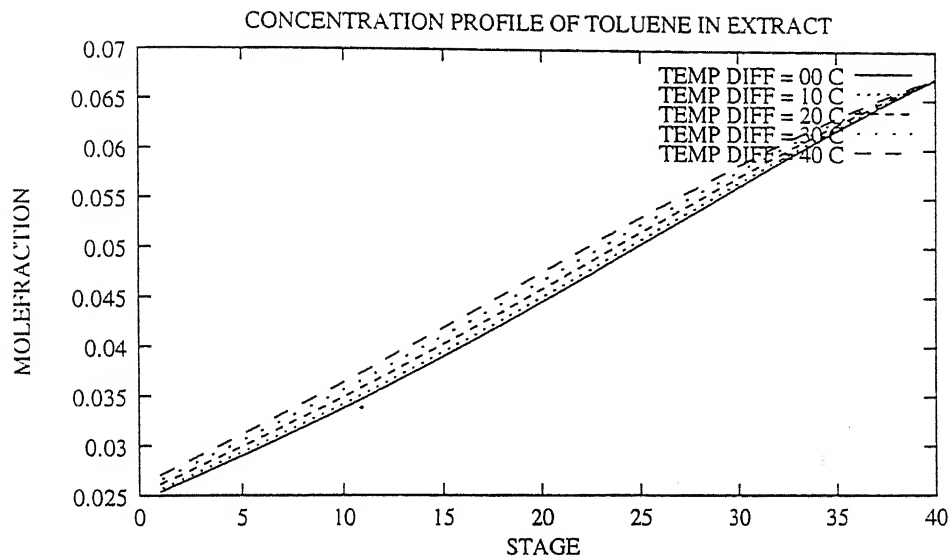


Fig. 4.23 Concentration of Toluene in Extract

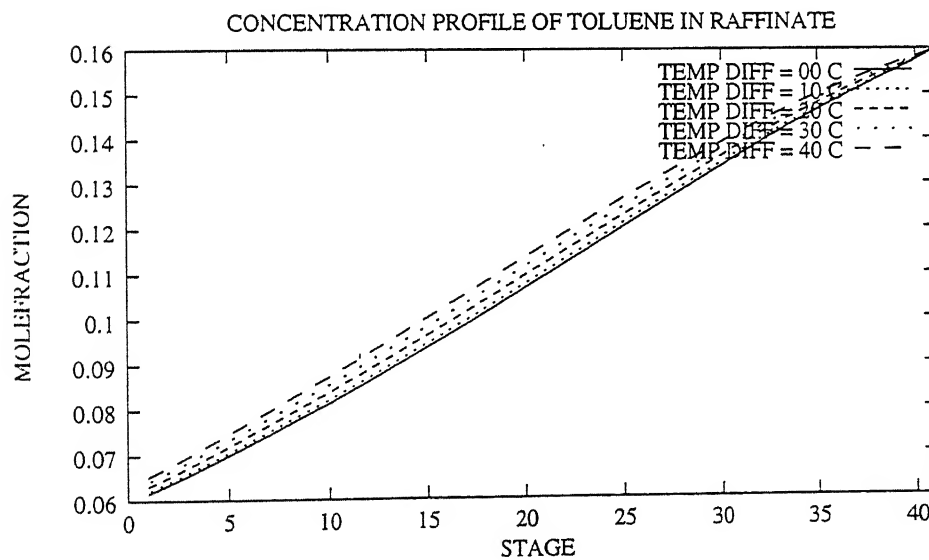


Fig. 4.24 Concentration of Toluene in Raffinate

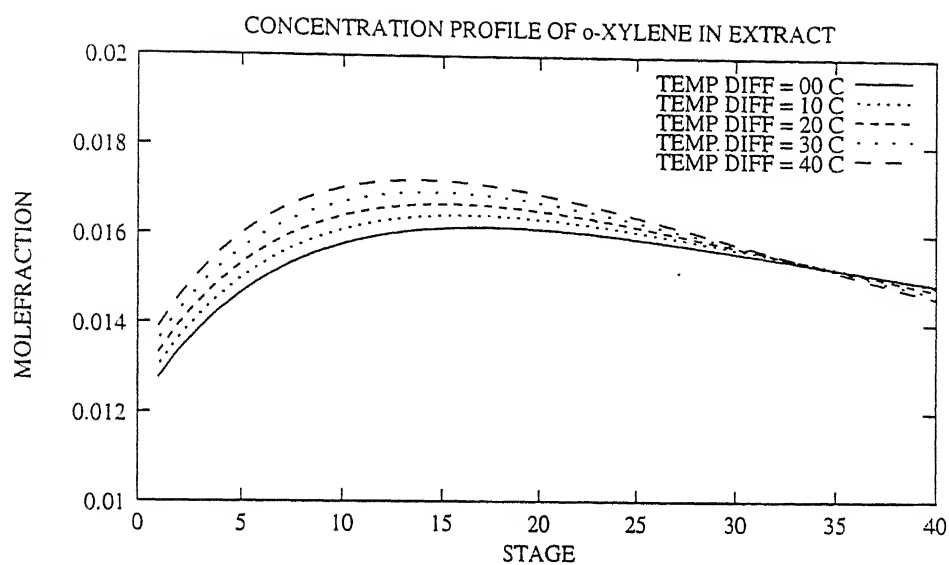


Fig. 4.25 Concentration of o-Xylene in Extract

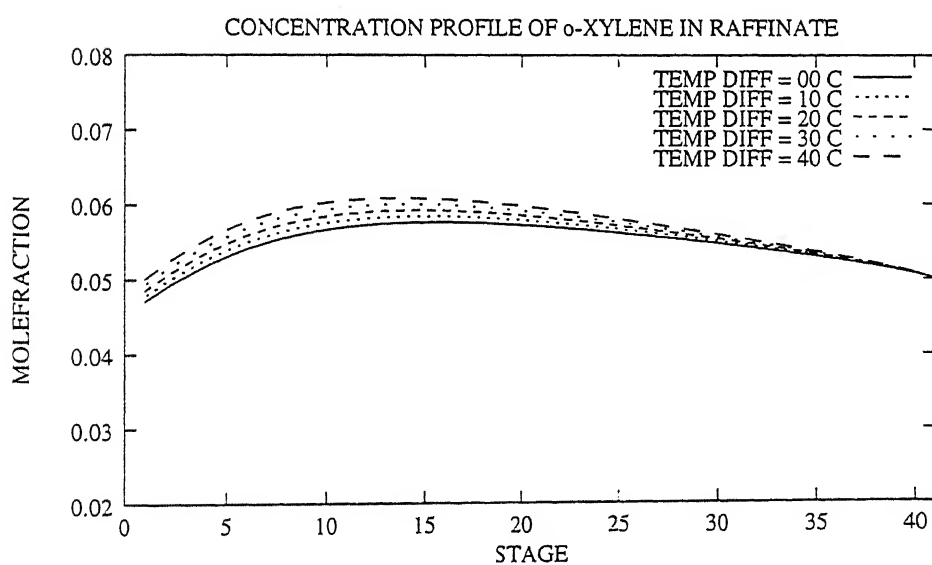


Fig. 4.26 Concentration of o-Xylene in Raffinate

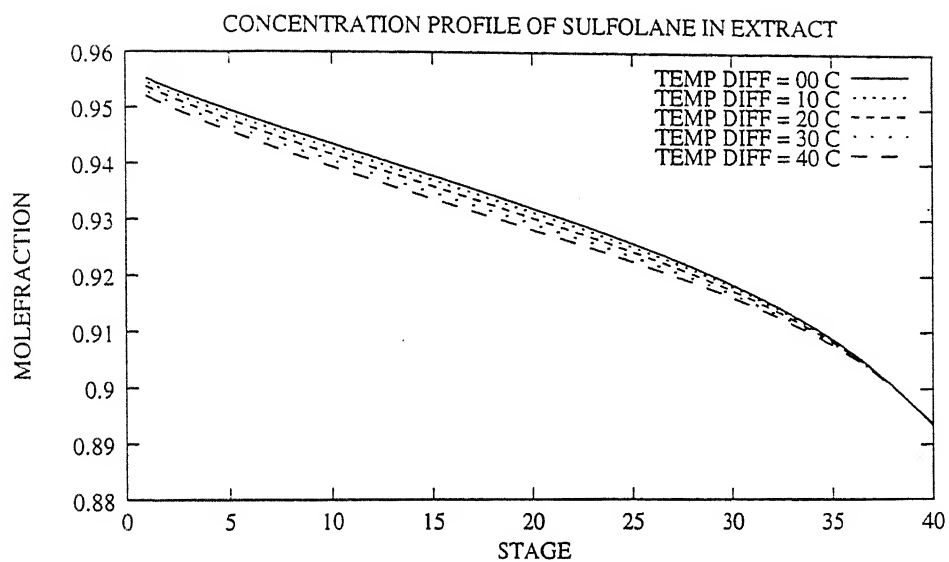


Fig. 4.27 Concentration of Sulfolane in Extract

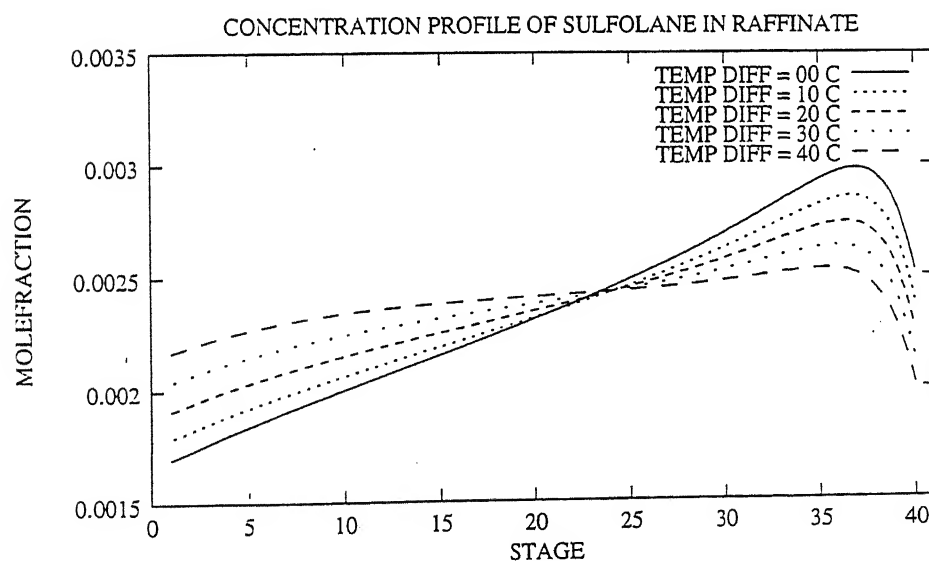


Fig. 4.28 Concentration of Sulfolane in Raffinate

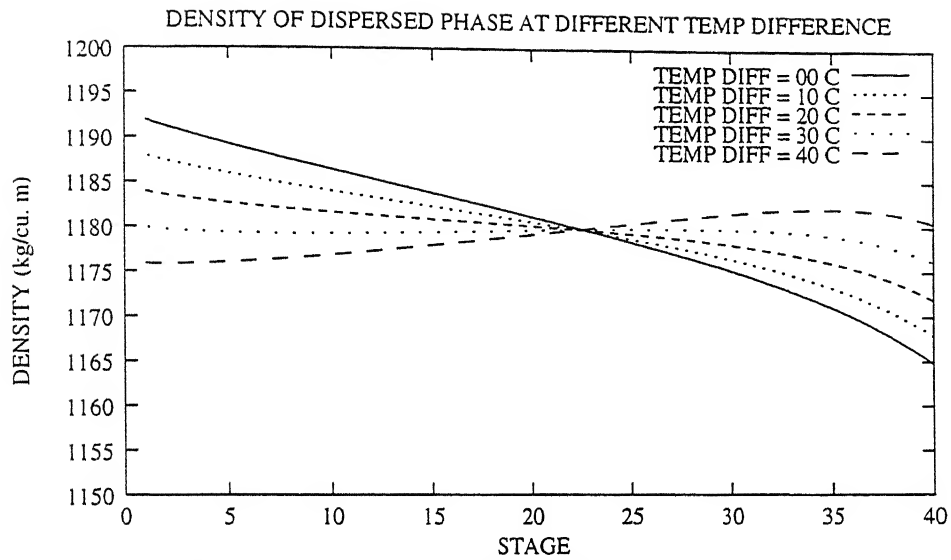


Fig. 4.29 Density of Dispersed Phase

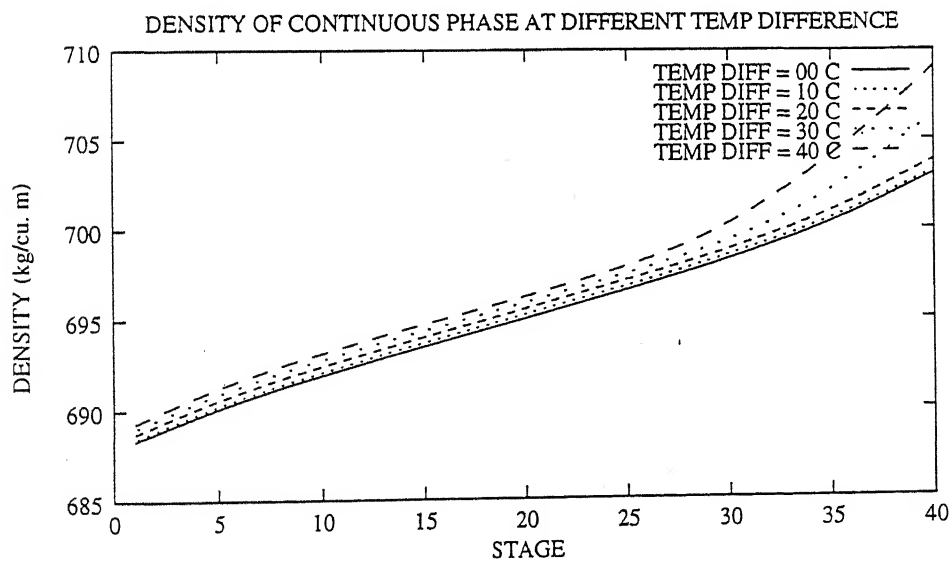


Fig. 4.30 Density of Continuous Phase

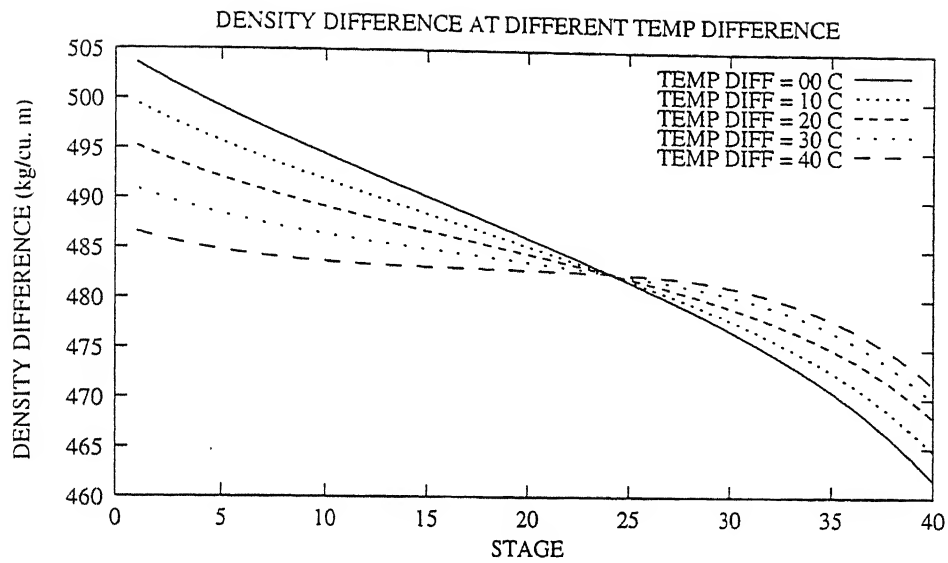


Fig. 4.31 Density Difference of Phases

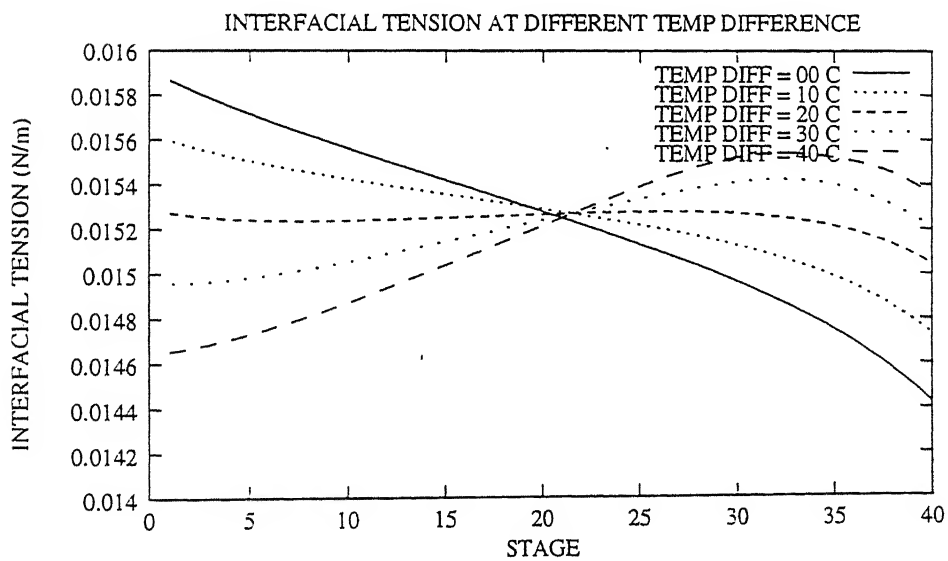


Fig. 4.32 Interfacial Tension between Phases

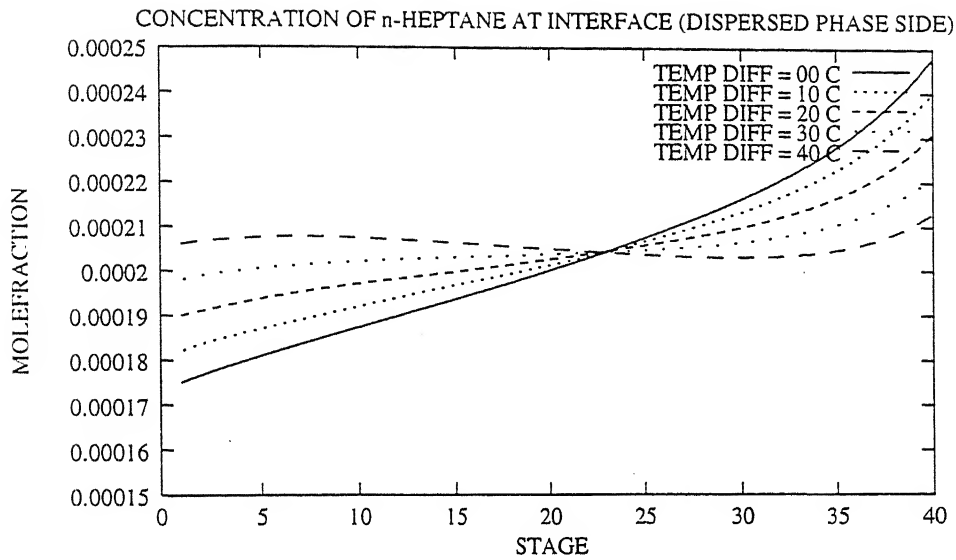


Fig. 4.33

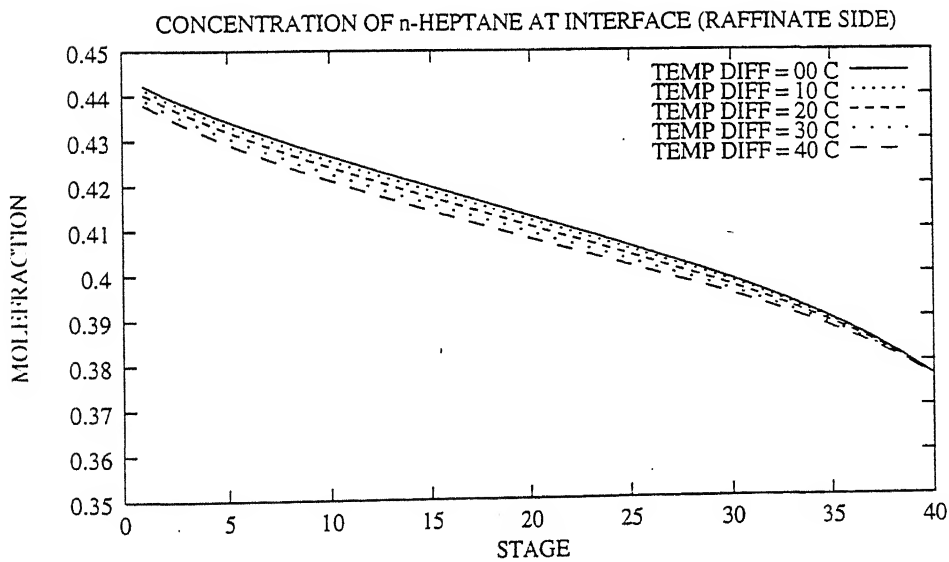


Fig. 4.34

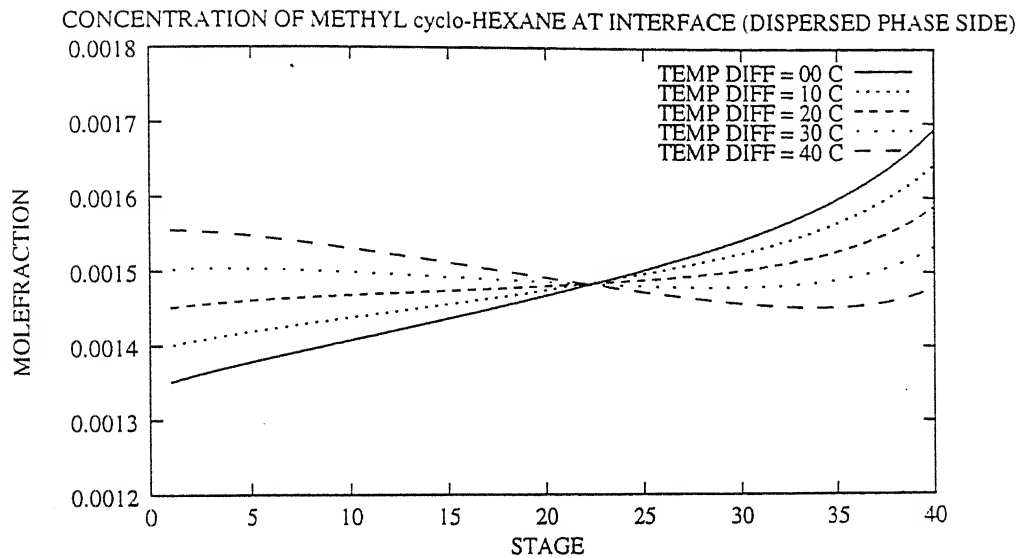


Fig. 4.35

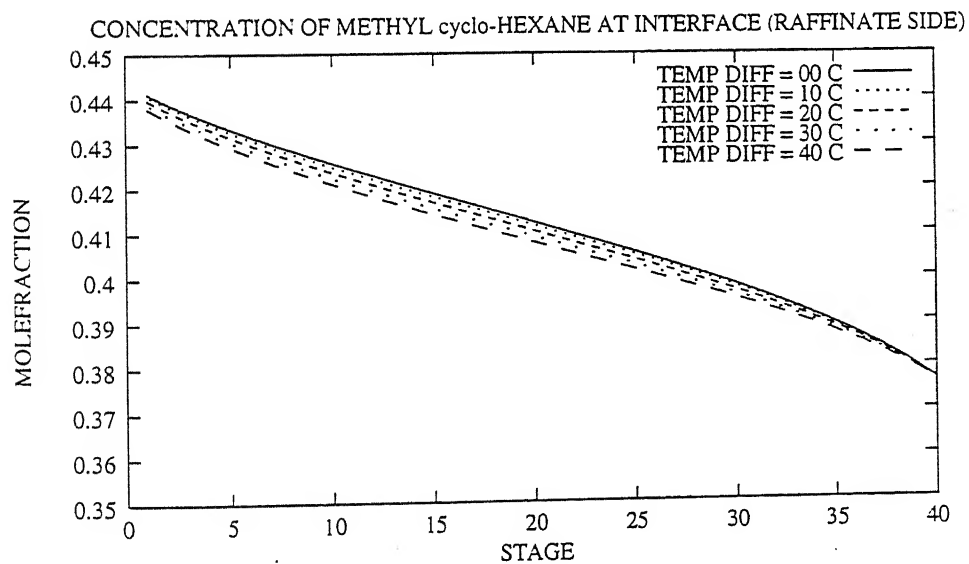


Fig. 4.36

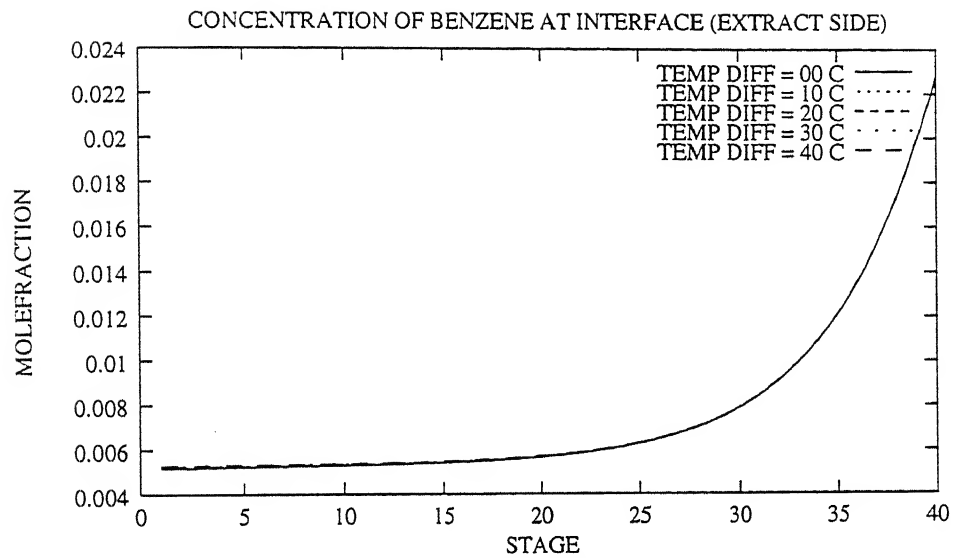


Fig. 4.37

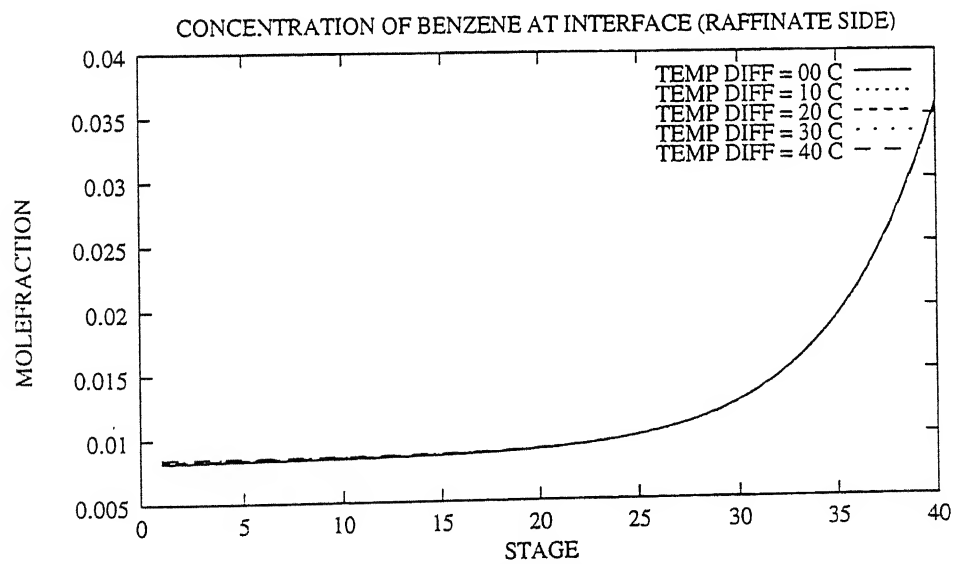


Fig. 4.38

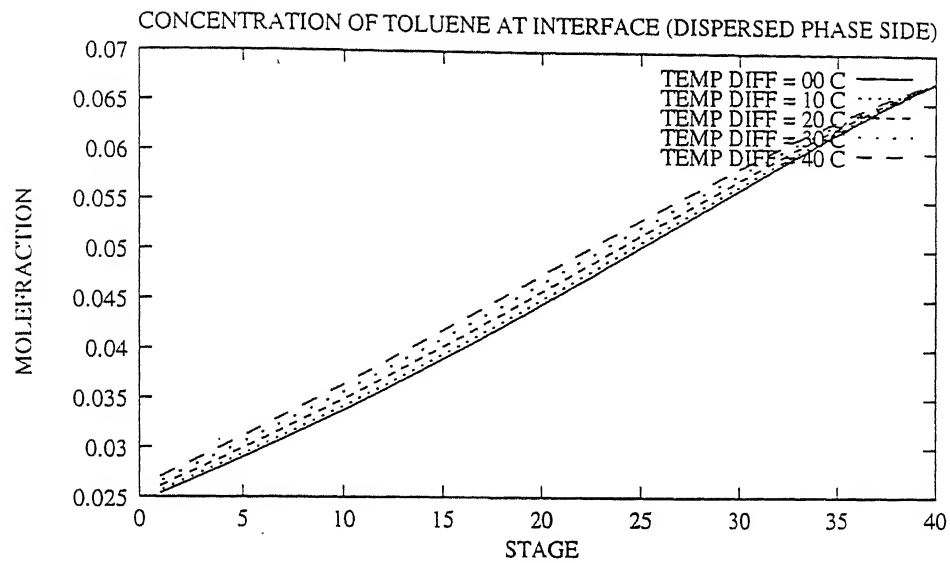


Fig. 4.39

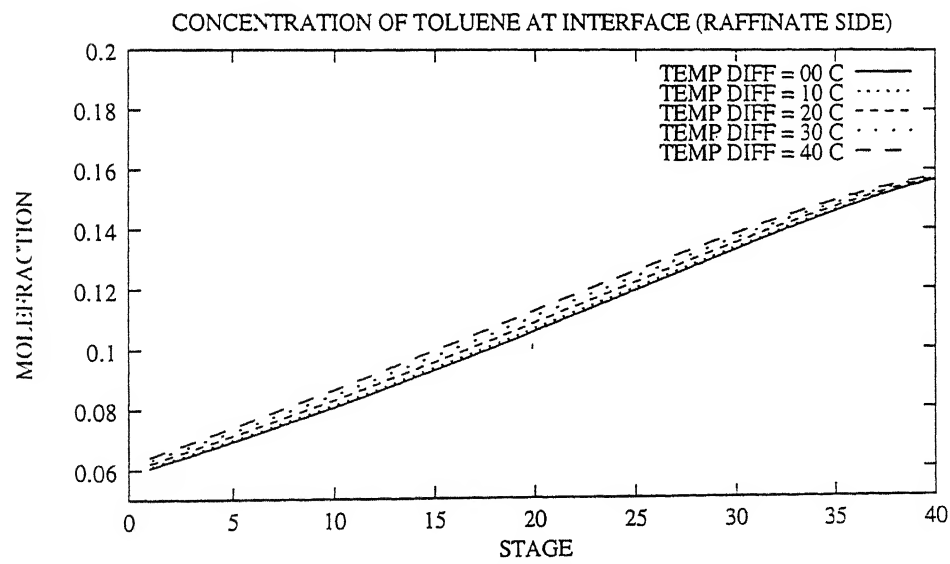


Fig. 4.40

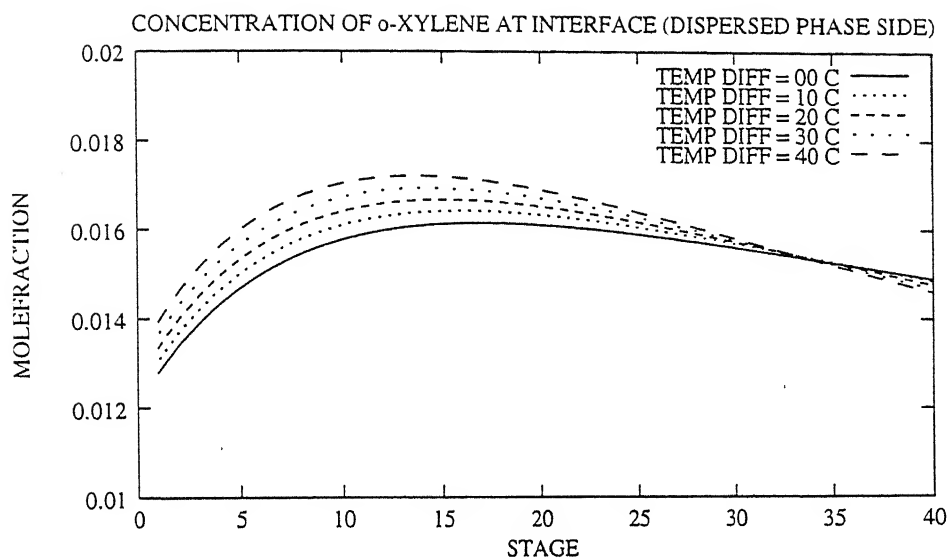


Fig. 4.41

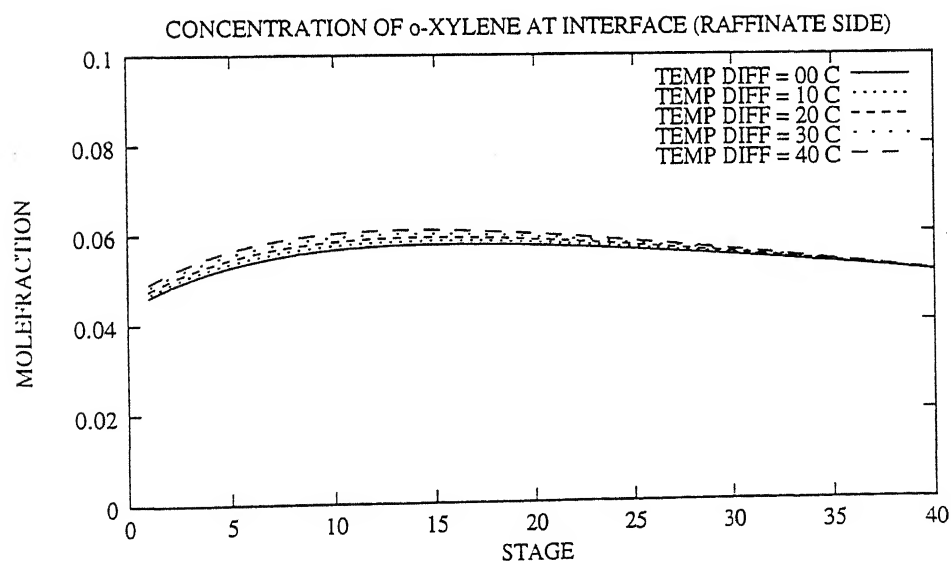


Fig. 4.42

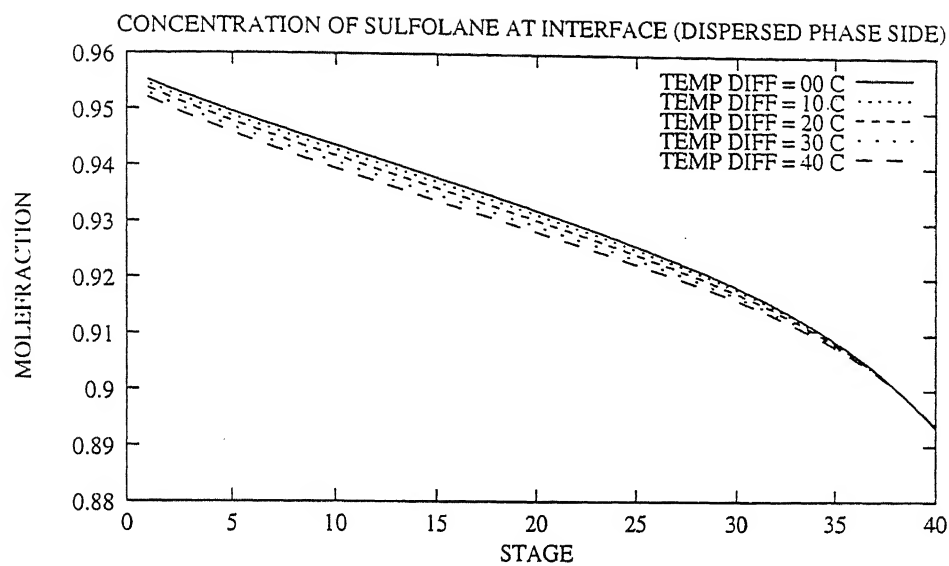


Fig. 4.43

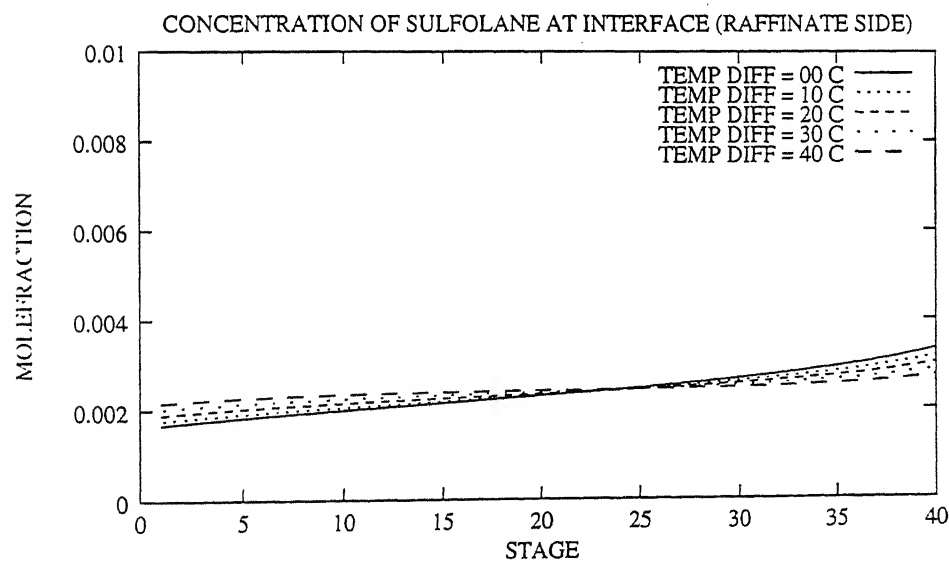


Fig. 4.44

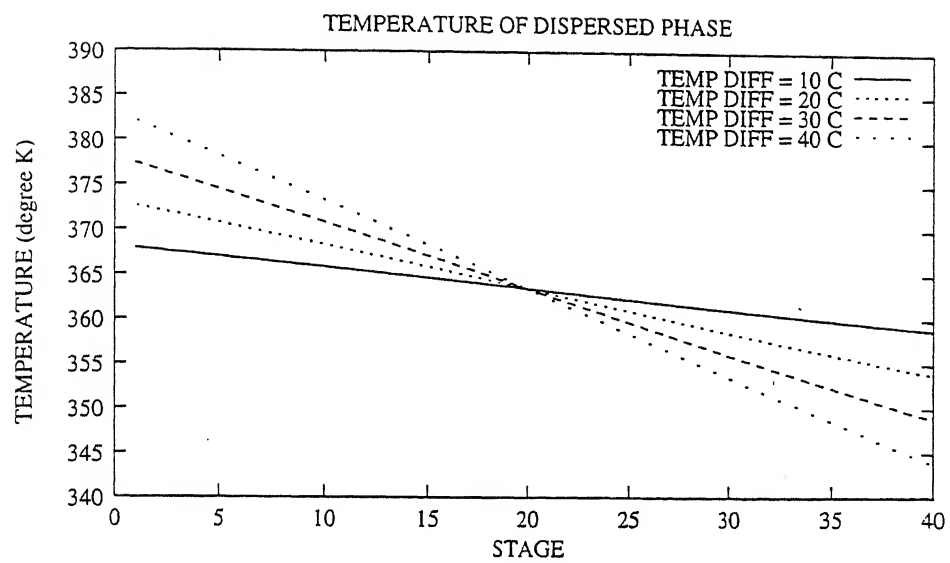


Fig. 4.45

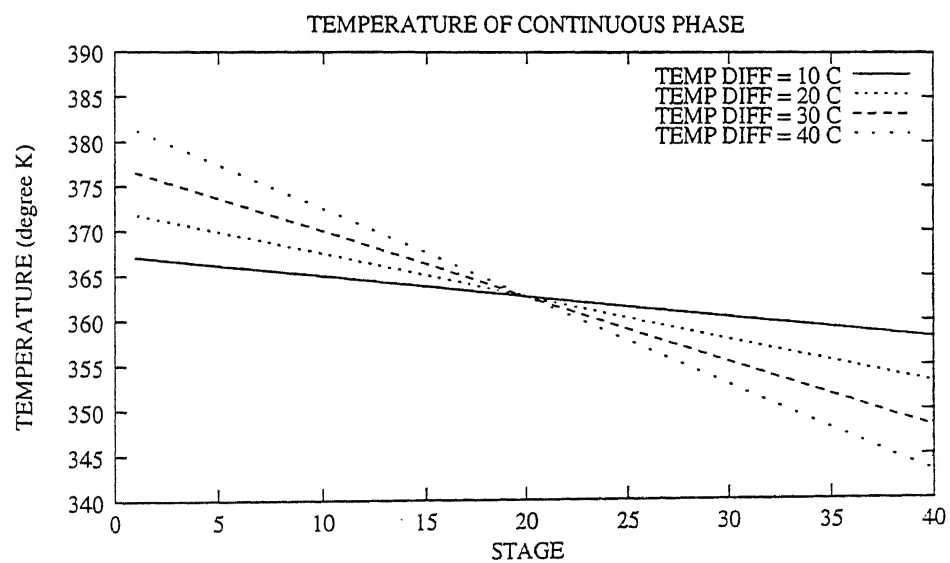


Fig. 4.46

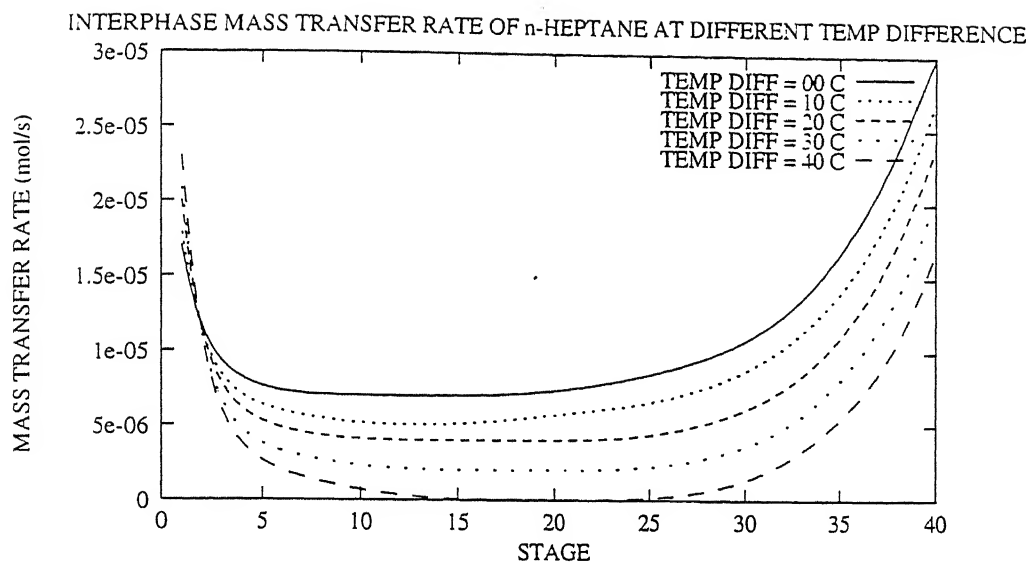


Fig. 4.47

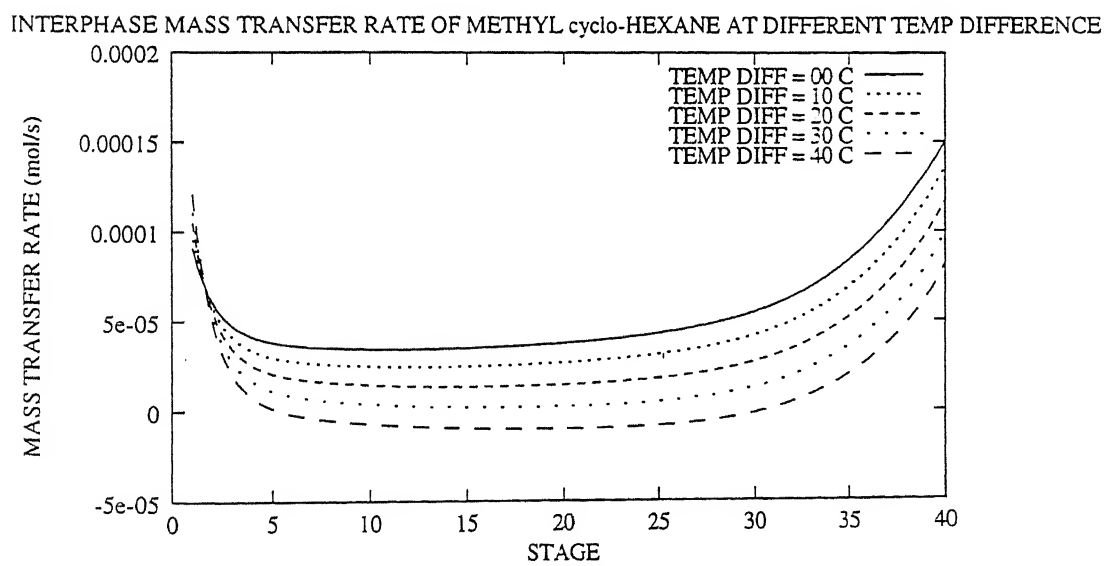


Fig. 4.48

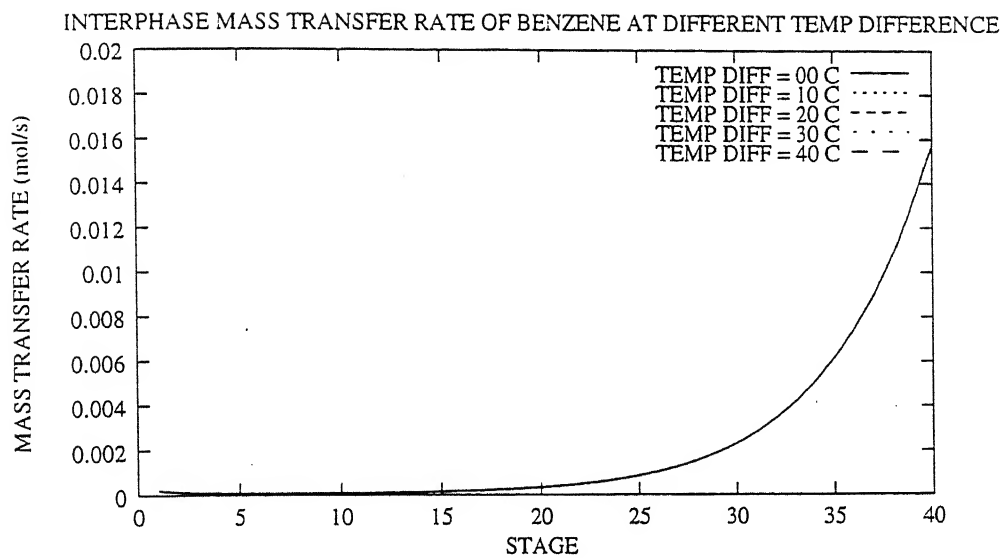


Fig. 4.49

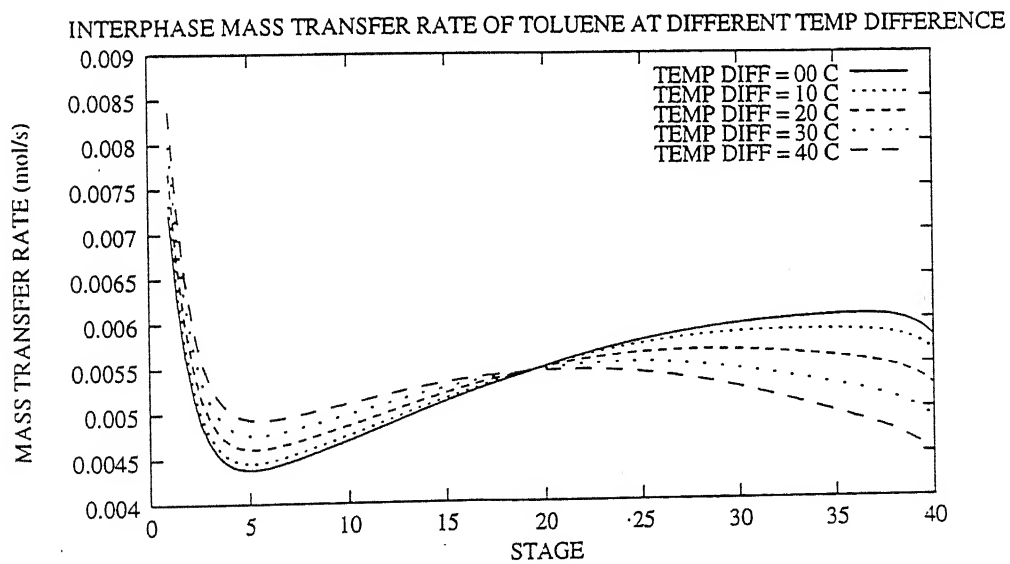


Fig. 4.50

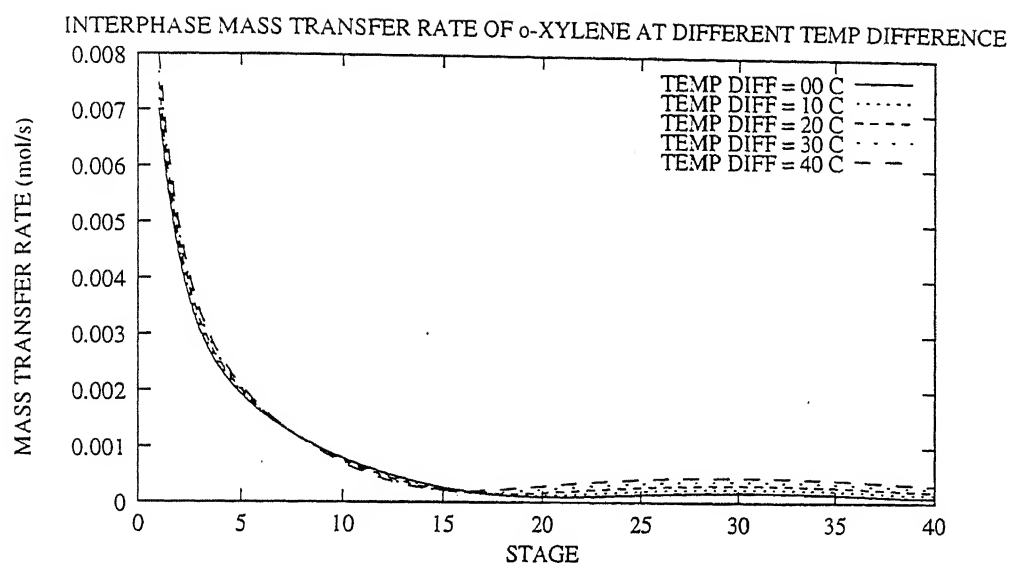


Fig. 4.51

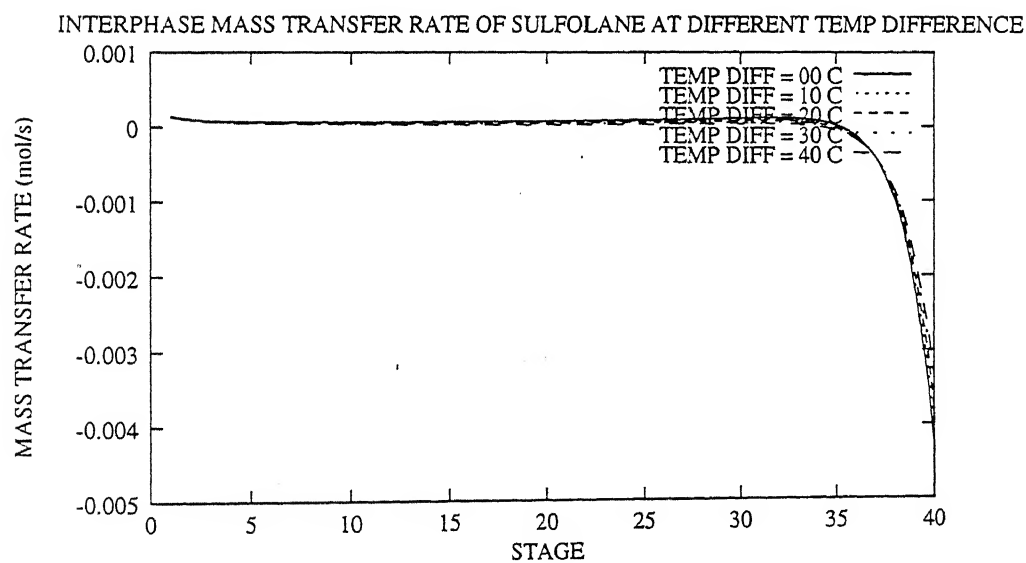


Fig. 4.52

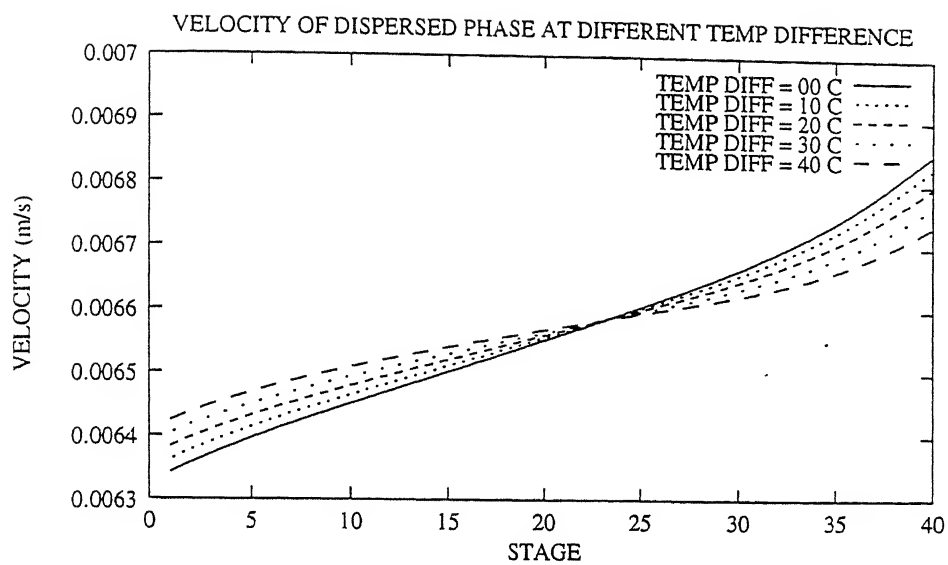


Fig. 4.53

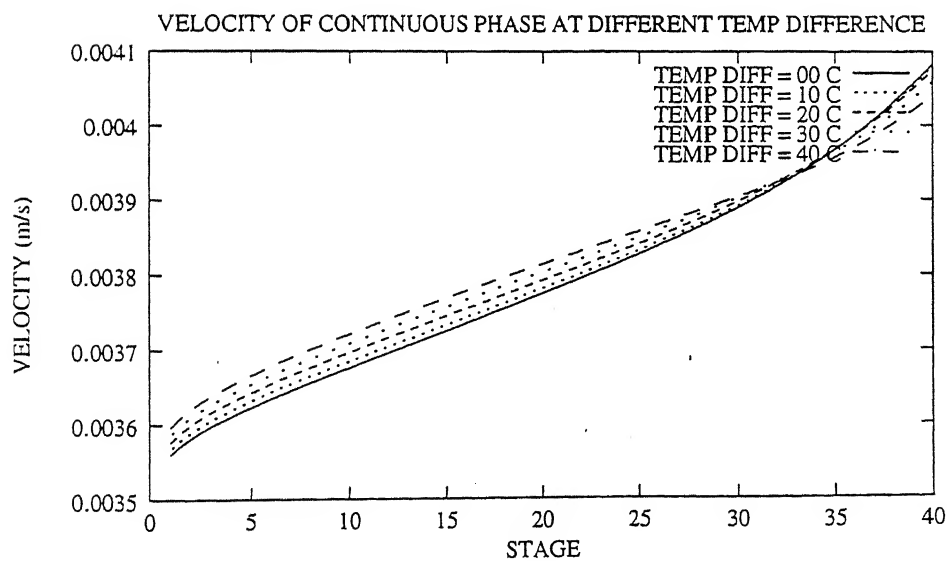


Fig. 4.54

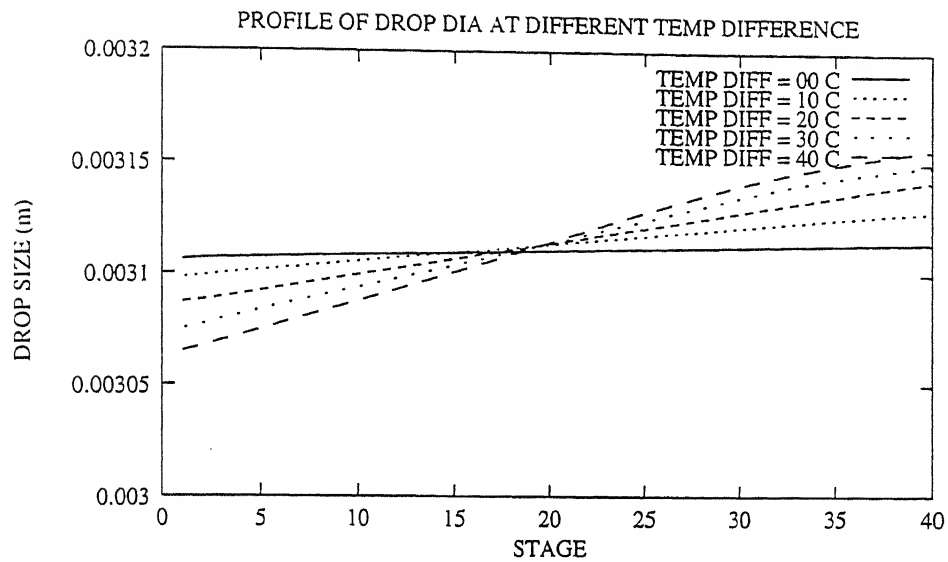


Fig. 4.55

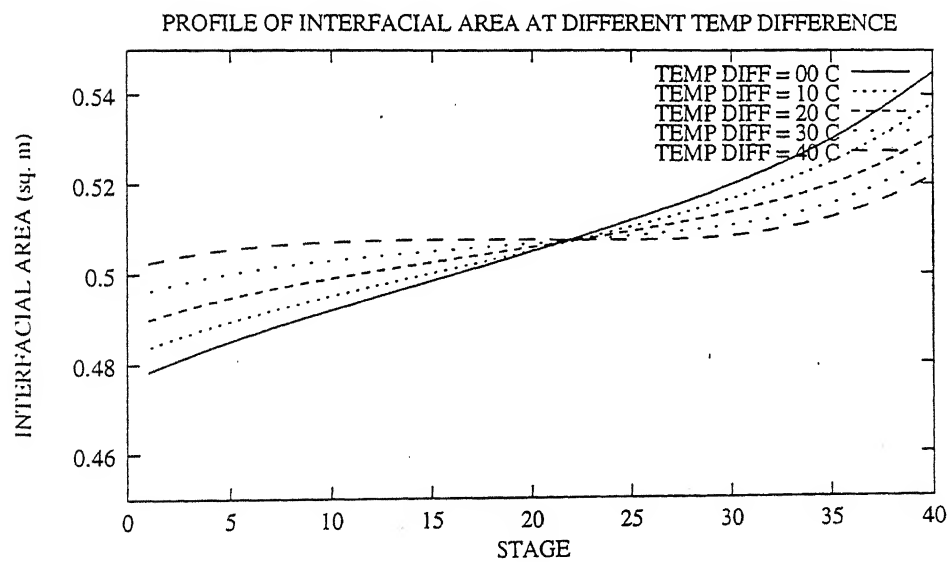


Fig. 4.56

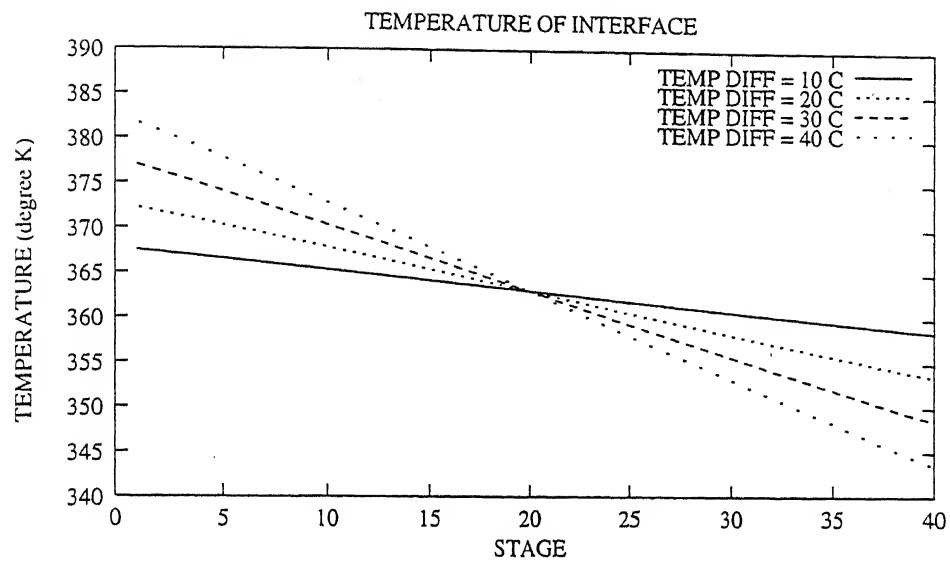


Fig. 4.57

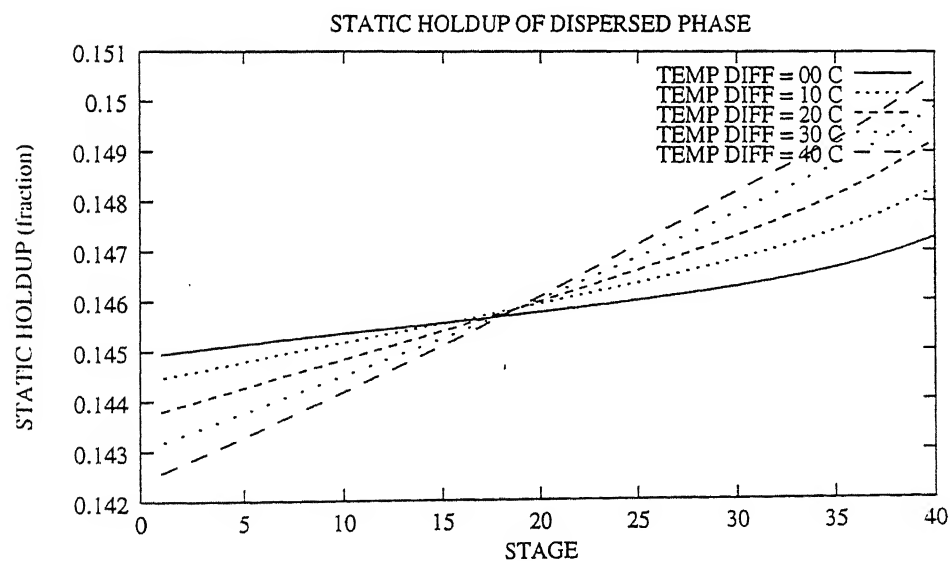


Fig. 4.58

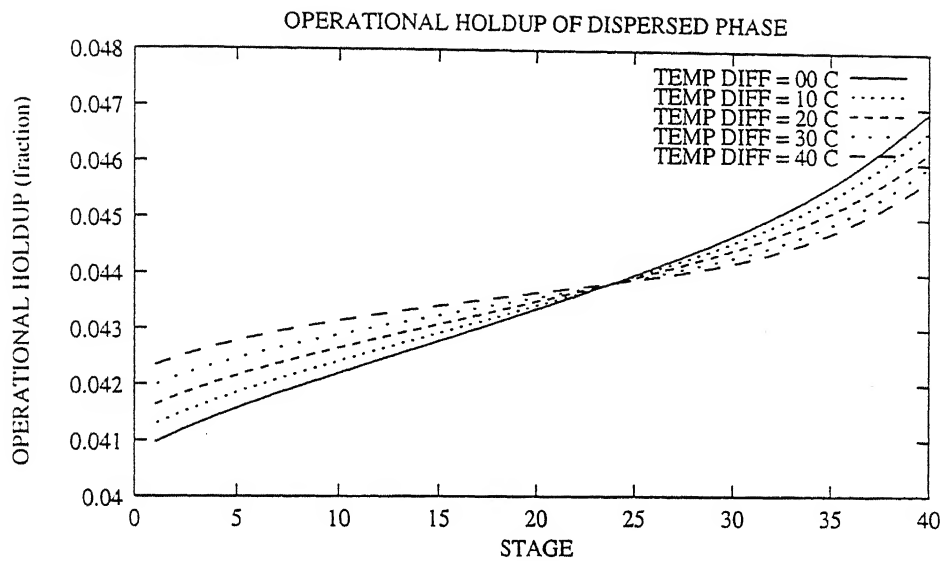


Fig. 4.59

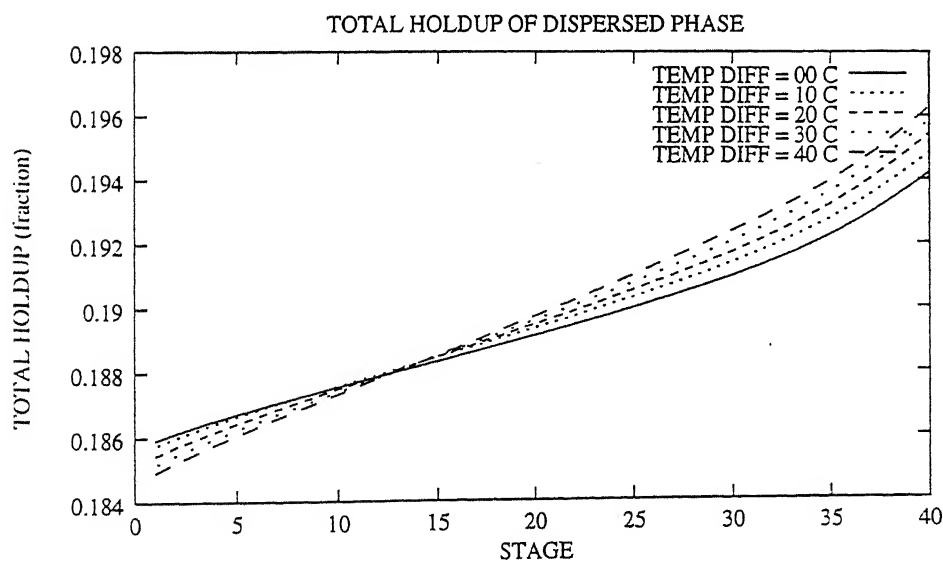


Fig. 4.60

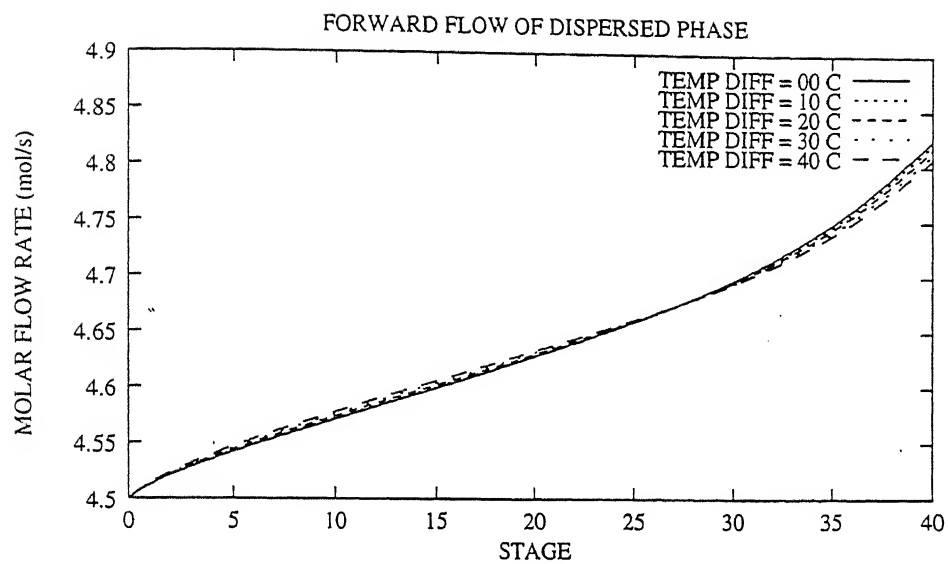


Fig. 4.61

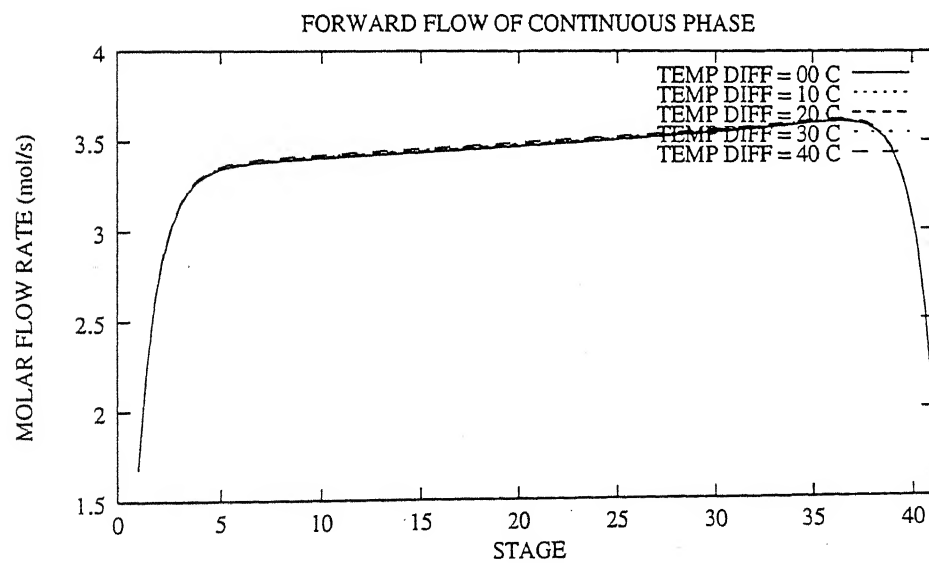


Fig. 4.62

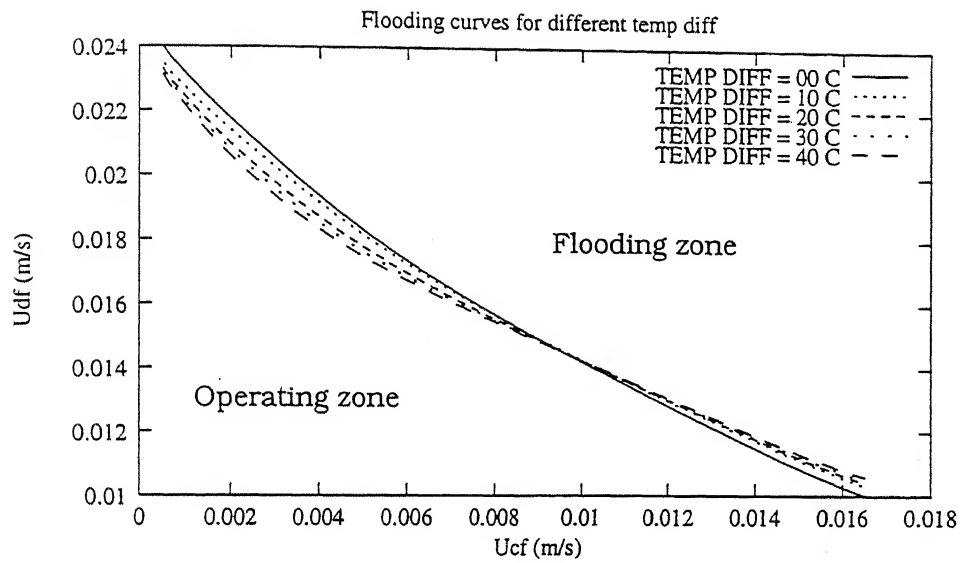


Fig. 4.63

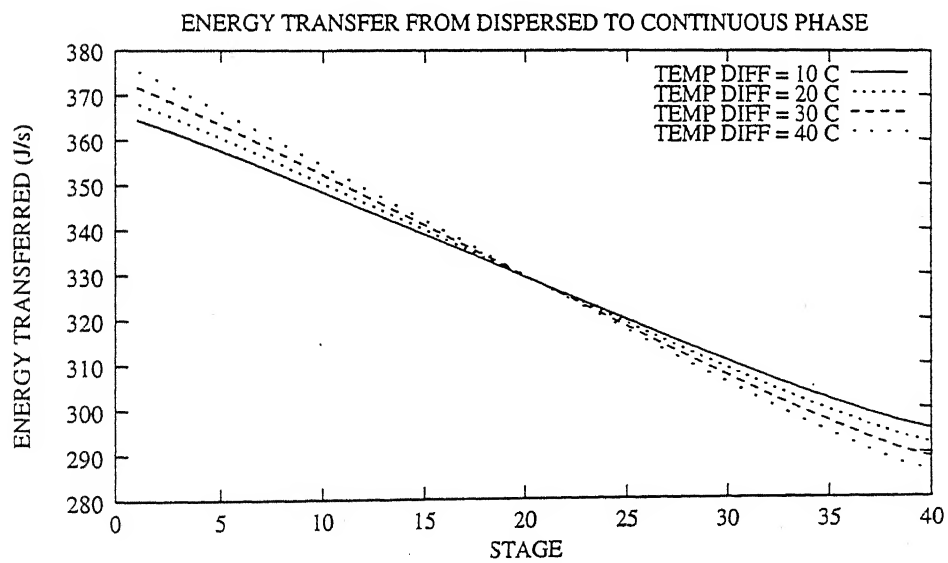


Fig. 4.64

CHAPTER 5

Conclusions and Suggestions

Simulation model selected for present thesis incorporates non-equilibrium rate-based mass transfer approach for non-isothermal operation. In general, results shown by the model are found satisfactory, when compared against ASPEN PLUS.

Axial dispersion coefficients for continuous and dispersed phases are assumed as model parameters and given suitable values as $D^c = 3.0 \text{ cm}^2/\text{s}$ and $D^d = 0 \text{ cm}^2/\text{s}$ during simulations.

The model has been run for 5 temperature differences across the column, keeping the average temperature 90°C . One of the runs is isothermal.

Some of the salient features found in the non-isothermal runs are:

1. The column shows hydrodynamically favorable behavior at higher temperature difference with respect to density difference, interfacial area, drop diameter, interfacial tension, operational holdup, etc.
2. The density difference profile tends to flatten towards constant value with increasing temperature difference; there exists an optimal temperature difference.
3. The distribution coefficients for components fall in three different magnitude ranges: 4×10^{-4} to 3×10^{-3} for non-aromatics, 0.27 to 0.65 for aromatics and 270 to 560 for solvent.
4. There is no effect of non-isothermal operation on the mass transfer rate of benzene (resulting in same composition profile for all runs). This effect is not found in case of toluene and o-xylene.
5. The percentage recovery of benzene and o-xylene increases with increasing temperature difference, whereas it slightly decreases for toluene.

6. Extract becomes purer with increasing temperature difference - non-aromatic concentration decreases by 13 - 14 % at 40 °C temperature difference compared to isothermal operation.
7. The simulation time has been greatly reduced by a factor of 30 after implementation of variables as arrays of stages. Now it is taking less than 1 minute for single iteration. It has been analyzed by getting profile of time consumption by various functions using *prof* command in UNIX.
8. Temperature and composition dependence of physical properties (like, density, density difference, viscosity, interfacial tension, etc) has been used to get actual picture of non-isothermal operation of extraction process.
9. The difference between dispersed phase temperature and continuous phase temperature on a stage has been found not to exceed 1 °C.

Suggestions for future work:

Study of any chemical process is a creative work and success of modeling and simulation is complete only when the model is validated against *real operating plant data*. Feedback from real process may further suggest some refinement in modeling aspects, which can't be envisaged just by theoretical study. To remove any bug and make the simulator versatile for study of any new extraction process, model must be tested for a variety of extraction systems. Other compositions for naphtha feed and mixed solvent may be incorporated. Some close boiling impurities must be included to study their effects.

Other suggestions and recommendations for improvement of the simulator are:

1. The simulator must be run for a span of average temperature along with a range of temperature difference across the column.
2. Present study has been done under isobaric condition. For realistic study, pressure drop across the stages must be incorporated.

3. Side feed streams and recycling of extract must be applied in future simulations.
4. Imposition of optimal temperature profile by fine tuning the temperature difference, feed streams' temperatures may be done to operate the some part of the column non-isothermally and rest isothermally.
5. Hydrodynamic parameters (jet diameter, jet velocity, operational holdup, etc) must be analyzed for a drop size distribution including drop breakage and coalescence, breaking efficiency must be analyzed and summarized results should be later included in the model.
6. Some of functions have been declared as arrays of stages, which results in reduction of CPU time. Other functions must be included for the same strategy for further reduction in CPU time.
7. Once SPEEDUP model runs successfully, the results may be compared and extended for process control, which is provided in SPEEDUP.
8. The model should be extended for dynamic simulation for non-isothermal operation.
9. In the present simulator, it has been found that T^d is approximately equal to T^c . Hence instead of using detailed energy balance, average temperature on stages may be imposed on simplified material balance equations.

Appendix A

Mathematical Formulation

The mathematical formulation for the steady state simulation consists of the following sections:

- Fluid dynamics
- Mass transfer relationship
- Heat transfer relationship
- Equilibrium relationship at the interface
- Normalization equations

A.1 Mass balance

The model proposed by Khani, Gourdon & Casamatta (1989) is discretized on the basis of real stages along the height of the column. The process variables vary according to the temperature at a particular stage.

The two phases contact at the interface. The dispersed phase in the form of drop spectrum is discretized in different drop-class. The interfacial area between the bulk and the drops of all drop-classes provides the medium for the mass and energy transfer between the two phases. A drop-class implies the drops of same diameter. The two films (one in each phase) at the interface offers the resistance to the mass as well as energy transfer. Each drop-class is described by the variable, P_{jk} , which is the volume fraction of drop-class j on the stage k . Summation over all the drop-classes at any stage k yields the operational holdup, ϕ_k , of the dispersed phase at any stage k .

$$\phi_k = \sum_{j=1}^{ND} P_{jk} \quad (A.1)$$

The mass balance relations at stage k for drop class j and component i are as follows:

MBD_{ijk} : Mass balance for dispersed phase

$$V_{jk-1}^+ x_{ijk-1} - (V_{jk}^+ + V_{jk}^-) x_{ijk} + V_{jk+1}^- x_{ijk+1} + N_{ijk} + F_{jk}^d x_{ijk}^f + \Pi_{ijk} = 0 \quad (\text{A.2})$$

MBC_{ik} : Mass balance for continuous phase

$$U_{k-1}^+ y_{ik-1} - (U_k^+ + U_k^-) y_{ik} + U_{k+1}^- y_{ik+1} - \sum_{j=1}^{ND} N_{ijk} + F_k^c y_{ik}^f = 0 \quad (\text{A.3})$$

where subscripts i, j, k take values as

i = 1, 2, ..., NC;

j = 1, 2, ..., ND;

k = 1, 2, ..., NS;

and superscripts + and - represent the direction along and opposite to the main flow of dispersed phase.

N_{ijk} represents the mass transfer rate (moles/s) in a stage from continuous phase to dispersed phase for drop-class j and component i. Π_{ijk} is a generation term due to drop breakage and coalescence Rajeev Kumar (1996).

A.2 Flow relationships

Flow streams V_{jk}^+ , V_{jk}^- , U_k^+ , U_k^- from a stage k to the adjacent stages consist of convective and diffusive contribution of the flow. Main flow direction contains both convective and diffusive (dispersion) flow; however only dispersion flow exists against the main flow causing backmixing. Axial dispersion coefficients D_k^c and D_k^d are used to represent axial dispersion in continuous and dispersed phases at stage k respectively.

Flow VP_{jk} : Forward flow of dispersed phase

$$V_{jk}^+ = (u_{jk}^d + \frac{D_k^d}{\Delta h_k}) P_{jk} c_{jk}^d S \quad (\text{A.4})$$

Flow VM_{jk} : Backward flow of dispersed phase

$$V_{jk}^- = \left(\frac{D_{k-1}^d}{\Delta h_{k-1}} \right) P_{jk} c_{jk}^d S \quad (A.5)$$

Flow UM_k : Forward flow of continuous phase

$$U_k^- = \left(u_k^c + \frac{D_{k-1}^c}{\Delta h_{k-1}} \right) (1 - \phi_k) c_k^c S \quad (A.6)$$

Flow UP_k : Backward flow of continuous phase

$$U_k^+ = \left(\frac{D_k^c}{\Delta h_k} \right) (1 - \phi_k) c_k^c S \quad (A.7)$$

Molar density of phases, c_k^c and c_k^d are assumed uniform in the k^{th} stage. u_k^c and u_{jk}^d represent the convective contribution to the main forward flow, whereas the axial dispersion and backmixing are described by axial dispersion coefficients.

Mixture molar densities are given as:

$$c_{jk}^d = \frac{\rho_{jk}^d}{\sum_{i=1}^{N_c} (x_{ijk} M_i)} \quad (A.8)$$

$$c_k^c = \frac{\rho_k^c}{\sum_{i=1}^{N_c} (y_{ik} M_i)} \quad (A.9)$$

Superficial velocity of the dispersed phase is expressed as:

$$u_{jk}^d = -u_k^c + u_{jk}^r \quad (A.10)$$

$$u_{jk}^r = (1 - \phi_k)^m u_{jk}^{r*} \quad (A.11)$$

where u_{jk}^r is the relative velocity and u_{jk}^{r*} is the characteristic velocity Laddha (1976). Exponent m (usually between 0 and 1) is a function of the hydrodynamic conditions, particularly the Reynolds number N_{Re} for the drop. Here it is assumed as a model parameter and kept unity. u_k^c (m/s) is the continuous phase superficial velocity.

A.3 Energy balance

The heat transfer depends on the temperature difference only. So a separate equation for each and every component and drop-class is not needed. Thus the energy balances are given as:

EBD_k: Energy balance equation for dispersed phase

$$\begin{aligned} & \sum_{j=1}^{ND} V_{jk}^- \sum_{i=1}^{NC} x_{ijk-1} H_{ik-1}^d - \sum_{j=1}^{ND} (V_{jk}^+ + V_{jk}^-) \sum_{i=1}^{NC} x_{ijk} H_{ik}^d + \sum_{j=1}^{ND} V_{jk+1}^- \sum_{i=1}^{NC} x_{ijk+1} H_{ik+1}^d + \\ & \sum_{j=1}^{ND} F_{jk}^d \sum_{i=1}^{NC} x_{ik}^j H_{ik}^j + \sum_{j=1}^{ND} \sum_{i=1}^{NC} \Pi_{ijk} H_{ijk}^d + \varepsilon^d = 0 \end{aligned} \quad (A.12)$$

where ε^d is the energy transfer across the interface based on the dispersed phase.

EBC_k: Energy balance equation for continuous phase

$$\begin{aligned} & U_{k-1}^- \sum_{i=1}^{NC} y_{ik-1} H_{ik-1}^c - (U_k^+ + U_k^-) \sum_{i=1}^{NC} y_{ik} H_{ik}^c + U_{k+1}^- \sum_{i=1}^{NC} y_{ik+1} H_{ik+1}^c + \\ & F_k^c \sum_{i=1}^{NC} y_{ik}^i H_{ik}^i - \varepsilon^c = 0 \end{aligned} \quad (A.13)$$

where ε^c is the energy transfer across the interface based on the continuous phase.

$$i = 1, 2, 3, \dots, NC;$$

$$j = 1, 2, 3, \dots, ND;$$

$$k = 1, 2, 3, \dots, NS.$$

A.4 Mass transfer relationships at the interface

The mass transfer relationships are described as:

MBIC_{ijk}: Mass balance at the interface based on the continuous phase

$$N_{ijk} = y_{ik} \sum_{l=1}^{NC} N_{il} + a_{jk} \sum_{m=1}^{NC-1} K_{imjk}^c (y_{mk} - y_{mj}^l) \quad (\text{A.14})$$

MBID_{ijk}: Mass balance at the interface based on the dispersed phase

$$N_{ijk} = x_{ik} \sum_{l=1}^{ND} N_{il} + a_{jk} \sum_{m=1}^{NC-1} K_{imjk}^d (x_{mk}^l - x_{mj}) \quad (\text{A.15})$$

K_{imjk}^c and K_{imjk}^d are mass transfer coefficients due to interaction effect in multi-component mixture.

Interfacial area a_{jk} is directly given by the drop size distribution at each stage in the column.

$$a_{jk} = 6.0 \left(\frac{V_k}{d_{jk}} \right) P_k \quad (\text{A.16})$$

The total interfacial area on a stage k is the summation over all the drop classes.

$$a_k = \sum_{j=1}^{ND} a_{jk} \quad (\text{A.17})$$

A.5 Energy transfer relationships at the interface

The energy transfer across the interface is described as follows:

EBID_k: Energy balance at the interface based on the dispersed phase

$$\varepsilon^d = h^d a_k (TD_k - TI_k) + \sum_{j=1}^{ND} \sum_{i=1}^{NC} N_{ijk} H_{ik}^d \quad (\text{A.18})$$

EBIC_k: Energy balance at the interface based on the continuous phase

$$\varepsilon^c = h^c a_k (TI_k - TC_k) + \sum_{j=1}^{ND} \sum_{i=1}^{NC} N_{ijk} H_{ik}^c \quad (\text{A.19})$$

where h^d and h^c are heat transfer coefficients for dispersed and continuous phases respectively. TD_k , TI_k and TC_k are the temperatures of bulk dispersed phase, interface and bulk continuous phase respectively. There is no accumulation of mass or energy at the interface. Hence

$$\varepsilon^d = \varepsilon^c \quad (A.20)$$

A.6 Interface model

In the present model equilibrium between the dispersed and continuous phases is assumed at the interface with no resistance to mass transfer as well as energy transfer. Equilibrium relation relates the interfacial composition of both the phases by the following equation:

EQ_{ijk}: Equilibrium relationship at the interface

$$y_{ijk}^I = K_{ijk} x_{ijk}^I \quad (A.21)$$

Distribution ratio K_{ijk} is calculated by means of the activity coefficients of component i in both the phases. It depends on temperature, pressure and composition of both the phases at the interface. There are different methods proposed by various authors such as UNIQUAC, NRTL, UNIFAC, etc based on the group contribution model. Modified UNIFAC model by Larsen (1987) consists of two group interaction parameters (which are temperature dependent) and the different combinatorial term than the original UNIFAC model of Fredenslund and Prausnitz (1975). Gmehling (1993) further modified this model. He proposed three group interaction parameters and slightly different combinatorial term by introducing empirical relation.

Here modified UNIFAC model of Gmehling (1993) has been used.

A.7 Normalization relations

The summation of the compositions in the bulk and the interface is unity.

$$NDI_{ik}: \quad \sum_{i=1}^{N^*} x'_{ik} = 1.0 \quad (A.22)$$

$$NCI_{ik}: \quad \sum_{i=1}^{N^*} y'_{ik} = 1.0 \quad (A.23)$$

$$ND_K: \quad \sum_{i=1}^{N^*} x_{ik} = 1.0 \quad (A.24)$$

$$NC_K: \quad \sum_{i=1}^{N^*} y_{ik} = 1.0 \quad (A.25)$$

Table A.1: Modified UNIFAC parameters

Line no.	Value
1	6
2	0.9011 0.6744 0.4469 0.5313 1.2663 4.0358
3	0.8480 0.5400 0.2280 0.4000 0.9680 3.2000
4	2 5 0 0 0 0
5	1 5 1 0 0 0
6	0 0 0 6 0 0
7	0 0 0 5 1 0
8	0 0 0 4 2 0
9	0 0 0 0 0 1
10	0.0 0.0 0.0 114.20 7.339 552.10
11	0.0 0.0 0.0 114.20 7.339 552.10
12	0.0 0.0 0.0 114.20 7.339 552.10
13	16.07 16.07 16.07 0.0 139.20 245.20
14	47.20 47.20 47.20 -45.33 0.0 -46.8
15	19.00 19.00 19.00 -61.10 476.0 0.0
16	0.0 0.0 0.0 0.0933 -0.4538 0.0
17	0.0 0.0 0.0 0.0933 -0.4538 0.0
18	0.0 0.0 0.0 0.0933 -0.4538 0.0
19	-2.998 -2.998 -2.998 0.0 -0.6500 0.0

Appendix B

```
TITLE
AROMATIC EXTRACTION USING SULFOLANE AS SOLVENT
****
FLOWSHEET
OUTPUT OF U_FEED IS INPUT 1 TO C1 TYPE LIQUID1
OUTPUT OF O_FEED IS INPUT 2 TO C1 TYPE LIQUID2
OUTPUT 1 OF C1 IS PRODUCT 1 TYPE LIQUID1
OUTPUT 2 OF C1 IS PRODUCT 2 TYPE LIQUID2
****
MODEL OVER_FEED
SET NOCOMP
TYPE
S      AS FLOW_MOL_2
Y_S    AS ARRAY(NOCOMP) OF MOLEFRACTION
STREAM
OUTPUT 1    S, Y_S
EQUATION
SIGMA(Y_S) = 1;
****
MODEL UNDER_FEED
SET NOCOMP
TYPE
F      AS FLOW_MOL_1
X_F    AS ARRAY(NOCOMP) OF MOLEFRACTION
STREAM
OUTPUT 1    F, X_F
EQUATION
SIGMA(X_F) = 1.0;
****
MODEL STAGE_SVT
SET NOCOMP, G=9.81, PI=3.14159, NO_HOLE=384, Dn=0.003175, STG_HEIGHT = 0.1,
AREA_STG = 0.070685835
TYPE
X_IN, X_P, X_OUT, X      AS ARRAY(NOCOMP) OF MOLEFRACTION
Y_IN, Y_OUT, Y_S, Y      AS ARRAY(NOCOMP) OF MOLEFRACTION
X_INT                    AS ARRAY(NOCOMP) OF MOLEFRAC_INT_1
Y_INT                    AS ARRAY(NOCOMP) OF MOLEFRAC_INT_2
U_IN, U_OUT, PROD_1      AS FLOW_MOL_1
V_IN, V_OUT, S           AS FLOW_MOL_2
    and so on.
STREAM
INPUT 1                  U_IN, X_IN
INPUT 2                  V_IN, Y_IN
INPUT 3                  S, Y_S
OUTPUT 1                  PROD_1, X_P
OUTPUT 2                  U_OUT, X_OUT
OUTPUT 3                  V_OUT, Y_OUT
EQUATION
#Dynamic mass balance equations #
# Flow Relationships #
# Mass transfer relationships
# Interface relationships #
# Normalization relationships #
    and so on.
PROCEDURE
(K_VALUE)                KLLVALUES (TEMP, P, X, Y)
(RHO_C)                  DENS_MASS_LIQ (TEMP, P, X)
```

and so on.

MODEL STAGE

SET as same as MODEL STAGE_SVT.

TYPE

as same as MODEL STAGE_SVT.

STREAM

as same as MODEL STAGE_SVT except that here 4 inputs & 4 outputs are present

EQUATION

as same as MODEL STAGE_SVT.

PROCEDURE

as same as previous model.

MODEL STAGE_L

SET as same as previous model.

TYPE

as same as previous model.

STREAM

as same as MODEL STAGE_SVT (here also 3inputs/3 outputs)

EQUATION

as same as previous model.

PROCEDURE

as same as previous model.

UNIT C1 IS A COLUMN

SET NS = 40, NOCOMP=6, G=9.81, PI=3.14159, NO_HOLE=384, Dn=0.003175, STG_HEIGHT = 0.1, AREA_STG = 0.070685775

UNIT O_FEED IS A OVER_FEED

SET NOCOMP = 6

UNIT U_FEED IS A UNDER_FEED

SET NOCOMP = 6

OPERATION

SET (used to specify fixed values of parameters; like flow rate of feed units, their compositions, etc.)

WITHIN O_FEED

S = 4.5E-3,

Y_S = < ,1E-6,1E-6,1E-6,1E-6,.999995>

WITHIN U_FEED

F = 2.0E-3,

X_F = <0.369999, 0.369999, 0.05, 0.16, 0.05, >

WITHIN "C1.STAGE_SVT"

here some parameters are specified.

WITHIN "C1.STAGE_L"

here some parameters are specified.

?REPEAT

WITHIN "C1.STAGE(? (ISTG))"

here some parameters are specified. This is valid for stage 2 to 39.

?WITH ISTG= <2:39>

PRESET (in this sub-section all the variables are given initial guess separately. Their lower and upper bounds are also specified.)

WITHIN "C1.STAGE_SVT"

WITHIN "C1.STAGE(*)"

WITHIN "C1.STAGE_L"

```

INITIAL      (In this sub-section the initial conditions are specified; like all the derivatives are
initialized to zero.)
WITHIN "C1.STAGE_SVT"
WITHIN "C1.STAGE_L"
?REPEAT
WITHIN "C1.STAGE(?ISTG)"
?WITH ISTG= <2:39>
****

MACRO COLUMN
?IF (NS > 2) ?THEN
MODEL STAGE_SVT
MODEL STAGE
MODEL STAGE_L
FLOWSHEET
?REPEAT
?IF (NOS = 1) ?THEN
    PRODUCT      1 IS OUTPUT  1 OF STAGE_SVT          TYPE LIQUID1
    FEED          2 IS INPUT    3 OF STAGE_SVT          TYPE LIQUID2
    INPUT 1 OF STAGE_SVT IS OUTPUT 1 OF STAGE 2        TYPE LIQUID1
    INPUT 2 OF STAGE_SVT IS OUTPUT 3 OF STAGE 2        TYPE LIQUID2
    OUTPUT 2 OF STAGE_SVT IS INPUT 2 OF STAGE 2         TYPE LIQUID1
    OUTPUT 3 OF STAGE_SVT IS INPUT 4 OF STAGE 2         TYPE LIQUID2
?ELSE ?IF (NOS = 2) ?THEN
    OUTPUT 1 OF STAGE ?(NOS+1) IS INPUT 1 OF STAGE ?(NOS) TYPE LIQUID1
    OUTPUT 3 OF STAGE ?(NOS+1) IS INPUT 3 OF STAGE ?(NOS) TYPE LIQUID2
?ELSE ?IF (NOS > 2) AND (NOS < NS-1) ?THEN
    OUTPUT 1 OF STAGE ?(NOS+1) IS INPUT 1 OF STAGE ?(NOS) TYPE LIQUID1
    OUTPUT 3 OF STAGE ?(NOS+1) IS INPUT 3 OF STAGE ?(NOS) TYPE LIQUID2
    OUTPUT 2 OF STAGE ?(NOS-1) IS INPUT 2 OF STAGE ?(NOS) TYPE LIQUID1
    OUTPUT 4 OF STAGE ?(NOS-1) IS INPUT 4 OF STAGE ?(NOS) TYPE LIQUID2
?ELSE ?IF (NOS = NS-1) ?THEN
    OUTPUT 2 OF STAGE ?(NOS-1) IS INPUT 2 OF STAGE ?(NOS) TYPE LIQUID1
    OUTPUT 4 OF STAGE ?(NOS-1) IS INPUT 4 OF STAGE ?(NOS) TYPE LIQUID2
?ELSE ?IF (NOS = NS) ?THEN
    FEED          1      IS INPUT    1 OF STAGE_L        TYPE LIQUID1
    PRODUCT 2      IS OUTPUT 3 OF STAGE_L                TYPE LIQUID2
    INPUT3 OF STAGE_L IS OUTPUT 4 OF STAGE ?(NOS-1)      TYPE LIQUID2
    OUTPUT 1 OF STAGE_L IS INPUT 1 OF STAGE ?(NOS-1)     TYPE LIQUID1
    OUTPUT 2 OF STAGE_L IS INPUT 3 OF STAGE ?(NOS-1)     TYPE LIQUID2
    INPUT 2 OF STAGE_L IS OUTPUT 2 OF STAGE ?(NOS-1)     TYPE LIQUID1
?ENDIF ?ENDIF ?ENDIF ?ENDIF ?ENDIF
?WITH NOS = <1 : NS>
?ELSE ?ERROR INVALID NO. OF STAGES ?END
?ENDIF
****

OPTIONS
ROUTINES      NEWTON      (other routines are FASTNEWTON & HYBRID for steady state
run)
              DAE         (other routines are SUPERDAE, EULER, RK4 for dynamic
simulation)
TRANSLATE
TYPECHECK     = ON
BLOCKRES      = ON
INLINE        = ON
PRINT (this is used to get information during runs. 1 - 6, 6 for max information)
DECLARE        1
FLOWSHEET      1
MACRO          1
MODEL          1

```

```

OPERATION      4
OPTIONS        1
PROCEDURE      1
TITLE          1
UNIT           1

```

```

EXECUTION
SCALING        = ON
PRINTLEVEL     = 3
PROPLEVEL      = 3
DEBUG          = OFF
TARGET         = FILE
REL_TOL        = 1E-11
ABS_TOL        = 1E-11
ITERATIONS     = 100
TIME_STEP      = 10
INTERVALS      = 100
EVENT_TOL      = 0.1
DERIVCHECK     = ON
WORKSPACE = 4

```

```
****
```

```
DECLARE
```

TYPE					
# VAR TYPE	DEFAULT	: MIN.	: MAX.	UNITS	
FLOW_MOL_1	= 2.0E-3	: 0.0015	: 0.003	UNIT = "kmol/s"	
FLOW_MOL_2	= 4.5E-3	: 0.0035	: 0.006	UNIT = "kmol/s"	
LIQFRACTION	= 0.045	: 0.03	: 0.06	UNIT = "-"	
MOLEFRACTION	= 0.1633	: 1e-7	: 1	UNIT = "kmol/kmol"	
K_VALUE	= 2.0	: 1E-5	: 1e6	UNIT = "-"	
MASS_TRANS_COEFF	= 1.0E-3	: 1e-6	: 50	UNIT = "kmol/s/m2"	
VELOCITY	= 0.0037	: 0.003	: 0.05	UNIT = "m/s"	
DIFFUS_LIQ	= 1.5E-5	: 1E-5	: 1E-4	UNIT = "CM2/S"	
TENS_C	= 0.023	: 0.0001	: 1.0	UNIT = "N/M"	
AREA	= 0.567	: 0.2	: 2.0	UNIT = "M2"	

and so on

```

STREAM LIQUID1
SET NOCOMP = 6
THERMO LIQUID
TYPE FLOW_MOL_1, MOLEFRACTION(NOCOMP)
COMPONENTS HEPTANE, MCH, C6H6, C7H8, OXYLENE, SULFOLANE
OPTIONS = UNIF-LL

```

```

STREAM LIQUID2
SET NOCOMP = 6
THERMO LIQUID
TYPE FLOW_MOL_2, MOLEFRACTION(NOCOMP)
COMPONENTS HEPTANE, MCH, C6H6, C7H8, OXYLENE, SULFOLANE
OPTIONS UNIF-LL

```

```
****
```

```

PROCEDURE DENS_MASS_LIQ : GPILD
INPUT TEMPERATURE, PRESSURE, MOLEFRACTION(NOCOMP)
OUTPUT DENS_MASS_LIQ

```

```
****
```

similarly other procedures are specified in separate PROCEDURE sections for calculations.

Bibliography

- Abrams D. S. and Prausnitz J. M., *AIChE J.*, **21**, 62, 1975.
- Allan J. M. and Teja A. S., Correlation and prediction of the viscosity of defined and undefined hydrocarbon liquids, *Can. J. of Chem. Engg.*, **69**, August, 1991.
- ASPEN PLUS User Manual, Vol. I, Aspen Technology, Cambridge, MA, 1996.
- ASPEN PLUS Reference Manual, Vol. III, Aspen Technology, Cambridge, MA, 1996.
- ASPEN PLUS PROPERTIES PLUS Reference Manual, Aspen Technology, Cambridge, MA, 1996.
- Baird M. H. I. and Lane S. J., Drop size and holdup in reciprocating plate extraction column, *Chem. Eng. Sci.*, **28**, 947-957, 1973.
- Baird M. H. I., Lo T. C. and Hanson C., *Handbook of solvent extraction*, John Wiley & Sons, 1983.
- Banerjee Phalguni, *Modeling and simulation of a non-isothermal liquid-liquid extraction column*, M. Tech. Thesis, I. I. T. Kanpur, 1997.
- Bird R. B., Stewart W. E. and Lightfoot E. N., *Transport Phenomena*, John Wiley & Sons, NY, 1960.
- Coulaloglou C. A. and Tavlarides L. L., Description of interaction process in agitated liquid-liquid dispersions, *Chem. Engg. Science*, **32**, 1289-1297, 1977.
- Edgar D. M. and Himmelblau T. F., *Chemical Process Optimization*, McGraw Hill, NY, 1989.

- Fredunslund A., Jones R. L. and Prausnitz J. M., Group contribution estimation of activity coefficients in non ideal mixtures, *AIChE J.* **21**(6), 1086-1098, 1975.
- Gmehling J., Li J. and Schiller M. A., Modified UNIFAC model: Present parameter matrix results for different thermodynamic properties, *Ind. Eng. Chem. Res.*, **32**, 178, 1993.
- Hakim D. I., Steinberg D. and Steil L. I., *Ind. Eng. Chem. Fundam.*, **10**, 174, 1971.
- Hankinson R. W. and Thomson G. H., *AIChE J.*, **25**, 653, 1979.
- Henley E. J. and Seader J. D., *Equilibrium stage separation operations in chemical engg.*, John Wiley and Sons, 1981.
- Holland C. D., *Fundamentals of multicomponent distillations*, McGraw Hill, NY 1981.
- Hsia M. A. and Tavlarides L. L., A simulation for homogenous dispersion in stirred tanks, *The Chemical Engg. J.*, **20**, 225-236, 1980.
- Hsia M. A. and Tavlarides L. L., Simulation Analysis of drop breakage coalescence and micromixing in liquid-liquid stirred tanks, *The Chemical Engg. J.*, **26**, 189-199, 1983.
- Jiricny V. and Kratky, Counter current flow of dispersed and continuous phase - I, *Chem. Engg. Sci.*, **34**, 1141-1149, 1979.
- Jiricny V. and Prochazka J., Measurement of holdup profiles and particle size distribution in a vibrating plate contactor, *Chem. Eng. Sci.*, **35**, 2237-2245, 1980.
- Khani S. D. A., Gourdan C. and Cassamata G., Dynamic and steady state simulation of hydrodynamics and mass transfer in liquid-liquid extraction column, *Chem. Engg. Sci.*, **44** (6), 1295-1305, 1989.

- King C. J., *Separation Processes*, 2nd edition, McGraw Hill, NY, 1980.
- Kirou and Tavlarides L. L., Flooding holdup and drop size measurements in multistaged column. *AIChE J.*, 34 (283), 843-848, 1988.
- Korchinsky W.J. Stagewise model of continuous liquid-liquid extraction. *Chem. Engg. Sci.*, **31**, 871-875, 1976.
- Krishna R. and Standart G. L., Mass and energy transfer in multicomponent systems, *Chem. Engg. Commun.*, **3**, 201, 1979.
- Krishnamurthy R., Reddy M. S. and Venkata Rao C., *Indian J. Technol.*, 6:53, 1968.
- Krishnamurthy R. and Taylor R. A., A non-equilibrium stage model of multicomponent separation process -1, *AIChE J.* **31**(3), 449-456, 1985a.
- Krishnamurthy R. and Taylor R. A., A non-equilibrium stage model of multicomponent separation process -2, *AIChE J.* **31**(3), 456-465, 1985b.
- Kumar A. and Hartland S., A unified correlation for the prediction of dispersed phase holdup in liquid-liquid extraction columns, *Ind. Eng. Chem. Res.*, **34**, 3925, 1995.
- Kumar R., *Modeling and simulation of liquid-liquid extraction column*, M. Tech. thesis, IIT, Kanpur, 1996.
- Laddha G. S. and Degaleesan T. E., *Transport Phenomena in Liquid Extraction*, Tata McGraw Hill, New Delhi, 1976.
- Larsen B. L., Rasmussen P. and Fredunslund A., A Modified UNIFAC group contribution model for prediction of phase equilibria and heats of mixing, *Ind. Eng. Chem. Res.*, **26**, 2274-2286, 1987.

- Latini G., Baroncini C. and Pierpaoli P., *Intern. J. Thermophys.*, **5**(4), 387, 1984.
- Li C. C., *AIChE J.*, **22**, 927, 1976.
- Magnussen T. and Fredunslund A., UNIFAC parameter table for prediction liquid-liquid equilibria, *Ind. Engg. Chem. Proc. Des. Dev.* **20**, 331-339, 1981.
- Mecklenbergi and Hartland. Design of differential counter-current extractor with back mixing, *Canadian Journal of Chem. Engg.*, **47**, 453-459, 1969.
- Mills A. L., *Recent advances in liquid-liquid extraction*, Pergamon Press, Oxford, 1972.
- Mukesh Kumar, *Simulation and model predictive control of aromatic extraction column*, M. Tech. thesis, IIT, Kanpur, 1998.
- Muthuravichandran B., Degaleesan T. E. and Laddha G. S., *Indian J. Technol.*, **27**, 125, 1989.
- Perry J. H., *Chemical Engineers' Handbook*, 6th edition, McGraw Hill, 1984.
- Ramkrishna D., The status of population balance, *Rev. Chem. Engg.*, **3**(1), 49-95, 1985.
- Reid R. C., Prausnitz J. M. and Poling B. E., *The properties of gases and liquids*, 4ed. McGraw Hill, NY, 1988.
- Renon H. and Prausnitz J.M., *AIChE J.*, **14**, 135, 1968.
- Ricker N. L. and King C. J., An efficient general method for computation of counter current separation process with axial dispersion, *AIChE J.*, **27**(2), 277-284, 1981.

- Rocha J. A., Fair J. R. and Humphrey J. L., Mass transfer efficiency of sieve tray extractors, *Ind. Eng. Chem. Process Des. Dev.*, **25**, 862, 1986.
- Rocha J. A., Cardenas J. C., Sosa C. and Rosales J., Flooding Velocities in sieve tray extractors, *Ind. Eng. Chem. Res.*, **28**, 1873, 1989.
- Rousseau R. W., *Handbook of Separation Process Technology*, John Wiley and Sons, 1987.
- Rowlinson J. S., *Liquid and Liquid Mixtures*, 2nd ed., Butterworth, London, 1969.
- Rubio L. M., Kumar A. and Hartland S., Drop size distribution and average drop size in a Wirz extraction column, *Trans. I. Chem. Engg. J.*, **26**, 189-199, 1983.
- Seader J. D., Rate-based modeling for staged separations, *Chem. Engg. Prog.*, **41**(9), 1989.
- Skelland A. H. P. and Minhas S. S., *AIChE J.*, **17**, 1316, 1971.
- Smith L. W. and Taylor R., Film model for multi-component mass transport: A statistical comparison, *Ind. Eng. Chem. Fund.*, **22**, 97-104, 1983.
- Sorenson J. M., DECHEMA chemistry data series Vol. I, II, III. Frankfurt, 1979-1980, LLE data collection.
- Souhrada F., Landau J. and Prochazka, *Can. J. Chem. Eng.*, **48**, 322, 1970.
- Sovava H. and Prochaska J., Breakage and coalescence of drops in a stirred vessel -1., *Chem. Engg. Sci.*, 163-171, 1981.
- Sovova H., A model of dispersion hydrodynamics in vibrating plate extractor, *Chem. Engg. Sci.*, **38**(11), 1863-1873, 1983.

equilibrium stage model incorporating a drop population model
Comput. Chem. Engg. Supp, S403-S410, 1992.

126233

Date Slip **A** 126233
turned on the

This book is to be returned on the
date last stamped.

This image shows a blank sheet of white paper with horizontal ruling lines. A single vertical line runs down the center of the page, creating two equal-width columns. The horizontal lines are evenly spaced and extend across the entire width of the paper. There is no handwriting or other markings on the page.

CHE-1998-M-JAI-SIM

